Carbon Energy

WILEY

CARBON ENERGY

REVIEW OPEN ACCESS

Typical Applications and Flame-Retardant Strategies for Organic Phase-Change Materials

Xiao-Mei Yang[1,2] | Tao Shi[3] | Xiaodong Wang[3] | Huan Liu[3] | De-Yi Wang[1,4] | Guang-Zhong Yin[1,4]

[1]Escuela Politécnica Superior, Universidad Francisco de Vitoria, Madrid, Spain | [2]Faculty of Diseño, Innovación y Tecnología, Universidad de Diseño, Innovación y Tecnología (UDIT), Madrid, Spain | [3]State Key Laboratory of Organic–Inorganic Composites, Beijing University of Chemical Technology, Beijing, China | [4]IMDEA Materials Institute, Madrid, Spain

Correspondence: Huan Liu (bucthuan@163.com) | De-Yi Wang (deyi.wang@imdea.org) | Guang-Zhong Yin (amos.guangzhong@ufv.es)

Received: 20 March 2025 | **Revised:** 20 June 2025 | **Accepted:** 17 July 2025

Funding: This study was supported by NEWSAFE (No.: PID2022-143324NA-I00) Projects funded by MICIU (Ministerio de Ciencia, Innovación y Universidades)/AEI (Agencia Estatal de Investigación)/10.13039/501100011033 and, as appropriate, by "ERDF/EU"; and Ramón y Cajal Fellowship (No.: RYC2023-045023-I) funded by MICIU, and, as appropriate, "ESF Investing in your future." This study was also partially supported by INC-UDIT-2025-PRO21 and INC-UDIT-2025-JCR24.

Keywords: bio-based | energy storage | flame retardant | nanocomposites | phase-change materials

ABSTRACT

This study begins by exploring the typical practical applications of phase-change materials (PCMs) in various industries, highlighting their importance in energy storage, temperature regulation, and thermal management. It then emphasizes the necessity of flame-retardant functionalization tailored to the specific application scenarios of PCMs, especially considering their use in safety-critical environments such as electronics, automotive, and construction. The classic characterization methods for assessing the flame-retardant properties of PCM are introduced in detail, including the limiting oxygen index, the vertical burning test, and the cone calorimeter, which are widely recognized standards in material safety testing. Additionally, newly developed methods for evaluating combustion safety are discussed, such as direct combustion tests, candle combustion experiments, and back temperature response, which offer a more comprehensive understanding of the material's fire resistance. Following this, this study provides a thorough summary and categorization of the flame-retardant strategies used in PCMs, divided into four main approaches: (1) incorporation of external flame retardants, (2) use of flame-retardant microcapsules, (3) development of flame-retardant support materials, and (4) creation of intrinsic flame-retardant PCMs. Each strategy is critically analyzed in terms of effectiveness, applicability, and potential challenges. Lastly, the conclusion provides an overview of the current state of flame-retardant PCMs, offering insights into future development directions, including the pursuit of more sustainable and efficient flame-retardant solutions, as well as prospects for their broader adoption in various industries.

1 | Introduction

Phase-change materials (PCMs) represent a class of substances capable of absorbing and releasing thermal energy through phase transformation processes. In contrast to conventional thermal energy storage (TES) approaches, including sensible heat storage systems and thermochemical reactions, PCM has distinctive characteristics that render it particularly advantageous for thermal regulation applications [1]. These materials demonstrate superior operational efficiency, characterized by their ability to maintain nearly isothermal conditions during energy exchange, thereby establishing themselves as one of the

Xiao-Mei Yang and Tao Shi contributed equally to the study.

Summary

- Systematized research and summary are presented of the applications of phase-change composite materials in thermoelectric energy harvest/conversion, battery modules' thermal management, electronic device thermal management, construction energy saving, and smart fibers/textiles.
- A detailed explanation of the testing methods for flame-retardant phase-change composite materials is presented.
- A detailed discussion of the flame-retardant strategies for functionalized phase-change composite materials is presented, providing guidance for future development and expansion of research on flame-retardant phase-change composites.

most effective solutions for thermal energy management and storage applications [2]. Some prospective and practical applications include building energy storage materials [3, 4], smart textiles [5–7], handheld devices [8, 9], food packaging [10], medical field [11, 12], renewable energy systems [13, 14], and TES systems [15, 16], among others. A key advantage of PCM is its remarkable tunability in the operational temperature range, enabling precise control over phase transition temperatures. This flexibility is particularly evident in organic PCM, where, for example, paraffin-based materials can be tailored by systematically adjusting the hydrocarbon chain length, thereby achieving phase transition temperatures spanning from −62°C to 86°C [17, 18].

PCM can be broadly classified into three categories: organic, inorganic, and eutectic PCM [19, 20]. The inorganic PCM family, which includes water, salt hydrates, molten salts, metals, and metal alloys, is frequently plagued by issues of high supercooling and phase separation, leading to phase transition hysteresis, reduced reversibility, and a shortened operational lifespan [21]. Eutectic PCMs are low-melting mixtures created by blending two or more components in specific ratios, categorized into inorganic–inorganic (e.g., NaCl–H_2O), organic–organic (e.g., lauric–palmitic acid), and organic–inorganic (e.g., fatty acid–metal salt) types [22]. As a typical example, Saher et al. [23] developed a eutectic phase-change system composed of boric acid and succinic acid that integrates latent heat storage, thermochemical transformation, and sensible heat capacity into a single trimodal energy storage strategy. This synergistic design achieves a high reversible energy storage density of 394 J/g, exceptional thermal cycling stability over 1000 cycles, and demonstrates strong potential for sustainable, low-cost TES in renewable energy applications. Common organic PCMs, such as paraffin wax (PW), fatty alcohols, fatty acids, polymers, and sugar alcohols, have attracted considerable attention due to their exceptional chemical stability, noncorrosive nature, and resistance to phase separation. Among these, PW is one of the most extensively studied due to the high phase-change enthalpy and favorable temperature range. For example, Wu et al. [14] developed an innovative strategy utilizing physically cross-linked dual-polymer networks combined with shear-aligned graphene nanoplatelets, achieving highly efficient paraffin encapsulation in multifunctional phase-change composites (PCCs). The resulting composite simultaneously shows high latent heat capacity, tunable mechanical strength, and enhanced thermal conductivity, demonstrating exceptional performance in thermal management applications for electronic devices and wearable systems. Fatty acids and alcohols, noted for their excellent biocompatibility, are well-suited for biomedical applications. Li et al. [24] developed a novel encapsulation strategy for fatty acid–based PCM by incorporating bio-based lauric acid into a flexible eugenol-derived epoxy resin (ER) network, achieving excellent compatibility, a high encapsulation rate, and a high enthalpy value. Although sugar alcohols offer the highest phase-change temperatures and enthalpies among organic PCM, their practical use is hindered by supercooling effects. Yang et al. [25] presented an effective thickening strategy by introducing carrageenan into erythritol, which substantially improves supercooling stability by enhancing both viscosity and solid–liquid interfacial energy. The resulting composite achieves an ultrastable supercooled state below −30°C for over 60 days while retaining a high latent heat (> 200 J/g), with crystallization controllably triggered via ultrasonication. Additionally, low-cost and functional polymer-based organic PCMs, such as polyethylene and polyethylene glycol (PEG), are increasingly being investigated for energy storage and thermal management applications.

Organic PCMs represent the most extensively studied and widely used category of PCMs, serving as attractive candidates for TES and thermal management applications [26]. However, the practical use of organic PCM is often constrained by the inherent flammability and relatively low thermal conductivity [27–30]. To address these limitations, significant advancements have been made in developing organic flame-retardant PCM (FRPCM). These include the incorporation of halogenated compounds, phosphorus-based additives, and nanomaterials to improve flame retardancy without compromising thermal performance [31–34]. Such innovations have significantly expanded the range of applications for organic PCMs, making them viable for high-performance systems in sectors such as battery modules, electronics, smart textiles, and building materials [35]. In addition, the development of eutectic organic PCM has further enhanced their performance by combining the beneficial properties of different components, resulting in a more synergistic effect for thermal energy management [36, 37]. These impacts might emerge as improved thermal conductivity or precisely tailored operational temperature ranges. As illustrated in Figure 1A, numerous research articles and review papers have been published on PCMs, exploring their applications in building materials, solar water heating systems, and sustainable technologies [38–42]. However, relatively few studies have specifically addressed the flammability of PCM. This issue presents a significant challenge that must be overcome before their widespread adoption, particularly in applications where fire safety is critical, such as building materials, electronics, and protective clothing. In light of this, the fire safety of PCM in essential applications has garnered increasing research attention (Figure 1B). Meanwhile, PCMs can absorb and release substantial latent heat through phase transition processes at specific temperatures, enabling effective thermal management and thus showing extensive interdisciplinary applications (Figure 1C). Consequently, enhancement of flame

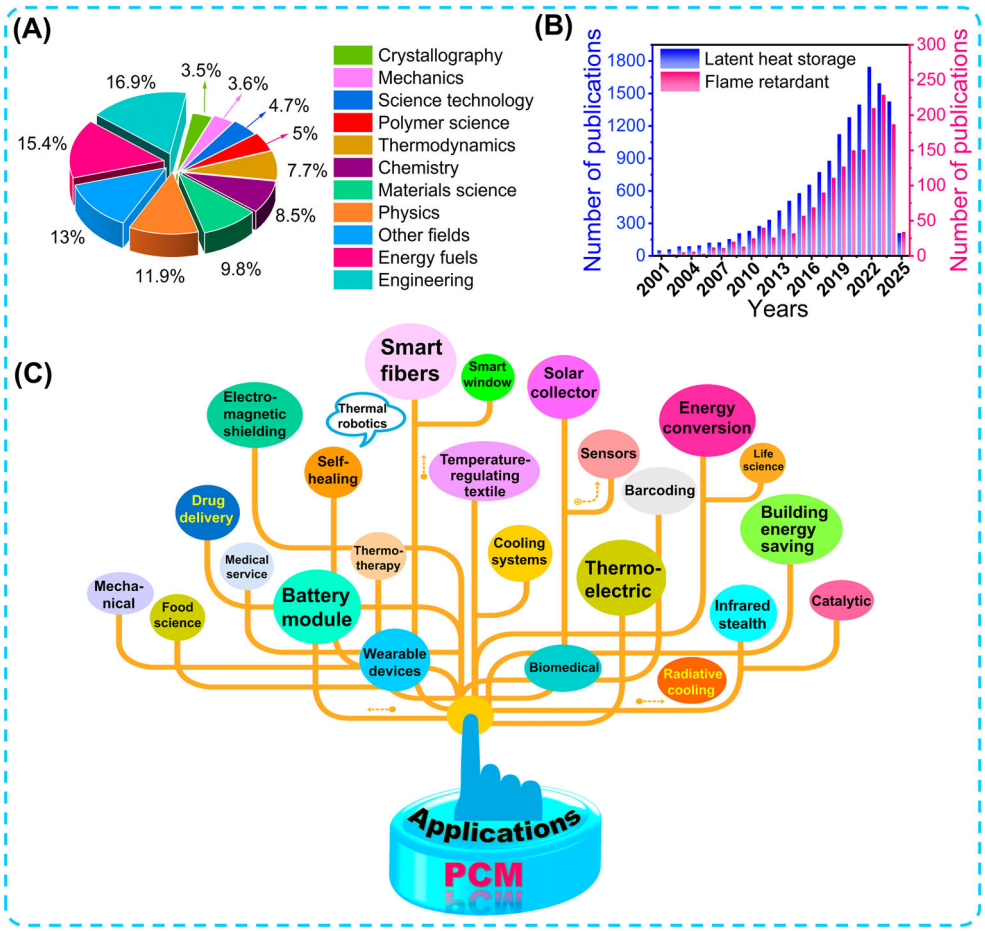

FIGURE 1 | (A) Data visualization of main application fields of organic PCMs. (B) Number of academic publications of fire-safe PCMs from 2001 to 2025. Data were extracted from Web of Science (May 2025). (C) Data visualization of the extensive application of organic PCMs.

retardancy can be regarded as a crucial prerequisite for the broader implementation of PCM in green buildings and other advanced fields.

In this review, we will begin by exploring the typical practical applications of PCMs (Figure 2) across various industries, emphasizing their importance in energy storage, temperature regulation, and thermal management. We then highlight the necessity of flame-retardant functionalization tailored to specific application scenarios, particularly in safety-critical fields such as electronics, automotive, and construction. Next, we will provide an in-depth overview of the flammability testing methods commonly used under laboratory conditions. The primary strategies to reduce the flammability of organic PCMs, as illustrated in Figure 2, will be examined in detail. Typically, a comprehensive investigation into the incorporation of various flame retardants into PCMs follows, covering strategies such as developing composite shape-stabilized PCMs, using bulk physical mixing processes, adding flame retardants to the shell or core of encapsulated PCMs, and designing intrinsically flame-retardant PCMs. The focus of these studies is on their impact on both flammability and phase-change properties. Finally, we provide an outlook on the research of PCM. We hope to collaborate with fellow researchers, inspire each other, and promote the safety, multifunctionality, and digitalization of PCMs, opening a new chapter for their widespread and scientifically efficient application.

2 | Typical PCM Applications

Against the backdrop of the "Carbon Peak and Carbon Neutrality" strategy, PCMs have emerged as pivotal components in energy management and thermal control due to their exceptional heat storage and temperature regulation capabilities. By leveraging reversible phase transitions, PCMs can efficiently absorb, store, and release substantial latent heat, thereby mitigating temperature fluctuations and enhancing energy utilization. These unique properties have enabled their widespread adoption in (1) thermoelectric conversion, (2) battery modules thermal management, (3) electronic device thermal management, (4) construction energy saving, and (5) smart fibers/textiles applications. In the following sections, we will discuss these five representative applications in detail, one by one.

2.1 | Thermoelectric Conversion

Thermoelectric generators (TEGs) use the Seebeck effect to convert heat directly into electrical energy, making them a viable option for emergency power supply. Their power generation efficiency is primarily determined by the temperature gradient between the hot and cold surfaces. PCMs effectively maintain and even increase this temperature difference, thereby

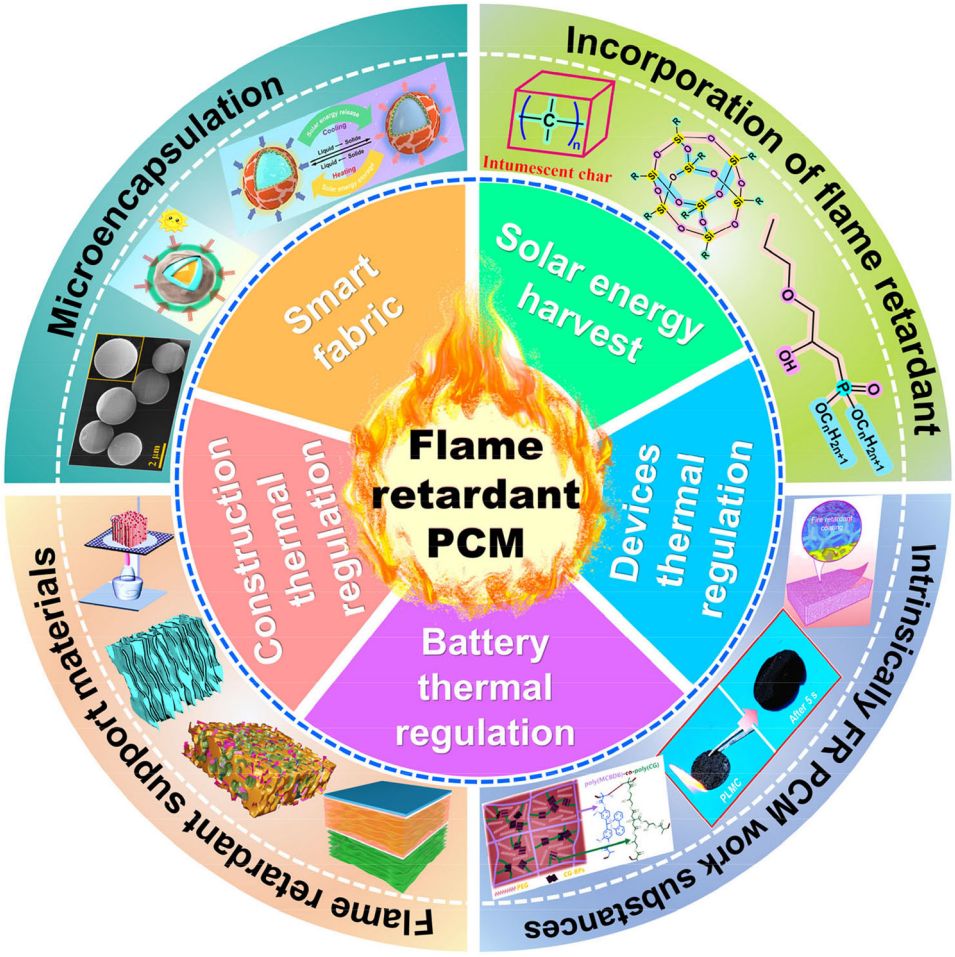

FIGURE 2 | Overview of typical applications and main flame-retardant strategies of flame-retardant PCMs.

improving the overall efficiency of TEGs. As illustrated in Figure 3A$_1$,A$_2$, PEG@thermoplastic polyurethane (TPU)/boron nitride nanosheets (BNNSs) act as a heat sink on the cold side of a TEG, effectively enhancing power generation. The TEG coupled with the composite can be used as an emergency power source during outdoor activities such as camping vacations and scientific expeditions. Notably, when using burning firewood as a heat source, this system remains operational during the night when solar power generation is inefficient (Figure 3A$_3$). This is a typical example of PCMs used on the cold side. In most cases, PCM is used on the hot side. We will present some examples to illustrate this below.

Covering approximately 71% of the Earth's surface, oceans receive solar energy at an average density of nearly 1367 W/m^2 [48]. However, most of this absorbed solar radiation is rapidly dissipated, influencing oceanic temperature and salinity dynamics [49, 50]. At present, solar–thermal–electric conversion technology based on the Seebeck effect is an attractive option for gathering clean and renewable solar energy [51, 52]. The combination of PCM (in the hot side) and optimized solar thermoelectric generator (STEG), rather than direct exposure of the thermoelectric module to incident solar radiation, provides excellent thermal conduction and conversion efficiency for long-term and stable power generation [53–55]. However, achieving complete leakage resistance across diverse application scenarios remains a significant challenge. Typically, in some cases, this is largely owing to the water solubility of frequently used organic PCMs and the low confinement capacity of supporting materials [56, 57]. Zhou et al. [44] developed a super-flexible PCM (SFPCM) with enhanced photoabsorption, mechanical properties, and thermal conductivity by incorporating MXene into a natural rubber (NR) network with dispersed PW microcapsules. The SFPCM-based STEG (Figure 3B) achieved an impressive 92% photothermal conversion efficiency, expanding the potential for efficient solar energy harvesting in oceanic applications. In addition, Ruirui Cao's research group [58] developed a phase-change aerogel (PCA)-based TEG to improve solar–thermal–electric energy conversion. The persistent thermal release of PCAs ensures that power production continues even after the heat source is eliminated. Proof-of-concept experiments in the study demonstrate the superior power capability of the PCA-loaded TEG, successfully lighting LEDs, powering portable electronics, and charging capacitors, with a voltage difference of up to 1.74 V compared to the bare TEG.

In recent years, thermoelectric devices have been widely used to power advanced low-power electronics [59–64]. However, the intermittent nature of natural sunlight poses challenges for stable energy harvesting and consistent power generation. Efficient photo-thermoelectric conversion requires high

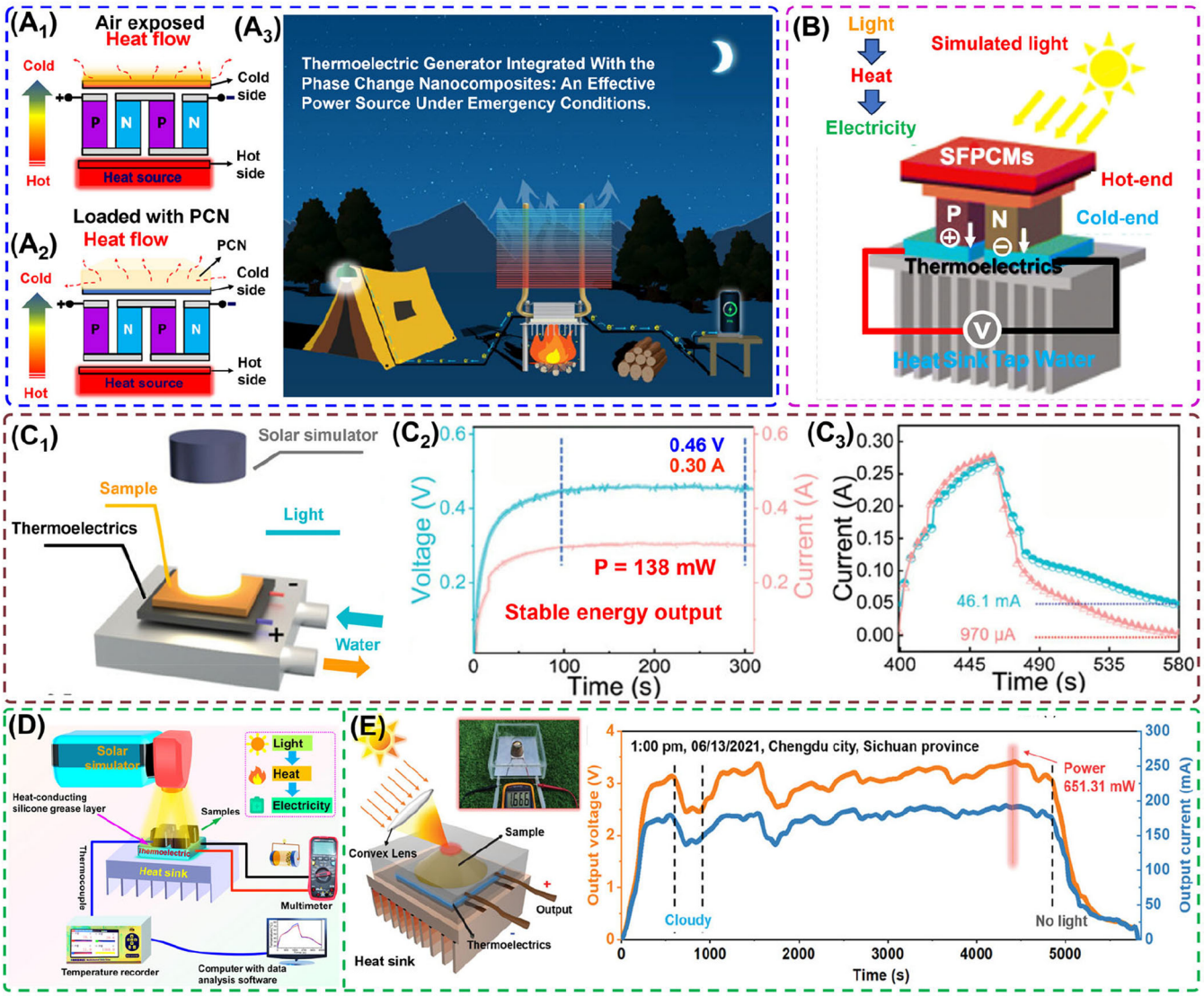

FIGURE 3 | Schematic mechanism of (A_1) TEG, (A_2) loaded with PEG@TPU/BNNS-es (PCN) exposed to air, and (A_3) conception diagram of potential application of TEGs integrated with the PCN film for outdoor activities. Reproduced with permission: Copyright 2023, Springer Nature [43]. (B) Experimental setup for solar–thermoelectric energy conversion of SFPCM. Reproduced with permission: Copyright 2023, The Royal Society of Chemistry [44]. (C_1) Designed device for light–thermal–electric conversion. (C_2) Output voltage and current of light thermoelectric device (LTED) based on the ethylene vinyl acetate/PW film with the stable light (one sun). (C_3) Output current of LTED based on ethylene vinyl acetate/PW film in a cycle. Reproduced with permission: Copyright 2023, Wiley [45]. (D) Schemes of a solar–thermal–electric conversion system. Reproduced with permission: Copyright 2024, American Chemical Society [46]. (E) Schematic of a homemade STEG system under environmental sunshine and power generation of a homemade STEG system. Reproduced with permission: Copyright 2021, Wiley [47].

conversion efficiency and a significant temperature gradient [65]. Achieving a sufficient temperature gradient requires rapid thermal charging of the heat source, which in turn depends on efficient and rapid collection of solar energy [66]. Thus, materials with high light-to-heat conversion efficiency and sustained energy delivery are necessary for improving the performance of traditional thermoelectric devices. In this regard, biomimetic composites have demonstrated great potential for enabling continuous solar energy harvesting and stable power generation in practical applications when integrated with thermoelectric systems [67]. Hu et al. [45] initially proved that the addition of PCM may considerably increase the photothermal-to-electrical conversion efficiency of thermoelectric devices, increasing the overall thermoelectric efficiency by 11.3%. The phase-change film ensures stable heat input, maintaining a constant output of 0.46 V and 0.30 A under illumination (Figure 3C). Even after the light is removed, the stored thermal energy sustains power generation, highlighting the potential of PCM-based designs as a simple and effective strategy for improving thermoelectric energy. Shi et al. [46] developed a magnetic phase-change composite with a 3D porous carbonized polyimide (PI)/Kevlar nanofiber aerogel, $CoFe_2O_4$ nanoparticles, PEG, and a polypyrrole photothermal coating for efficient solar–thermal–electric energy conversion. This unique structure enables efficient heat and electron transfer, ensuring high photothermal conversion (Figure 3D). This study highlights the potential of PCM-based magnetic materials in solar–thermal–electric conversion systems, expanding TES options and enhancing power generation

TABLE 1 | Summary of the performance of solar–thermo–electric energy conversion.

PCM work substances	Melting enthalpy (J/g)	Thermal conductivity (W m^{-1} K^{-1})	Solar irradiation power (mW cm^{-2})	Solar–thermal conversion efficiency (%)	Output voltage (mV)/ current (mA)	Output power (mW)	References
PW	126.8	0.38	200	92.0	410/–	—	[44]
PW	160.5	—	100	—	236.1/136.5	138.00	[45]
PEG–4000	150.0	0.41	200	84.8	259.7/27.1	7.01	[48]
			400		405.9/36.9	15.03	
D–mannitol	> 90	10.00	78	—	3410/1191	20.83	[47]
PEG–10000	138.2	22.36	800	—	~25	—	[56]
Methoxy poly (ethylene glycol) mono-methacrylate	158.0	—	200	—	144/14.8	2.13	[59]
PEG–10000	145.9	0.33	400	82.9	~120/~25	—	[68]
			800		~200/~45	—	
PEG–10000	122.2	1.30	400	72.7	~130/~28	—	[69]
			800		~120/~26	—	
PEG–10000	147.5	2.94	78	80.5	251/64.2	—	[67]
PW	146.4	0.85	200	97.1	246.9/–	—	[70]
PEG–8000	107.1	0.56	500	92.9	323.1/100.7	35.8	[71]
PEG–8000	101.2	0.59	200	94.4	491/100.5	54.8	[72]
PW	144.9	—	495	81.7	720/–	—	[60]

efficiency. Zhang et al. [47] developed a phase-change composite with a circular truncated cone structure and actinomorphic polybenzobisoxazole fibers, enabling efficient TES and discharge. Integrated into an STEG system with a Fresnel lens for solar concentration, the composite reached a record high power of 651.31 mW, comparable to commercial photovoltaics (Figure 3E).

Notably, Table 1 lists the key parameters for the use of PCMs in STEG systems. PEG- and PW-based work substances are widely explored. Using common PCM, such as PW, the output voltage is generally low, typically ranging between 100 and 400 mV. However, with D-mannitol, the output voltage can reach up to 3 V. The possible reason for this could be the difference in melting points between the PCM, which provides a higher temperature gradient.

2.2 | Battery Modules' Thermal Management

The long cycle or intermittent charge and discharge electrochemical processes for power battery, overheating, and uneven temperature distribution at high discharge rates will inevitably lead to severe degradation of power system performance, decrease in reliability, and early failure of the power system [73, 74]. However, traditional thermal management systems for battery modules focus on air cooling and liquid cooling technologies. Natural convection air cooling systems are less efficient, and forced-air cooling systems have large space requirements and uneven temperature distributions [75]. Among various cooling technologies, PCM cooling systems stand out for their energy-free operation, ease of installation, and low maintenance requirements [76, 77]. In particular, organic PCM is capable of efficiently absorbing a substantial quantity of heat produced by the power battery. Owing to its high latent heat, it further mitigates the temperature increase and maintains outstanding temperature uniformity. This allows the PCM cooling system to not only maintain the peak temperature within a reasonable range but also ensure a uniform temperature distribution [78, 79].

However, the majority of existing organic composite PCMs currently available are susceptible to combustion, leading to potential thermal risks, including fires and detonations within battery modules [80]. Therefore, the advancement of high-performance flame-retardant phase-change composites for large-scale power battery systems can restrict the maximum temperature to a reasonable level and ensure consistent temperature distribution among battery modules [81]. As a typical example, Weng et al. [82] developed a novel tubular organic PCM with a cellular structure using physical flame-retardant modification technology to improve the thermal safety of PCM-based battery modules, and the study provided valuable insights into improving battery safety. In addition, more studies have explored battery safety at multiple levels, including intrinsic safety through material development, active safety through fault avoidance control, and passive protection through fault energy limitation [83, 84].

Various functional components to improve the intrinsic safety of batteries have also been developed in recent years (Table 2). The following are some typical examples. Li et al. [85] demonstrated that smart firewalls combining non-flammable PCM with flexible silica nanofiber mats show thermally triggered, switchable thermal properties. As shown in Figure 4A, these firewalls incorporate a variety of functions, such as cooling, fire suppression, and thermal insulation. Compared to pure thermal insulation materials, the PCM-enhanced firewalls offer superior heat absorption and cooling capabilities. As shown, commonly used PCMs include PEG, PW, stearyl alcohol, and other working substances. It can be observed that organic PCMs are widely selected as suitable materials for battery thermal management due to their appropriate phase-change temperature range (35°C–65°C). The temperature regulation performance of the final battery pack is largely influenced by factors such as thermal conductivity, melting enthalpy, and battery model. Among these, the regulation capability is generally positively correlated with the melting enthalpy of the PCM. In fact, this is one of the core development indicators for PCM—the key technical challenge for multifunctional PCM lies in maximizing melting enthalpy while maintaining good thermal conductivity, flame retardancy, and leakage resistance.

A multifunctional composite PCM (MTPCM) tailored for end-of-life battery modules was developed by Mingyu Cheng et al. [88]. The MTPCM3 module effectively mitigates heat accumulation, ensuring that battery temperatures remain below 50°C and maintaining a uniform temperature distribution (within a 5°C range) during long-cycle operations (Figure 4B). This study has significant potential to improve the safety and performance of battery systems. Hu et al. [79] have successfully developed an intrinsically flexible, high-enthalpy phase-change composite (PW-SBS/CNT) and demonstrated its efficacy in controlling the operating temperature of commercial lithium-ion batteries (LiBs). When applied to the battery's base, the composite significantly reduces temperature gradients compared to areas without the material, thereby enhancing thermal uniformity (Figure $4C_1$–C_3). The PW-SBS/CNT composite can also be used as a photo-thermal and temperature-controlled board to maintain the temperature of the roof. The application mechanism of the PW-SBS/CNT energy-saving board is briefly illustrated in Figure $4C_4$. During the day, under sufficient solar radiation, the PW is in a melting state due to the thermal excitation of the solar energy, which enables energy storage. The phase-change process will absorb the excess heat in the house and maintain a cool indoor environment. At night, without solar radiation, the liquid PW will return to a solid state, and the stored heat will be slowly released into the room, because of which an optimal temperature can be maintained in the room. The temperature evolution curves of samples under solar irradiation are illustrated in Figure $4C_5$. This study provides insight into the design of flexible PCM for electronic thermal management and solar TES. Wu et al. [87] developed phase-change composites (PCCs) with a dual encapsulation strategy, utilizing a polyurethane/graphite nanoplatelet hybrid network to achieve superior cooling performance. The composite efficiently manages thermal conditions in LiBs by preheating at low temperatures and absorbing excess heat at high temperatures through phase transition and latent heat (Figure $4D_1$,D_2). Infrared images show a more uniform temperature distribution, highlighting the exceptional cooling capability of the PCCs (Figure $4D_3$).

As lithium battery technology becomes widely used, an effective thermal management system is essential to maintaining battery performance and safety in all climates. Cheng et al. [88] developed a dual-layer thermal management system for lithium batteries using a PW/olefin block copolymer/expanded graphite (EG) (POE). This integrated active–passive system uses a two-layer PCM structure to achieve multifunctional thermal regulation. During preheating, the POE layer forms a thermal loop with the battery, whereas under high-temperature conditions, it effectively mitigates heat accumulation, ensuring optimal thermal management (Figure 4E). Wu et al. [83] addressed the problem of low thermal conductivity in PCM by developing highly thermally conductive PCCs incorporating large, aligned graphite sheets. When heat flows along the alignment of the graphite sheets, the thermal charging power is more than twice that observed when heat flows across the alignment (Figure $4F_1$,F_2).

2.3 | Electronic Device Thermal Management

The growing demand for high-performance portable electronic devices has spurred rapid advancements in thinness, lightweight design, miniaturization, integration, and intelligence [95, 96]. Generally speaking, portable electronic systems with integrated smart units often have increased power density, which leads to excessive heat build-up due to the limited heat dissipation of miniaturized devices [97, 98]. Thus, this unwanted heat build-up can lead to degraded performance of the electronics and thermal discomfort or even injury to the skin [99]. To address this practical issue, scientists have utilized the characteristics of PCMs, such as heat absorption during phase change and a relatively narrow phase-change temperature range, to regulate the operating temperature of devices like mobile phones and digital cameras (Figure 5). Below, some recent typical reports are presented.

Thermal management strategies for portable devices have been developed using boron nitride (BN) aerogel films, as reported by Wang et al. [100]. The BN aerogel film effectively reduced heat transfer from electronics to the skin, demonstrated by its ability to protect a green leaf from burning when placed on a flame for 15 s (Figure $5A_1$,A_2). Additionally, BN PCC films (PCCFs), with organic PCMs, absorbed excess heat through a solid–liquid phase transition, cooling the electronics (Figure $5A_3$). Infrared images from a 5G phone test further highlighted the thermal protection, maintaining a temperature of around 52.4°C during heavy use (Figure $5A_4$). In addition, the composite film has low thermal conductivity, which promotes the thermal insulation effect (Figure $5A_5$). Li et al. [101] developed shape-stable phase-change composites (SSPCCs) made from polypropylene, carbon nanotubes (CNTs), ferroferric oxide, and PW, which show superior thermal management and flexibility. Demonstrations of the SSPCC with 8 wt% Fe_3O_4 (P8) applied to a smartphone showed its ability to effectively regulate temperature, prevent rapid heat accumulation, and maintain thermal stability (Figure 5B). The simple manufacturing process underlines its promising potential for advanced thermal management in future integrated circuits.

TABLE 2 | Summary of the thermal properties of different PCMs and thermal management performance in batteries.

PCM work substances	Melting temperature (°C)	Melting enthalpy (J/g)	Thermal conductivity (W m^{-1} K^{-1})	Battery model	Maximum temperature difference (°C)	References
Silica sol	127	1920	0.026	50 Ah $LiNi_{0.5}Co_{0.2}Mn_{0.3}O_2$ (NCM523)	512	[85]
PW	47.5	125.7	1.39	32650-lithium iron phosphate	5	[86]
PW	61.6	147.63	0.39	Commercial lithium-ion battery	12.1	[79]
PEG	46.5	163.5	27.0	18650 ternary	15	[87]
PW	35–50	~110	19.3	18650 MH	—	[88]
Stearic acid	67.7	122.8	> 10	18650 ternary	13.2	[83]
PW	48–57	165	7.2	18650 ternary	60	[76]
PW	34.9	117	—	Battery thermal management system	5.87	[80]
Octadecyl acrylate	46.1	71.5	1.26	18650 ternary	4.1	[82]
PW	46.3	81.2	1.05	18650 ternary	1.36	[89]
PEG–6000	57.7	78.7	0.252	18650 ternary	405	[90]
n-docosane	~40.5	153.7	0.335	LF32	11.93	[91]
Lauric acid	40.2	107.7	0.3	18650 Li ion	11.1	[92]
PW	~42	292.7	30.75	14500 cells	~60	[93]
PW	42	152.1	2.31	18650 Li ion	4.8	[94]

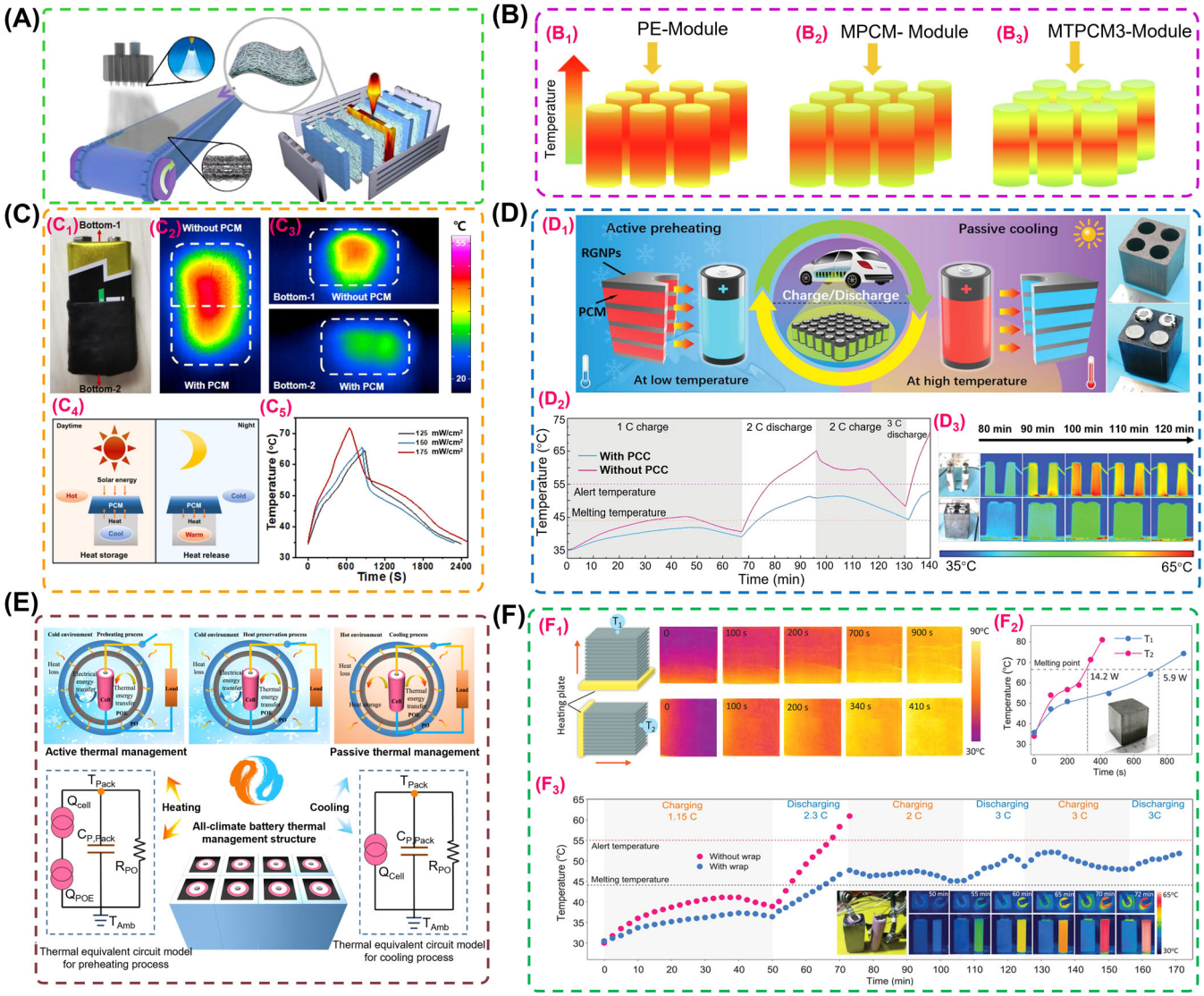

FIGURE 4 | (A) Fabrication process for the smart firewalls. Reproduced with permission: Copyright 2021, Elsevier [85]. (B) Schematic diagram of the battery temperature distributions of (B_1) the PW/ethyl vinyl acetate (PE) Module, (B_2) the PW/EG/melamine PCM (MPCM) Module, and (B_3) the MTPCM3 Module. Reproduced with permission: Copyright 2022, Elsevier [86]. (C_1) Digital photos of batteries with a wrap of PW-styrene-butadiene-styrene (SBS)/carbon nanotube (CNT). (C_2, C_3) Infrared images of batteries during charging. (C_4) Schematic illustration of a flexible PW-SBS/CNT composite charged by solar irradiation for energy-saving buildings. (C_5) Time–temperature evolution curves of PW-SBS/CNT composite as a function of irradiation light power. Reproduced with permission: Copyright 2022, Elsevier [79]. (D_1) Schematic of PCC-based battery thermal management for electrothermal-driven active preheating at low temperature and phase-change–driven passive cooling at high temperature. The digital images on the right side show a LiBs pack wrapped with a PCC block. (D_2) Comparison of temperature evolution curves of the LiB packs with and without PCC cooling in a hot environment (35°C). (D_3) Digital photos of LiB packs with and without a PCC wrap and the corresponding infrared images during the charge/discharge process. Reproduced with permission: Copyright 2021, Wiley [87]. (E) Schematic illustration of the battery packs and working instructions for different processes. Reproduced with permission: Copyright 2022, Elsevier [88]. (F_1) Comparison of 1D coordinated and uncoordinated heat conduction. The temperature of the heating plate is maintained at 90°C. (F_2) Temperature profiles of the measured points. The inset shows a digital photo of the composite block. (F_3) Temperature profiles for two battery monomers. The insets show the digital photos of tested battery monomers and their infrared images during the discharging process from 50 to 72 min. Reproduced with permission: Copyright 2019, Wiley [83].

Bioinspired PCCs with high thermal conductivity hold great potential for effective thermal management. Hu et al. [102] mimicked the hierarchical structure of trees by using a phloem-inspired cross-linked ethylene–vinyl acetate copolymer (EVA)/PW film for heat storage and a xylem-inspired EVA/EG film for fast heat conduction. The composite, with annual-ring and multilayer structures, shows rapid heat diffusion and excellent thermal management (Figure $5C_1$). The above two components were assembled to develop PCCs with annual-ring and multilayered structures. The heat diffusion from the center of the PCCs was monitored by an IR camera (Figure $5C_2$), and the speed of heat diffusion can be roughly judged via the color and area of real-time pictures. The MEP-9.0 with higher thermal conductivity diffuses the absorbed heat out of the center more rapidly, and thus, no

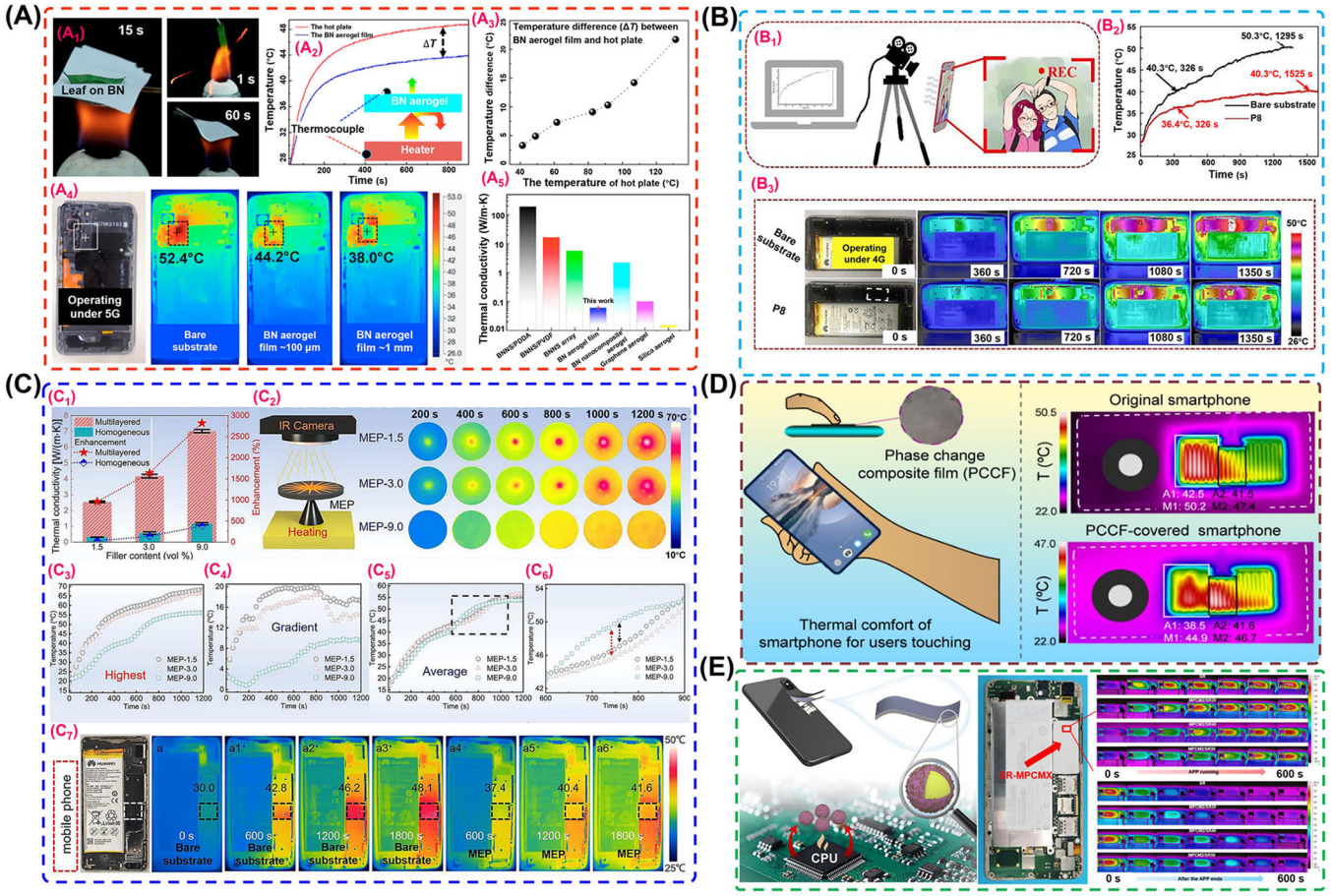

FIGURE 5 | Examples of PCM applications for thermal management of electronic devices. (A_1) Thermal insulation and protection of a BN aerogel film on the flame. (A_2) Temperature–time curves of a BN aerogel film. (A_3) Chart of the temperature difference between a BN aerogel film and a heater. (A_4) Photograph and infrared (IR) images of the backside of a working 5G smartphone. (A_5) Thermal conductivity of a BN aerogel film and other materials. Reproduced with permission: Copyright 2020, American Chemical Society [100]. (B_1) Schematic illustration of the setup for thermal management. (B_2) Temperature–time curves of P8 and the bare substrate of a working smartphone. (B_3) Photographs and IR images of a smartphone. Reproduced with permission: Copyright 2021, Elsevier [101]. (C) Thermal conductivity and thermal management characterizations of multilayered EVA/EG (MEPs). (C_1) Thermal conductivities of MEPs. (C_2) Setup for temperature monitoring of MEPs and in-time IR pictures of MEPs heated from the center. (C_3) Highest temperature, (C_4) temperature gradient, and (C_5, C_6) average temperature curves of MEPs heated from the center. (C_7) In-time IR pictures of thermal management characterization of MEP on a mobile phone. Reproduced with permission: Copyright 2023, Elsevier [102]. (D) Thermal comfort of smartphones for users in terms of touch. Reproduced with permission: Copyright 2023, American Chemical Society [103]. (E) Schematic illustration showing cooling of a mobile phone by a silicone sheet containing micro PCM, and thermal IR images of mobile games during and after the game. Reproduced with permission: Copyright 2020, Elsevier [104].

obvious temperature gradient is observed. The time–temperature curves simultaneously quantitatively differentiate the different temperature distributions (Figure 5C_3–C_6). When applied to a mobile phone, the MEP-9.0 composite effectively prevented rapid temperature rise, demonstrating its potential for advanced thermal management solutions (Figure 5C_7). Despite numerous investigations into encapsulating solid–liquid PCMs within porous networks for thermal energy dissipation in electronic devices, the synthesis methods often remain intricate and expensive [105]. The obtained PCCF often shows insufficient mechanical strength to withstand external pressure, and its thickness is too large for integration into electronic devices. In addition, their in-plane dimensions are usually not suitable for applications in larger devices such as tablets or laptops. Therefore, there is an urgent need to develop PCCFs that combine high thermal conductivity, superior structural stability, high phase-change enthalpy, and ultrathinness to manage heat distribution in smartphones and other electronic devices efficiently.

Li et al. [103] developed a flexible, leakproof sodium alginate (SA)/carboxymethyl cellulose@CNT-PEG film using a simple, eco-friendly method with a stainless-steel mesh. The film demonstrated excellent shape stability and thermal management performance in electronic devices. Thermal tests on a smartphone showed that the PCCF-0.7 reduced its peak temperature by 5.3°C, enhancing user comfort (Figure 5D).

The above examples use aerogel or polymer blending techniques to prepare PCMs. Additionally, many researchers have widely utilized microencapsulation technology to produce PCMs. Specifically, Zhu et al. [104] developed a microencapsulated PCM with a core–shell structure and high payload, prepared using a Pickering emulsion stabilized by regenerated nano chitin and interfacial polymerization with isocyanate. They tested the performance of MPCM2, combined with silicone rubber in sheet form, to delay temperature rise under high processor demands, such as gaming and

multitasking. As shown in Figure 5E, without micro PCM, the sample reached 50°C in 235 s, whereas MPCM2/SR50 delayed the temperature rise by 8.7°C at 265 s, protecting devices from overheating during processor surges.

2.4 | Construction Energy Saving

As living standards improve, the demand for thermal comfort in buildings is increasing [106]. In building applications, the phase-change process—such as melting and solidification—results in significantly higher heat storage and release compared to sensible heat alone [107]. Generally, PCM absorbs solar energy during the day and releases stored heat energy at night, improving the indoor temperature distribution, reducing indoor temperature fluctuations, and having the effect of peak shaving and troughing [108], which can be applied as thermal regulators either in new construction buildings or for thermal energy. Solid–liquid PCMs can be used to regulate indoor temperatures in buildings, thereby reducing energy consumption and saving energy [109]. At the same time, PCMs used in building structures and decorative materials can improve the usable area and space utilization efficiency of a building to a certain extent compared to conventional air conditioning systems or other heat transfer devices.

For typical examples, Lei et al. [110] investigated the energy performance of building envelopes incorporating PCM to reduce cooling loads in Singapore using numerical simulations. The study found that the incorporation of PCM into the building envelope can reduce the effect of cooling loads in tropical air-conditioned buildings. Also, the addition of a 10 mm layer of PCM with a phase-change temperature of 28°C to the external surface of vertical concrete walls in heating, ventilation, and air conditioning (HVAC) systems effectively reduced heat gain in the building envelope. This highlights the significant advantages of using PCM in tropical regions compared to other climates.

An active phase-change heater for buildings in marine climates has been proposed by Zhang et al. [111]. This system utilizes low-cost electricity during off-peak periods to store thermal energy and discharges it during peak periods (Figure 6A). A numerical model was developed to simulate phase change and convective heat transfer between PCM and indoor air. The study evaluated the heater's performance in regulating indoor temperature, phase-change behavior, and operation, reducing energy consumption in buildings. Kalbasi et al. [108] conducted an annual analysis of a building using numerical methods to simulate PCM phase change and account for radiation effects from all directions. Adding PCM to the walls improved both sensible and latent heat performance, with installation near the uppermost layer enhancing energy savings by 3.72 kWh/m^2 (Figure 6B). The study also highlighted the efficiency of thermally activated building systems (TABS), where liquid (typically water) circulates through pipes embedded in ceilings, walls, floors, or roofs for heat transfer. Figure 6C illustrates the differences between buildings equipped with conventional HVAC systems and those with TABS incorporating PCM into their structural partitions. It shows how TABS with PCM can reduce indoor temperature variations and maintain thermal comfort throughout the day when the system is optimally installed. Anter et al. [106] studied the long-term thermal performance of building walls incorporating different types and thicknesses of PCMs during the hot summer season in Aswan, Egypt. The analysis compared the performance of the wall with and without the PCM layer under different external weather conditions. Figure 6D shows that placing the PCM on the outside of the wall improved the internal performance. In addition, dividing the PCM thickness between the exterior and the interior yielded better results than placing it on either side alone. Zhang et al. [113] proposed a novel building wall design incorporating a PCM layer, optimized by computational fluid dynamics analysis. The PCM layer dynamically exchanges positions with the insulation layer, sandwiched between the outer brick layer and the insulation during the day, and reverses at night. Compared to two control walls—one with no PCM and one with a static PCM layer—the proposed design demonstrated superior thermal performance, achieving up to 89% energy savings for heating in cold winters (Figure 6E). Schossig et al. [115] investigated the integration of microencapsulated PCM into building materials like plaster and walls. The results indicated that temperatures above 26°C could be effectively reduced, as shown in Figure 6F. In addition, Li et al. [116] investigated the thermal performance of different types of roofs, both with and without PCM, in the northeastern and cold regions of China, including conventional roofs and PCM-integrated roofs. The results showed that PCM roofs significantly delayed temperature peaks in the room, with a delay of over 3 h compared to conventional roofs, as shown in Figure 6G. The graph clearly demonstrates the remarkable peak-shaving and valley-filling effect of the PCM. Yu et al. [117] found that roofs with an external PCM layer help to release condensation heat during summer nights, significantly reducing heat transfer through the roof and lowering the peak internal surface temperature. This makes such roofs more suitable for energy saving in buildings in hot regions with long summers.

Although organic PCMs maintain the temperature of building elements constant by absorbing a large amount of latent heat during the phase-change process, thus reducing room-temperature fluctuations, one of the drawbacks of organic PCMs in building applications is the possible risk of their leakage from the molten state, which can lead to safety issues [113, 118]. Organic PCMs also have the disadvantage of being flammable, especially hydrocarbon PCM, so when organic PCMs are incorporated into building materials, appropriate fire and environmental safety measures are required, in addition to leakage prevention [119]. Research on fire safety will be further discussed in Section 4.

2.5 | Smart Fibers/Textiles

Smart temperature–regulating textiles originate from smart fibers, which in turn rely on the integration of PCMs into fibers using various techniques to achieve thermal regulation. The typical fabrication methods can be broadly categorized into three main types: (1) microcapsule technology; (2) core–shell fiber-based encapsulation technology; and (3) coating technology.

2.5.1 | Microcapsule Technology

Encapsulated PCM capsules are micro-sized core–shell particles, with PCM as the core and a protective shell. This encapsulation not only prevents leakage and reduces the reactivity of the core material (e.g., n-alkanes) but also increases the heat

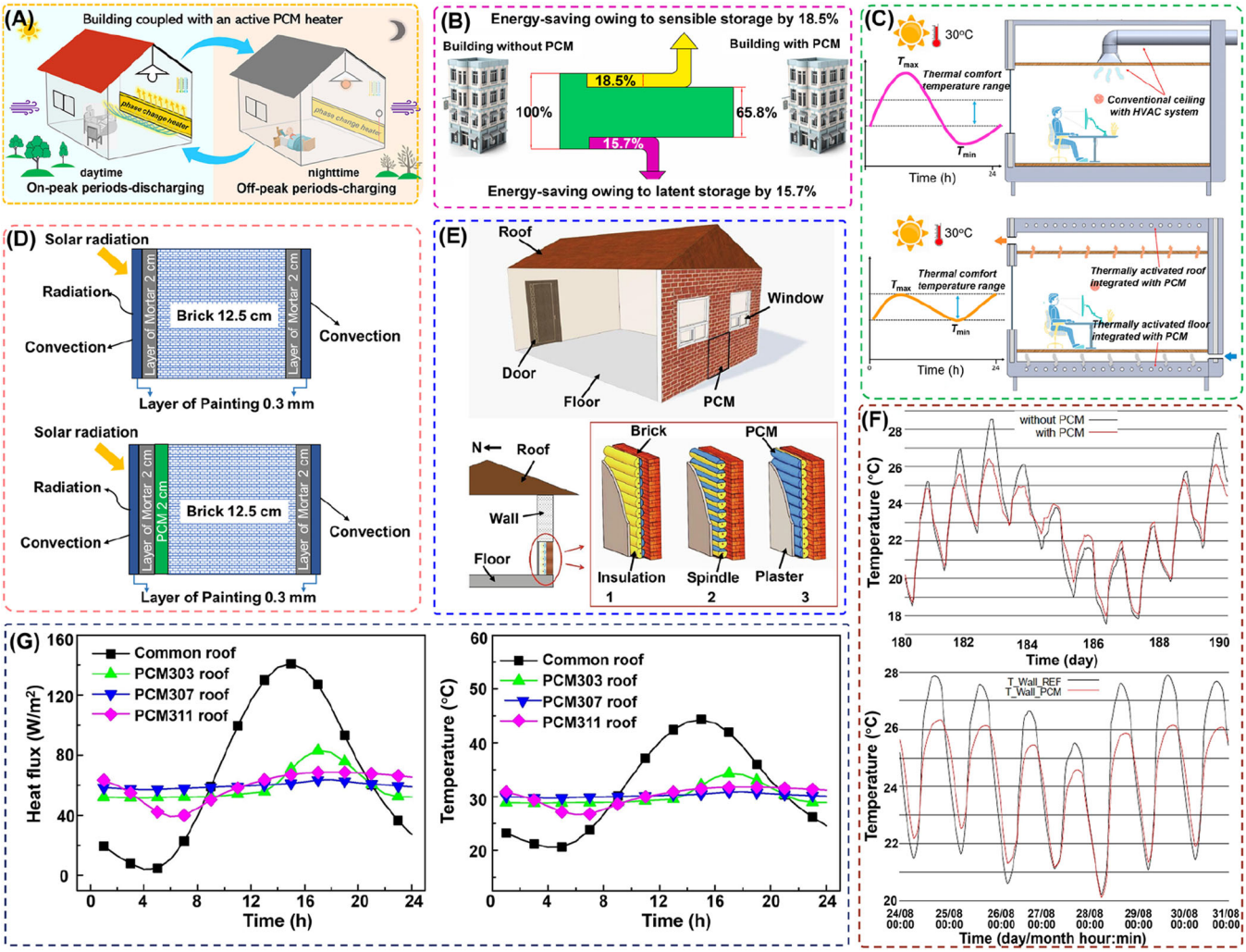

FIGURE 6 | Typical examples of PCMs for building energy saving. (A) Building coupled with an active PCM heater. Reproduced with permission: Copyright 2023, Elsevier [111]. (B) Schematic illustration of the setup for thermal management. Reproduced with permission: Copyright 2022, Elsevier [108]. (C) Schematic showing the difference between a conventional HVAC-cooled office and an office integrated with TABS and PCM. Reproduced with permission: Copyright 2019, Elsevier [112]. (D) Wall without a PCM and with a PCM layer, outdoor varied boundary conditions, and computational domain. Reproduced with permission: Copyright 2023, Elsevier [106]. (E) Room with a dynamic PCM wall system and PCM orientations, with position 1 during the daytime and position 3 during the nighttime. Reproduced with permission: Copyright 2021, Elsevier [113]. (F) Plaster and wall with and without PCM. Reproduced with permission: Copyright 2023, Elsevier [114, 115]. (G) Average temperature and heat flux of the upper surface in base layer heat flux and temperature. Reproduced with permission: Copyright 2015, Elsevier [116].

exchange surface area [120–122]. Microencapsulation refers to the process of encapsulating PCMs in protective capsules. Among several techniques, in situ polymerization is commonly used due to its ability to form strong, fast capsules ideal for TES. At present, encapsulated n-alkanes are widely studied for TES applications, including solar energy storage, waste heat recovery, thermally regulated textiles, and energy-efficient construction [4, 123, 124].

Recently, flexible multifunctional textiles have gained significant attention for their ability to respond to external stimuli and maintain a comfortable microclimate. Smart textiles are increasingly being integrated into wearable devices and protective systems, playing a key role in personal thermal management. Textiles embedded with microencapsulated PCMs can efficiently regulate temperature by absorbing and releasing latent heat, offering both thermoregulatory and energy-saving benefits. For example, Yu et al. [125] developed a biomimetic strategy to produce corncob-like, superhydrophobic, and phase-changeable nanofibers through one-step electrospinning (Figure 7A). The resulting nanofibrous membranes showed excellent water repellency and hybrid thermoregulatory performance. This makes them promising candidates for the next generation of smart clothing. Wang et al. [126] designed a core–sheath fiber incorporating phase-change microcapsules to capture and store solar energy, thereby mitigating extreme temperature fluctuations on the skin (Figure 7B). This thermoregulating textile shows slow heating and cooling rates, enhancing thermal comfort and providing adaptable solutions for personal temperature control. He et al. [127] developed an elastic, multi-responsive PCM-based fiber via continuous wet spinning for efficient personal health care and thermal management (Figure 7C). This highly elastic fiber, with strong Joule heating and

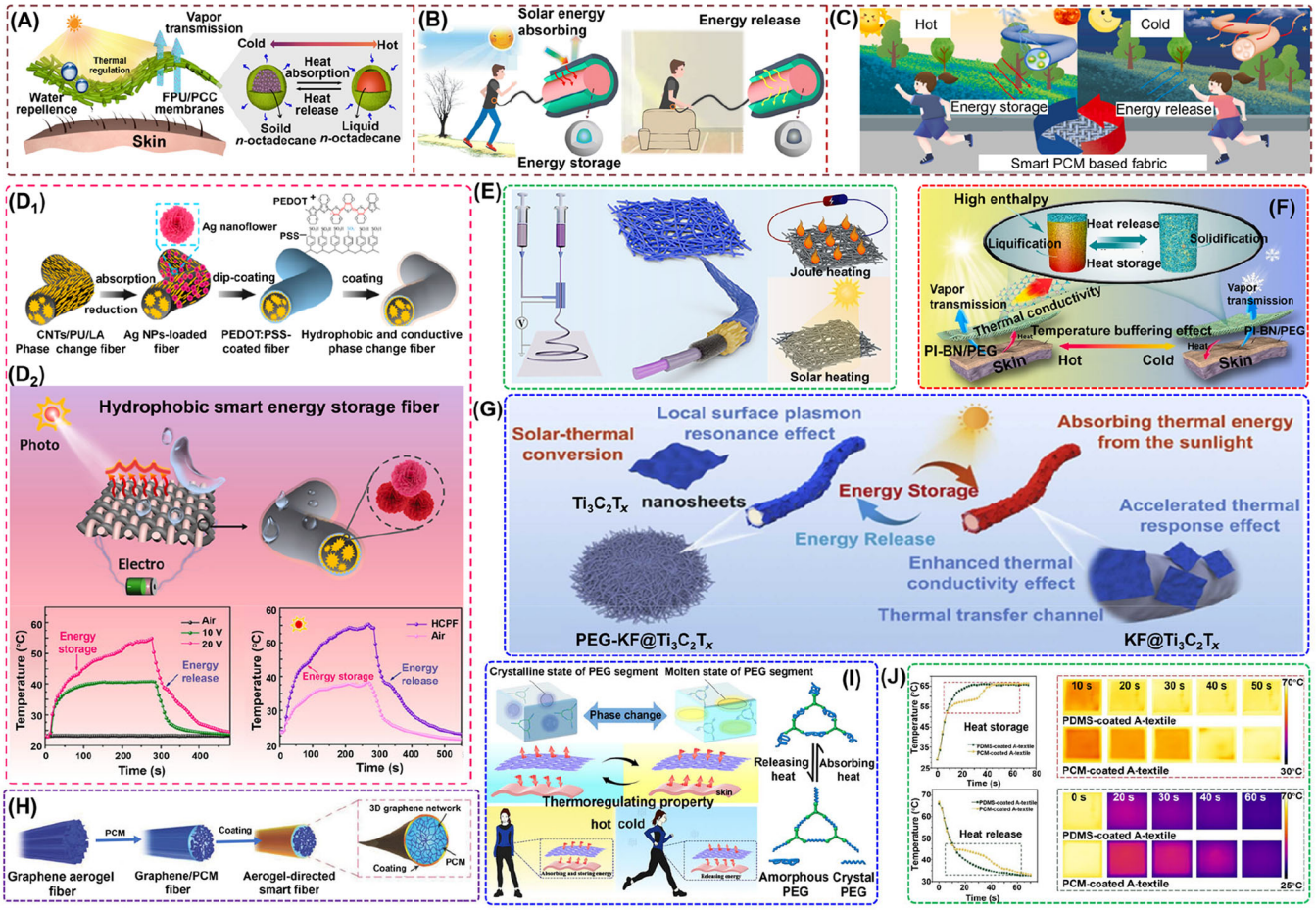

FIGURE 7 | (A) Schematic demonstration of water-repellent, breathable, and thermoregulating performance of FPU/PCC membranes. Reproduced with permission: Copyright 2020, American Chemical Society [125]. (B) Schematic illustration of solar energy conversion and storage in the fibers under sunlight and latent heat release to keep warm without sunlight. Reproduced with permission: Copyright 2019, Royal Society of Chemistry [126]. (C) Temperature regulation schematic of heat storage and release processes in smart CNTs-G-PCM@PU-based fabrics. Reproduced with permission: Copyright 2023, Elsevier [127]. (D_1, D_2) Graphical abstract and schematic description of the processes of hydrophobic conductive phase-change fibers. Reproduced with permission: Copyright 2021, Elsevier [128]. (E) Joule heating and solar heating diagram of a phase-change fiber membrane with flexible core–shell structure. Reproduced with permission: Copyright 2022, American Chemical Society [129]. (F) Schematic illustration of the thermoregulating performance of PI-BN/PEG textile. Reproduced with permission: Copyright 2022, Elsevier [130]. (G) Schematic of solar–thermal conversion and storage mechanism of PEG-KF@$Ti_3C_2T_x$. Reproduced with permission; Copyright 2023, Elsevier [131]. (H) Schematic description of the processes of graphene/PCM smart fibers. Reproduced with permission: Copyright 2018, Wiley [132]. (I) Schematic diagram of the thermoregulating performance of structural colored textiles with high stability and color visibility for intelligent thermoregulating performance and the obtained textiles. Reproduced with permission: Copyright 2023, Elsevier [133]. (J) Temperature curves of the textiles under heating and cooling conditions and the corresponding infrared thermal images. Reproduced with permission: Copyright 2023, Elsevier [134].

photothermal effects, maintains excellent responsiveness even under mechanical deformation, making it ideal for self-powered, personalized thermal management.

2.5.2 | Core–Shell Fiber-Based Encapsulation Technology

In addition to the above-mentioned microcapsule technology, leakage-free and flexible PCM fibers can also be obtained by directly preparing fibers with a core–shell structure. Typically, Niu et al. [128] presented a phase-change fiber (PCF) with tunable phase-change temperature and high energy storage using a novel wet spinning method (Figure $7D_1$). This high-performance PCF integrates conductive nanoflowers, PEDOT:PSS, and fluorocarbon resins with fast electronic and photonic responsiveness for efficient solar thermal energy conversion under sunlight (Figure $7D_2$). By integrating solar and Joule heating, these fibers provide multi-source energy, enabling efficient energy storage, longer life, and broader application scenarios. Herein, Wu et al. [129] reported a fibrous membrane with a core–sheath structure for tri-mode thermal management (Figure 7E). The membrane encapsulates high-enthalpy-density PCM to buffer temperature fluctuations in the clothing microclimate. It achieves a photothermal saturation temperature of 70.5°C and an electrothermal conversion temperature of 73.8°C through a conductive coating. Integrating reversible phase change, multi-source heating, and energy storage, these membranes show significant potential for energy-efficient wearable thermal management. Zhang et al. [130] fabricated PI/BN composite aerogel fibers with high porosity and mechanical strength by freeze

spinning (Figure 7F). This textile is promising for advanced smart clothing applications. Guo et al. [131] successfully developed a form-stable PEG-kapok fiber@$Ti_3C_2T_x$ nanosheet composite, achieving high thermal conductivity and solar–thermal conversion efficiency, as shown in Figure 7G. The strong solar absorption of $Ti_3C_2T_x$ and the composite's black surface enabled efficient thermal conversion, demonstrating the composite's potential for thermal energy management and high solar–thermal conversion. Furthermore, Li et al. [132] developed robust graphene aerogel (GA) composite fibers with tunable thermal conversion and storage capabilities (Figure 7H). Composed of porous GA and an organic PCM coated with hydrophobic fluorocarbon resin, these fibers show a wide range of phase transition enthalpies. When woven into fabrics, these fibers show self-cleaning superhydrophobic surfaces, excellent multi-responsive properties to external stimuli (electronic, photonic, and thermal), and reversible energy storage and conversion.

2.5.3 | Coating Technology

Intelligent textiles with structural color are gaining attention for their potential in advanced photonic applications. A key mechanism to enhance color visibility and thermoregulating performance is essential for advancing these textiles. Herein, Kong et al. [133] developed structural colored textiles with high color visibility and stability, incorporating PCM for intelligent thermoregulation (Figure 7I). These textiles adjust to temperature changes by absorbing and releasing energy around the phase-change temperature, providing effective solutions for personal thermal management. Liang et al. [134] developed multifunctional polymer textiles incorporating silver nanowires (AgNWs) encapsulated within a solid–solid PCM coating using a scalable dip-coating method. The coating was achieved by cross-linking PEG with 3-isocyanatopropyltriethoxysilane, preserving the phase-change behavior while ensuring shape stability. The resulting textiles have high Joule heating efficiency, effective heat storage and release, superior heat dissipation, and infrared anti-counterfeiting capabilities (Figure 7J). These properties make them highly promising for applications in wearable smart clothing, thermal management, and electromagnetic radiation protection.

Coating technology provides a flexible and efficient pathway for the application of microencapsulated PCM, supporting thermal management solutions across various fields. The integration of microencapsulated PCM with coating processes not only enhances their adaptability but also expands their potential applications in diverse scenarios. Typically, Su et al. [135] presented microencapsulated PCMs with four distinct melting temperatures and applied them to flame-resistant fabrics for thermal protective clothing. The PCM layer's bidirectional thermal regulation enhances the comfort of firefighters by reducing the risk of skin burns due to overheating.

2.6 | Brief Summary

In addition to the five important applications mentioned above, PCMs have many other applications, such as solar heat collectors, solar water heaters, and cold chain transportation. However, a significant drawback of organic PCM is their inherent flammability, as they are generally composed of combustible materials. In environments with fluctuating temperatures or potential ignition sources, this flammability poses serious safety risks. For instance, if organic PCMs are used in building materials or electronic devices, they could accelerate fire spread in case of overheating or electrical malfunctions. This fire hazard limits the application scope of organic PCM, especially in sectors where safety standards are stringent. The research content and core aspects of flame-retardant PCMs include flame-retardant characterization techniques, equipment, and methods, as well as flame-retardant strategies and advanced technologies for PCMs. In the following chapters, we will elaborate on these two major modules in sequence.

3 | Characterization Methods for Flame-Retardant PCMs

3.1 | General Pathways

Scientific and standardized flammability testing methods are essential for evaluating the performance of flame-retardant materials. They provide a fundamental basis for the design and optimization of flame retardants, while also serving as a key reference for ensuring the safety of product applications. The most commonly used methods for evaluating flame retardancy are currently the limited oxygen index (LOI), cone calorimetry, and vertical flammability tests. The LOI test measures the minimum oxygen concentration required to sustain combustion, providing a direct indication of a material's intrinsic flammability. Cone calorimetry simulates realistic fire conditions and provides comprehensive data on heat release rate (HRR), total heat release (THR), ignition time, and smoke production. Vertical flammability tests assess flame spread and dripping behavior, which are critical for evaluating fire propagation risks in real-world scenarios. Together, these complementary methods provide a comprehensive framework for characterizing and comparing flame-retardant performance.

3.1.1 | Cone Calorimetry

Cone calorimetry is the most powerful laboratory flammability evaluation tool because it provides quantitative information on the flammability of a material, as illustrated in Figure 8A. The sample is exposed to a constant heat flux (typically 35 kW/m^2 for ISO 5660 and 50 kW/m^2 for ASTM E1354). Typically, using the ASTM E1354-2009 test criteria, each specimen (approximately $100 \times 100 \times 3.0\ mm^3$) was wrapped in aluminized paper within an iron holder. The results accurately predicted the burning characteristics of composites in real-fire scenarios [136]. Various parameters, including the HRR, smoke production, mass loss rate, ignition time, flame extinction time, and total heat of combustion, are monitored during the sample combustion process. In addition, the peak heat release rate (pHRR) can be conveniently obtained, which is one of the most important parameters indicating the ease of combustion and the intensity of the flame [137].

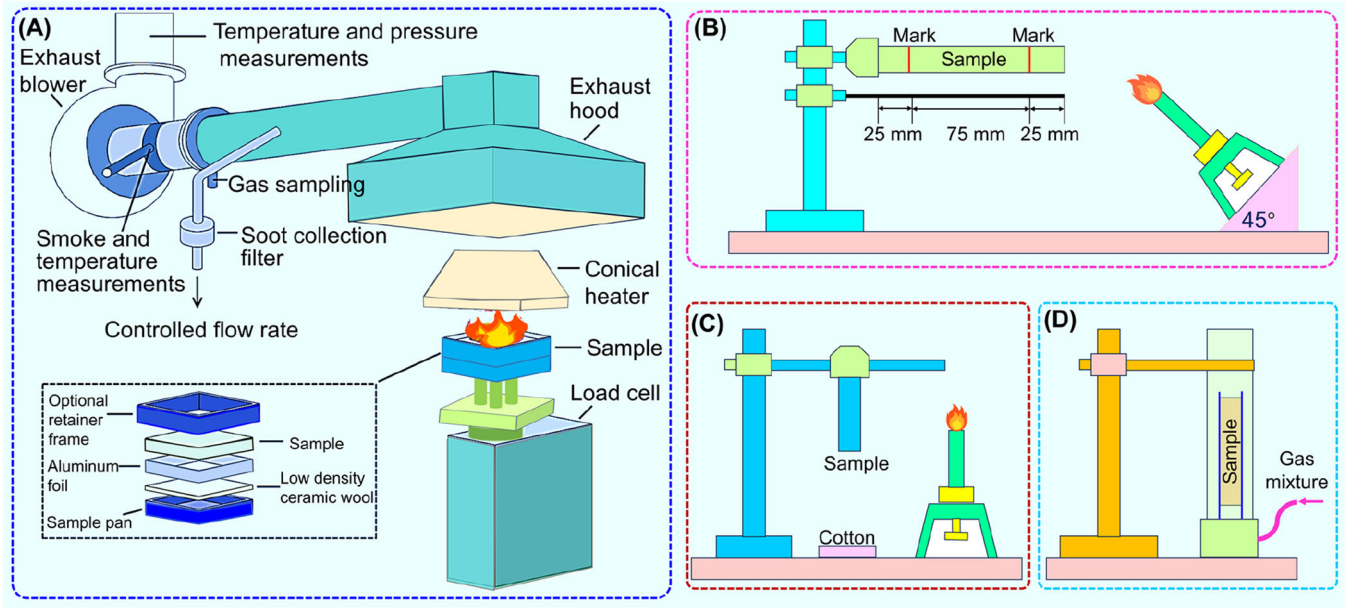

FIGURE 8 | Schematic diagram of (A) a cone calorimeter, (B) a UL-94 horizontal flame, (C) a UL-94 vertical flame, and (D) the limited LOI test.

3.1.2 | Vertical Burning (UL-94) Test

UL-94 testing is performed on both horizontal (Figure 8B) and vertical burn meters. The vertical way is currently widely used for polymeric composites. The specimens are clamped vertically and exposed to an ignition source for 10 s twice, as illustrated in Figure 8C. The flame-retardant effect depends on the time taken for the flame to self-extinguish and whether burning droplets are observed. UL-94 test results are classified as V-0, V-1, V-2, or NR (no rating) burning ratings [138]. The best burning rating is V-0, which requires the sample to self-extinguish within 10 s, and no flame droplets are observed. For example, Zhao et al. [139] fabricated a polymethylsilsesquioxane/cellulose/-MXene composite aerogel with excellent fire resistance, thermal insulation, and hydrophobicity. In the vertical UL-94 tests, whereas the bacterial cellulose sample ignited and burned out within 10 s, PCM-3 self-extinguished within 1 s after 10 s of ignition. Infrared thermal imaging confirmed the rapid temperature drop of PCM-3 once the heat source was removed (Figure 9A). This study expands the potential of biomass-based aerogels in high fire safety applications.

3.1.3 | LOI

The LOI is measured using a high-temperature oxygen index meter in accordance with the ASTM D2836 standard. The dimensions of the samples are $130 \times 6.5 \times 3\ mm^3$ [136]. The LOI represents the minimum oxygen concentration required to support combustion of the material. If the LOI falls below 21 (the atmospheric oxygen concentration), the material will continue to burn after the ignition source has been removed. The test is conducted by igniting a sample in a nitrogen–oxygen mixture within a vertical glass column [139], as illustrated in Figure 8D.

3.2 | Direct Combustion

3.2.1 | Self-Extinguishment Test

Generally, the self-extinguishing performance of flame-retardant PCMs is evaluated using the candle burning test [143]. By designing a candle test to compare the effect of pure PCMs, the flame-retardant self-extinguishing performance of flame-retardant modifiers on PCCs can be further analyzed. Burning time and residual rate are important indicators for evaluating the self-extinguishing properties of materials. Chen et al. [140] designed a candle test to evaluate the self-extinguishing properties of flame-retardant PCMs (Figure 9B). The introduction of flame-retardant additives, particularly phosphorus groups, significantly reduced the burning time of hexadecanol. Phosphorus free radicals and phosphorus acid released during combustion helped to extinguish the flame. In the vertical burning test (Figure 9C), the TPCM composite burned intensely with rapid flame spread, whereas the phosphorus/ammonium-based non-formaldehyde flame-retardant modified wood-stabilized PCM composites (PTPCM-1 and PTPCM-5) self-extinguished quickly, maintaining structural integrity [141].

For another type of non-three-dimensional shape-stable regular sample, a similar method can also be applied. In a combustion test using a homemade candle setup, loose polystyrene and polystyrene microcapsules were placed in separate beakers. Upon ignition of the wick, the candle containing loose polystyrene continued to burn, whereas the candle with polystyrene microcapsules self-extinguished after a few minutes. During the combustion of microencapsulated polystyrene, nitrogen was released, leading to the formation of a char layer on the surface. This char layer acted as a barrier, blocking oxygen and resulting in self-extinguishment [144]. It is worth noting that this mainly applies to new types of PCM working substances, which do not have fixed external dimensions or phase-change shape stability. The typical advantages of this method are its ease of operation and direct test results. However,

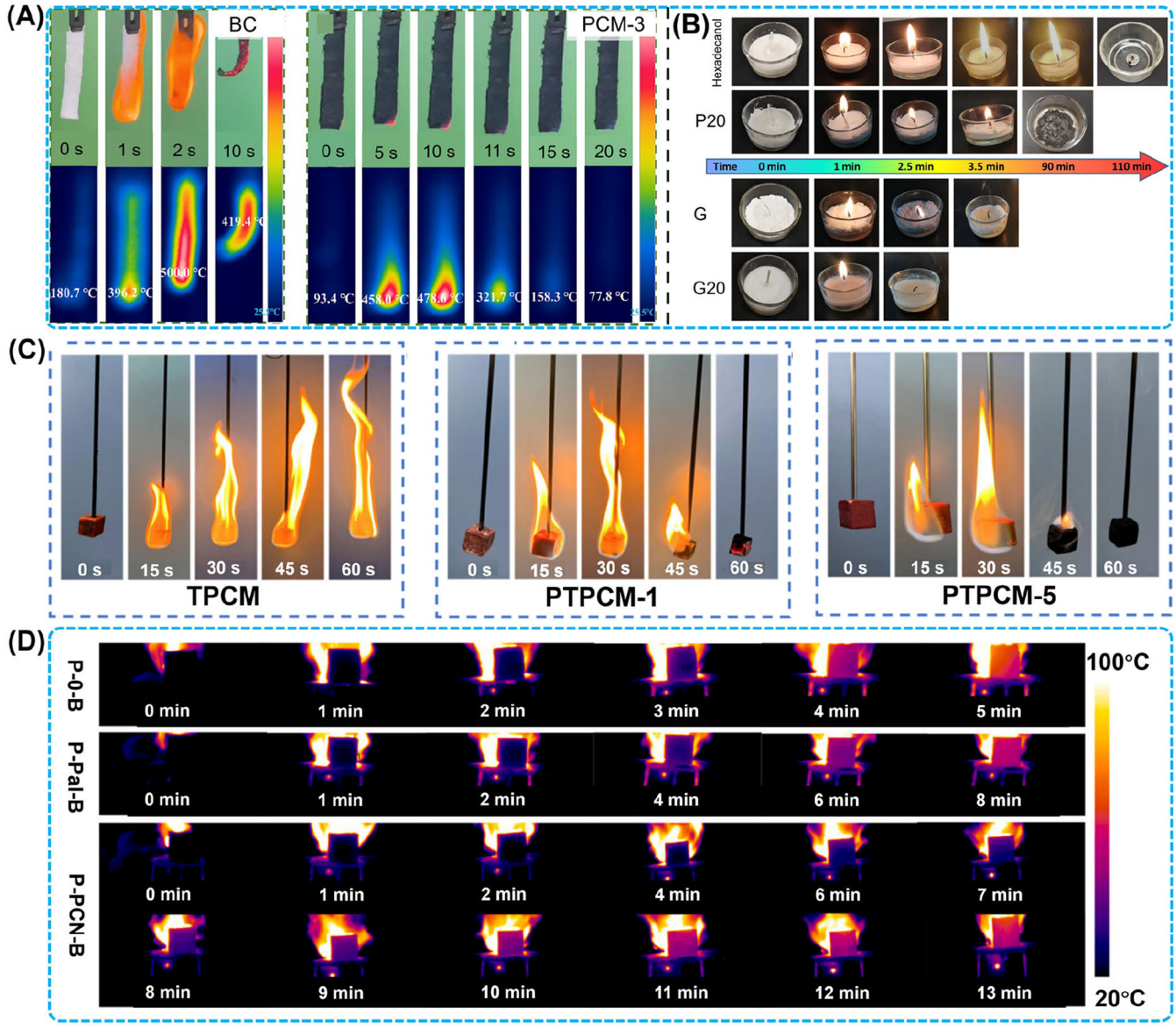

FIGURE 9 | (A) Video snapshots of the UL-94 tests and the corresponding thermographic images of bacterial cellulose and PCM-3. Reproduced with permission: Copyright 2023, Elsevier [139]. (B) Self-extinguishment test of PCM candles. Reproduced with permission: Copyright 2019, Elsevier [140]. (C) Digital photos of the UL-94 test. Reproduced with permission: Copyright 2023, American Chemical Society [141]. (D) Infrared thermography of P-0-B, P-Pal-B, and P-PCN-B during combustion. Reproduced with permission: Copyright 2022, Elsevier [142].

the resulting drawback is that the test results are only a qualitative assessment.

3.2.2 | Direct Combustion Test

The combustibility of pure PEG, MXene@PEG, and MXene@PEG/$Mg(OH)_2$ films was evaluated through combustion experiments [145]. This is somewhat similar to the UL-94 test, except that the test samples are of non-standard dimensions. Combustion tests were carried out using a spirit lamp, with each sample lit for 4 s before being withdrawn from the flame. Pure PEG melted and became liquid after 2 s, indicating low heat stability. In contrast, the MXene@PEG film retained its form near the flame, indicating much increased thermal stability. Finally, the MXene@PEG/$Mg(OH)_2$ film maintained better thermal stability throughout the test, showing that $Mg(OH)_2$ greatly improved the film's flame retardancy.

3.2.3 | Temperature Monitoring

In addition, researchers have also used back temperature monitoring methods to characterize the fire integrity of PCM. To visualize the difference between the real-time temperature of the material and the background temperature, the data are accurately recorded using a thermal infrared imager. The samples were treated with a flame gun combustion while placed on a bracket, and surface temperatures were recorded using infrared thermal imaging. Infrared thermal images of

the Palygorskite-based building materials (P-0-B), PW-palygorskite–based building materials (P-Pal-B), and PW-porous composite microspheres-based building materials (P-PCN-B) during combustion are shown in Figure 9D. The results indicate that PW absorbs heat, delaying temperature rise and providing more time for escape in a fire [142].

4 | Flame-Retardant Strategies for Organic PCM

4.1 | Physical Incorporation of Flame Retardants

4.1.1 | Typical Flame Retardants

Both the original ammonium polyphosphate (APP) and its modified form (f-APP) have demonstrated excellent flame-retardant performance in the modification of PCMs. As a specific example, a fire-safe PCM has been developed by Yin et al. [146] by directly combining APP into poly(glycerol-itaconic acid) (PGI)-loaded PEG (Figure 10A). The results showed that increasing APP content greatly improved flame retardancy, with the LOI increasing from 21.6% to 28.7% at 15 wt% APP. At this level, the material obtained a UL-94 V-0 rating and lowered pHRR by 36.15%.

APP is often used in combination with other charring agents and expandable graphite. For example, (1) *Triazine char-forming agent* (CFA). Flame-retarded PCMs have been created by combining eutectic mixtures of solid and liquid PW with polypropylene, a triazine CFA, and APP, as reported by Li et al. [151]. The PCM received a UL-94 V-0 rating at 30% APP/CFA loading. Furthermore, cone testing revealed a decrease in pHRR, THR, and smoke output, emphasizing the material's outstanding flame retardancy. (2) *EG*. A flame-resistant composite PCM for battery modules was created by Zhang et al. [89] using PW, EG, APP, red phosphorus, and ER (Figure 10B). The composite PCM provided considerable cooling and temperature balancing benefits for battery

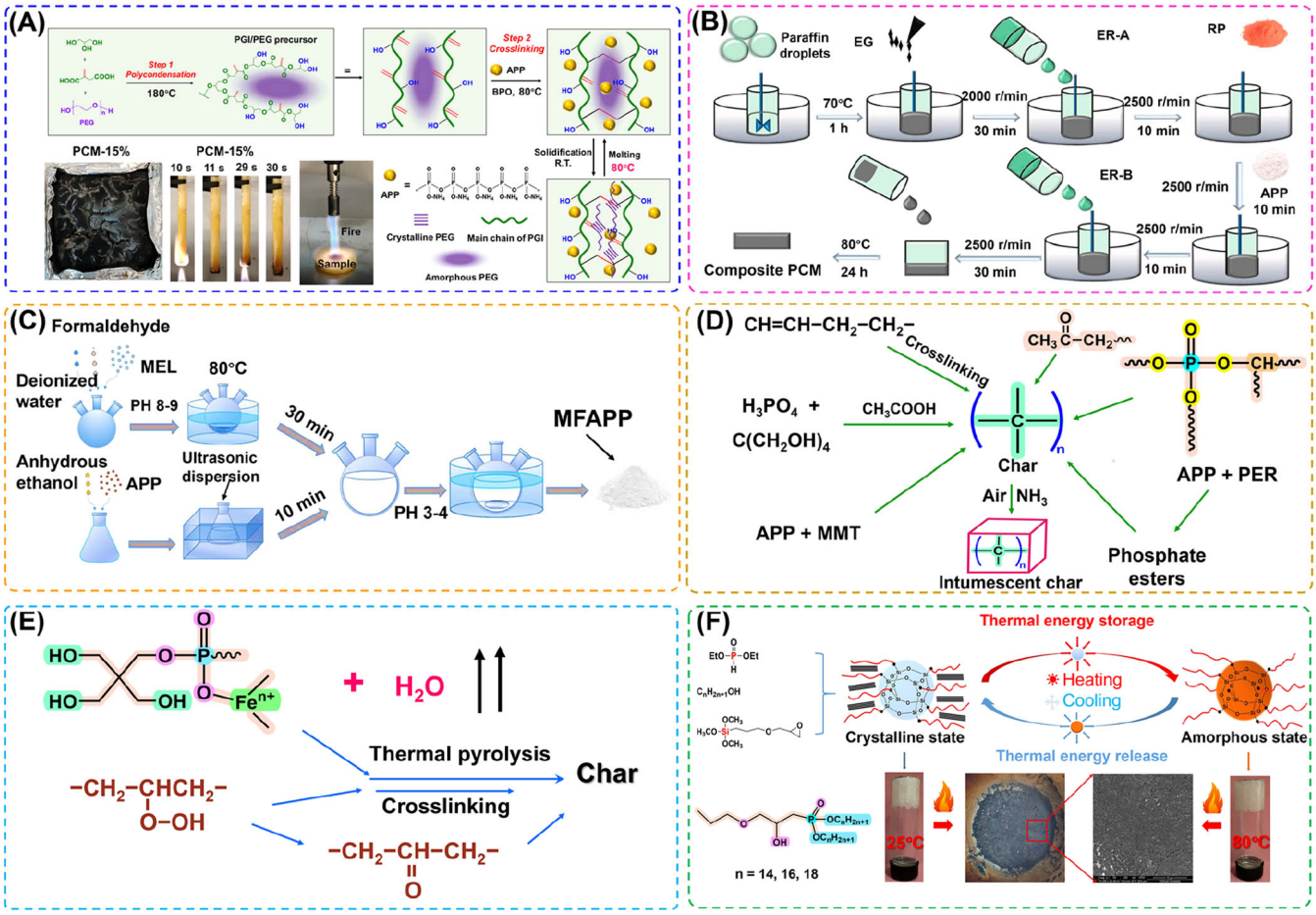

FIGURE 10 | (A) PGI/PEG synthesis by polycondensation, schematic diagram of the precursor with vinyl and hydroxyl groups, cross-linked precursor induced by dibenzoyl peroxide (BPO), and mixing an APP flame retardant at 80°C, and the reversible phase transition illustration and sample (PCM-15%) as a typical example to show the fire resistance. Reproduced with permission: Copyright 2022, Elsevier [146]. (B) Schematic diagram showing the preparation of a flame-retardant composite PCM. Reproduced with permission: Copyright 2020, Elsevier [89]. (C) Preparation of microencapsulated APP. Reproduced with permission: Copyright 2022, Elsevier [147]. (D) Shape-stabilized PCM intumescent formulations. Reproduced with permission: Copyright 2006, Elsevier [148]. (E) Possible reaction mechanisms of char formation during the combustion of the PW/HDPE/IFR system with iron [149]. (F) Schematic of the melting and crystallization mechanism of a novel phosphorus- and silica-containing morphologically stable PCM. Reproduced with permission: Copyright 2018, Elsevier [150]. MEL, melamine; MFAPP, microcapsule-coated ammonium polyphosphate; MMT, montmorillonite; PER, pentaerythritol.

modules, lowering the peak temperature by 44.7% while maintaining a maximum temperature differential of 1.36°C at a 3 C discharge rate at 25°C. In addition, a flame-retardant solid–solid PCM for battery heat control was created by Xu et al. [147], using PEG as the phase-change matrix and *N*,*N*′-methylenebisacrylamide as the crosslinking agent. A flame-retardant material was created by combining microcapsule-coated ammonium polyphosphate (MFAPP), EG, and a carbon source (Figure 10C). The results revealed that the composite with 19% MFAPP had outstanding flame retardancy, having an LOI of 32.6% and passing the V-0 grade vertical combustion test.

In addition to its inherent flame-retardant properties, APP can show a pronounced intumescent flame-retardant effect when combined with other flame retardants in specific systems. Here, we present several representative examples. Shape-stabilized phase-change nanocomposites have been prepared by Cai et al. [148] using a twin screw extruder. These nanocomposites are based on a high-density polyethylene (HDPE)/EVA alloy, organophilic montmorillonite (OMT), PW, and an intumescent flame retardant (IFR). The composition of 60% PW, 15% HDPE-EVA, 5% OMT, and 20% APP-pentaerythritol (PER) showed good flame retardancy (Figure 10D). Zhang et al. [149] created a flame-retardant shape-stabilized PCM (FSPCM) made of PW, HDPE, an IFR (containing APP, PER, and melamine), and iron. The study found that iron could be successfully disseminated in the composite matrix made of HDPE and PW (Figure 10E). Because of iron's strong intrinsic thermal conductivity, the inclusion enhanced the IFR's flame retardancy as well as the thermal conductivity of the FSPCM.

In addition to the commonly used APP, phosphorus-containing flame retardants also include diethyl phosphite. When used in combination with silicon-containing flame retardants, they can also achieve excellent flame-retardant performance. As reported by Jiang et al. [150], the synthesis process involves transesterifying diethyl phosphite with alcohols, followed by ring-opening and hydrolytic condensation with the silane coupler KH-560. The cross-linked silicon network efficiently stopped the leaking of molten higher alcohols. The combination of phosphorus and silica enhanced char formation, which improved thermal stability and fire resistance (Figure 10F).

4.1.2 | Advantages and Disadvantages Analysis

The series of parameters for the flame-retardant PCM research cases reported above are listed in Table 3. The direct incorporation of flame retardants into conventional PCM systems represents the most straightforward and widely adopted strategy for flame-retardant modification. However, achieving effective flame retardancy often necessitates high loading levels, which can markedly reduce the phase-change enthalpy and result in suboptimal thermal efficiency (typically < 70%). This performance degradation is primarily attributed to the diminished proportion of active PCM components, as well as the impurity effect introduced by excessive flame retardants, which can impede PCM crystallization and lower its crystallinity.

We thus believe that blending modification has the following typical advantages: simple modification process, flexible processing form, and the ability to achieve functionality through traditional step-by-step processes. Of course, the addition of exogenous flame retardants has significant shortcomings. Because the introduction of exogenous flame retardants may lead to a decrease in crystallization and reduce the load efficiency of PCM, the enthalpy value of phase transition will also decrease accordingly. The addition of external additives can significantly reduce the core performance of PCM. Therefore, development of efficient flame retardants is central to the preparation technology of flame-retardant PCCs. Additionally, the development of bio-based, environmentally friendly flame retardants is an essential pathway in the field of flame-retardant PCMs and the entire flame-retardant industry.

4.2 | Flame-Retardant Microcapsules

The initial approach to address the flammability of PCMs involved incorporating flame-retardant additives directly into the bulk material. However, the flame-retardant additive reduces the amount of PCMs, decreasing energy storage efficiency, and the flame retardant is not sufficiently dispersed, reducing long-term stability. The development of flame-retardant phase-change microcapsules represents a key area of research in material science, aiming to combine TES and enhanced fire safety. The advancement of microencapsulation technology offers a more effective approach to incorporating flame retardants. By integrating flame-retardant elements such as phosphorus, boron, and nitrogen into the shell materials encapsulating the PCM, this technique imparts flame resistance while preserving the PCM's functionality. It significantly enhances thermal stability, prevents PCM leakage, and achieves higher flame-retardant efficiency compared to methods of directly introducing additive. Below are some specific reports. Kang et al. [152] developed halloysite nanotube (HNT)-doped PCM microcapsules (H-PCM) for ER coatings (H-PCM-EP) to improve temperature control. H-PCM microcapsules, with a distinct core–shell structure, show higher thermostability and thermal conductivity than pure PCM microcapsules. The addition of HNT decreased the melting temperature of capric acid while increasing the latent heat. Flammability studies revealed that adding HNT to PCM microcapsules considerably decreased fire risks in epoxy composites.

4.2.1 | SiO_2 Shell–Based Flame-Retardant Microcapsules

Layered double hydroxide (LDH) has great application potential in the flame-retardant field, and it has attracted considerable attention due to its nontoxicity, high water content, and remarkable smoke reduction effect [153]. Zhang and colleagues [154, 155] created two new flame-resistant phase-change microcapsules to improve temperature control and fire safety in silicone rubber foam (SRF). The first, M-EPCM, has a SiO_2 shell modified with LDH, which improves both thermoregulation (latent heat of 15.4 J/g) and flame retardancy (LOI > 31%, pHRR decrease of 36.4%), as shown in Figure 11A. Flame-retardant mechanisms include barrier effects and catalytic crosslinking. The second design combines PW core capsules with a multilayer shell that includes SiO_2, tannic acid, and

TABLE 3 | Summary of typical parameters of flame-retardant PCM obtained by physical incorporation of flame retardants.

Flame retardant (Contents%)	PCM	Preparation method	ΔH_m (J/g)	Enthalpy efficiency (η)	Thermal conductivity ($W\,m^{-1}\,K^{-1}$)	LOI (%)	UL-94	pHRR reduction (%)	THR reduction (%)	References
MA/TPP (10/15 wt%)	PW	Melt blending	125.7	55.7%	1.39	—	V-0	75.4	19.3	[86]
APP/RP/ER (23/10/25 wt%)	PW	Physical mixing and dispersing	81.2	36.4%	1.05	27.6	V-0	35.9	15.1	[89]
PCN-B (80 wt%)	PW	Calcined + vacuum impregnation	130.2	67.7%	0.53	—	—	—	—	[142]
APP (15 wt%)	PEG	Polycondensation cross-linking	70.1	39.8%	0.38	28.7	V-0	36.1	21.4	[146]
MFAPP (19 wt%)	PEG	Esterification reaction and cross-linking	76.3	56.7%	1.0	32.6	V-0	28.5	41.4	[147]
APP/PER (20 wt%)	PW	Extrusion	88.2	52.8%	—	—	—	—	—	[148]
IFR (20 wt%)	PW	Extruded	79.9	56.0%	—			40.2		[149]
DOP, DHP, DTP	Tetradecanol, hexadecanol, octadecanol	Ring-opening reaction, hydrolytic condensation	81.5, 107.4, 116.9	35.1%, 45.0%, 46.7%	—	—	—	—	—	[150]
APP + CFA (30 wt%)	PW	Blending	126.8	52.9%	—	32.8	V-0	88.6	13.2	[151]

Abbreviations: APP, ammonium polyphosphate; BPO, dibenzoyl peroxide; CFA, char-forming agent; DHP, dihexadecyl phosphite; DOP, dioctadecyl phosphite; DTP, ditetradecyl phosphite; ER, epoxy resin; IFR, containing ammonium polyphosphate, pentaerythritol, and melamine; MA, melamine; MFAPP, microcapsule-coated ammonium polyphosphate; PCN-B, porous composite microsphere-building materials; PW, paraffin wax; RP, red phosphorus; TPP, triphenyl phosphate.

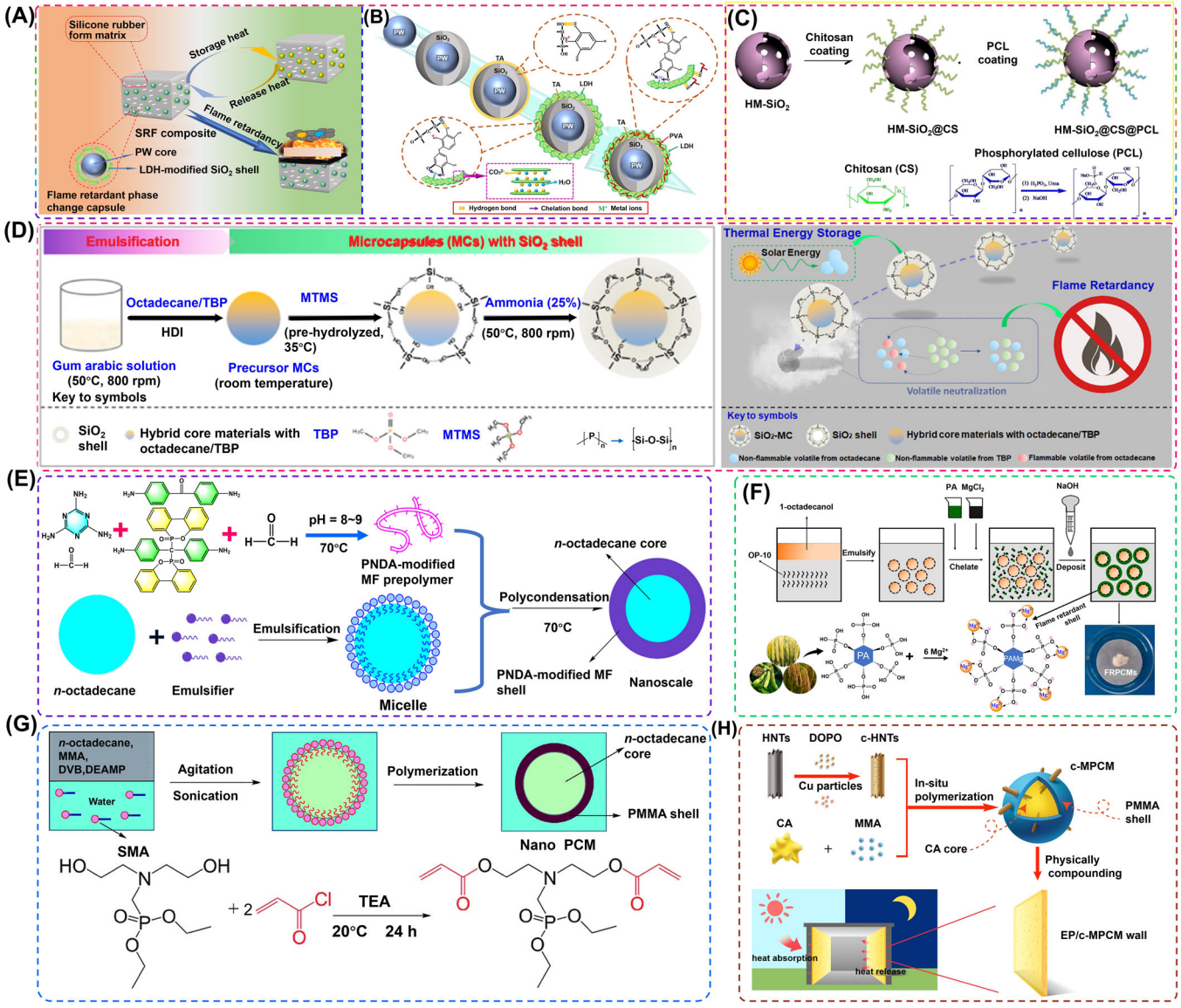

FIGURE 11 | (A) Schematic representation of the thermal management capability and flame-retardant properties of silicone rubber foams filled with flame-retardant phase-change capsules. Reproduced with permission: Copyright 2023, Elsevier [154]. (B) Schematic illustration of preparation of a multilayer shell PCM. Reproduced with permission: Copyright 2022, Elsevier [155]. (C) Synthetic route of hollow mesoporous multilayer-coated silica (HM-SiO_2@CS@PCL). Reproduced with permission: Copyright 2017, Elsevier [156]. (D) Schematic illustration of formation of microcapsules with a silica shell and an octadecane/TBP hybrid core. Reproduced with permission: Copyright 2021, American Chemical Society [157]. (E) Schematic fabrication of NanoC18. Reproduced with permission: Copyright 2018, American Chemical Society [158]. (F) Schematic diagram of the preparation process of flame-retardant PCMs. Reproduced with permission: Copyright 2021, Elsevier [159]. (G) Schematic fabrication of the nano PCM and synthetic route of DEAMP. Reproduced with permission: Copyright 2018, Royal Society of Chemistry [160]. (H) Experimental flowchart of the experiment. Reproduced with permission: Copyright 2023, Elsevier [161]. MC, microcapsule; MTMS, methyltrimethoxysilane; TBP, tributyl phosphate.

LDH layers for increased flame resistance (Figure 11B). The resultant SRF composite obtains UL-94 V-1 certification and self-extinguishes, showing improved fire safety. Jiang et al. [156] created a multifunctional bio-based polyelectrolyte hollow mesoporous multilayer-coated silica (HM-SiO_2@CS@PCL) by layering hollow mesoporous silica, chitosan, and phosphorylated cellulose (Figure 11C). This flame retardant enhanced the thermal properties and fire resistance of ER, with the synergistic effects of P, N, and Si, reducing the pHRR by 51%, highlighting its potential for improved fire safety. In addition, Hu et al. [157] successfully synthesized silica- and poly(urea formaldehyde)-shelled microcapsules using octadecane/tributyl phosphate as hybrid core materials (Figure 11D). This method of encapsulating PCM/flame retardants in an inorganic shell has considerable promise for fire protection in buildings and environmental sustainability.

4.2.2 | Other Polymer-Based Flame-Retardant PCMs

4.2.2.1 | Phosphorus–Nitrogen–Containing Diamine (PNDA) Shell. A flame-retardant *n*-octadecane (nanoC18) with a PNDA-modified melamine–formaldehyde (MF) shell was synthesized by Du et al. [158] via in situ polymerization (Figure 11E). The incorporation of PNDA significantly

increased the LOI value, residual weight, and fire resistance of ER/nanoC18 composites while reducing heat and smoke release. This flame retardant nanoC18 has significant promise for TES in energy-efficient buildings and thermoregulated fabrics.

4.2.2.2 | PMMA + P-Compound. FRPCMs with a 1-octadecane core and a bio-based magnesium phytate (PAMg) shell were successfully synthesized by Liao et al. [159] using a chelation-deposition strategy (Figure 11F). The PAMg shell effectively prevents leakage and enhances flame resistance, increasing the LOI and lowering the THR. The composite shows promise in heat energy storage and thermal management. Du et al. [162] synthesized flame-retardant nano-PCM with *n*-octadecane as the core and PMMA as the shell, using a phosphorus-based flame retardant (DEAMP) as the cross-linking agent (Figure 11G). The incorporation of DEAMP significantly reduced the heat and smoke release while increasing the LOI value and residual weight of the EP/nano-PCM composites. HNTs are widely used as flame-retardant fillers. Kang et al. [161] successfully incorporated 9,10-dihydro-9-oxa-10-phospha-phenanthrene-10-oxide (DOPO) and Cu-doped HNTs (c-HNTs) into MPCM to improve flame retardancy and heat transfer (Figure 11H). The modified c-HNTs reduced pHRR and THR, demonstrating their effectiveness in improving fire safety.

4.2.3 | Microspheres

Interestingly, there are some reports of flame-retardant encapsulation similar to microcapsules in spherical shape. Zhao et al. [163] developed a PW/expanded perlite (P/EP) composite FSPCM with high latent heat storage (174.6 ± 2.20 J/g) and long-term stability. EP acted as a noncombustible shell, effectively inhibiting heat and fire transfer, enhancing the composite's flame retardancy.

We present a summary of some recent reports on flame-retardant PCM parameters (Table 4). Based on the above research reports, it is not difficult to find that microcapsules are typically not used as the final form of PCM. They often require further compounding, processing, and shaping. As listed in Table 4, both enthalpy and enthalpy efficiencies are usually lower than those encapsulated in 3D aerogels [165–169]. In addition, the LOI index is also low, which may be because it is compounded in a polymer matrix. However, it is undeniable that microencapsulation technology has irreplaceable and significant advantages. Specifically, it can be used as a multifunctional filler to realize flame-retardant composite materials with smart fabrics and other thermal regulation functions.

4.3 | Flame-Retardant Support Materials

4.3.1 | Inorganic Aerogels

Aerogels, which are known as potential thermal protective materials, have sparked great research interest due to their high porosity and light weight [170, 171]. Silica aerogels, for example, have been intensively researched as fire-protective

TABLE 4 | Summary of typical parameters of flame-retardant PCMs fabricated by a microcapsule strategy.

Flame retardant	PCM (core)	Shell	ΔH_m (J/g)	Enthalpy efficiency (η)	Thermal conductivity ($W\ m^{-1}\ K^{-1}$)	LOI (%)	pHRR reduction (%)	THR reduction (%)	References
Halloysite nanotube	Capric acid	PMMA	100.8	59.21%	—	—	20.25	—	[152]
Layered double hydroxides	PW	SiO_2	120	—	1.109		—	—	[155]
PNDA	*N*-octadecane	Melamine–formaldehyde	125.9	52.22%	—	25.1	32.8	30.3	[158]
Magnesium phytate	*N*-octadecane	PAMg	118–158.5	53.08%–71.3%	—	19.5–21.6	18.5–25.1	26.31–39.5	[159]
DOPO/Cu-HNTs	Capric acid	PMMA	113.2	80.17%	—	—	30.23	17.77	[161]
DEAMP	*N*-octadecane	PMMA	109.1	45.25%	0.263	25.1	39.68	18.43	[162]
M-CNT	Capric acid	PMMA	90.3	63.93%	—	—	43.24	16.57	[164]

Abbreviations: DEAMP, diethyl bis (2-hydroxyethyl acrylate) aminomethylphosphonate; DOPO/Cu-HNTs, 9,10-dihydro-9-oxa-10-phosphaphenanthrene-10-oxide/Cu-halloysite nanotubes; M-CNT, 4,4′ – methylene diphenyl diisocyanate (MDI)-grafted carbon nanotube; PNDA, phosphorus–nitrogen–containing diamine.

clothing coverings due to their ultra-low heat conductivity and intrinsic non-flammability. Niu et al. [172] developed a low-thermal-conductivity flame-retardant PCC to mitigate thermal runaway propagation in battery modules. The flame-retardant coating enables the material to achieve a V-0 rating in the UL-94 test and an LOI of 56.31%, together with effective thermal insulation at 700°C.

4.3.1.1 | EG-Based PCM. EG is widely used as a porous inorganic material for PCM encapsulation due to its superior adsorption capacity. Its high thermal conductivity, surface compatibility, fire resistance, non-toxicity, and chemical stability make it an ideal candidate for PCM retention. Wang et al. [173] developed a cost-effective thermal management material for LiBs by stabilizing a hydrated salt–PW composite (HPC) in porous EG (Figure 12A). The HPC@EG composite showed excellent shape stability and improved thermal conductivity, and the intrinsic fire resistance of the hydrated salt and EG further enhanced its safety performance. Alkhazaleh et al. [177] developed a leakage-free thermal storage composite by incorporating an 80/20 butyl stearate/isopropyl palmitate eutectic PCM into EG. With 10% of this composite integrated into a cemented test room's south wall, flammability analysis confirmed its potential for enhancing indoor thermal regulation and reducing building energy consumption. Wang et al. [178] developed a flame-retardant PCM with enhanced thermal performance by incorporating MXene to improve enthalpy and conductivity, and the synergistic effect of APP and zinc hydroxy stannate increased the carbon residue, achieving a V-0 flame-retardant rating.

4.3.1.2 | Graphene Porous Materials-Based PCM. Inspired by the intricate structural synergy in hydrocotyle vulgaris, Zhu et al. [174] designed a plant leaf mimetic network using a laser-induced graphene method to encapsulate PCM (Figure 12B). The structured 3D porous graphene enabled efficient heat transfer and self-extinguishing behavior, highlighting its potential for solar energy harvesting and thermal management.

4.3.1.3 | MXene-Supported PC. Composite PCMs with a 3D porous biomass aerogel matrix were synthesized by Huang et al. [175], where Ag/MXene enhanced conductivity and structural stability, enabling efficient energy conversion and promising flame-retardant potential (Figure 12C). Luo et al. [179] synthesized flame-retardant PCMs by incorporating phosphorus-modified stearyl alcohol into an MXene framework. Increasing the MXene content significantly reduced the pHRR and THR, highlighting its low flammability and potential for TES. Liang et al. [180] developed 3D MXene/wood-derived porous carbon aerogels with excellent electrical conductivity,

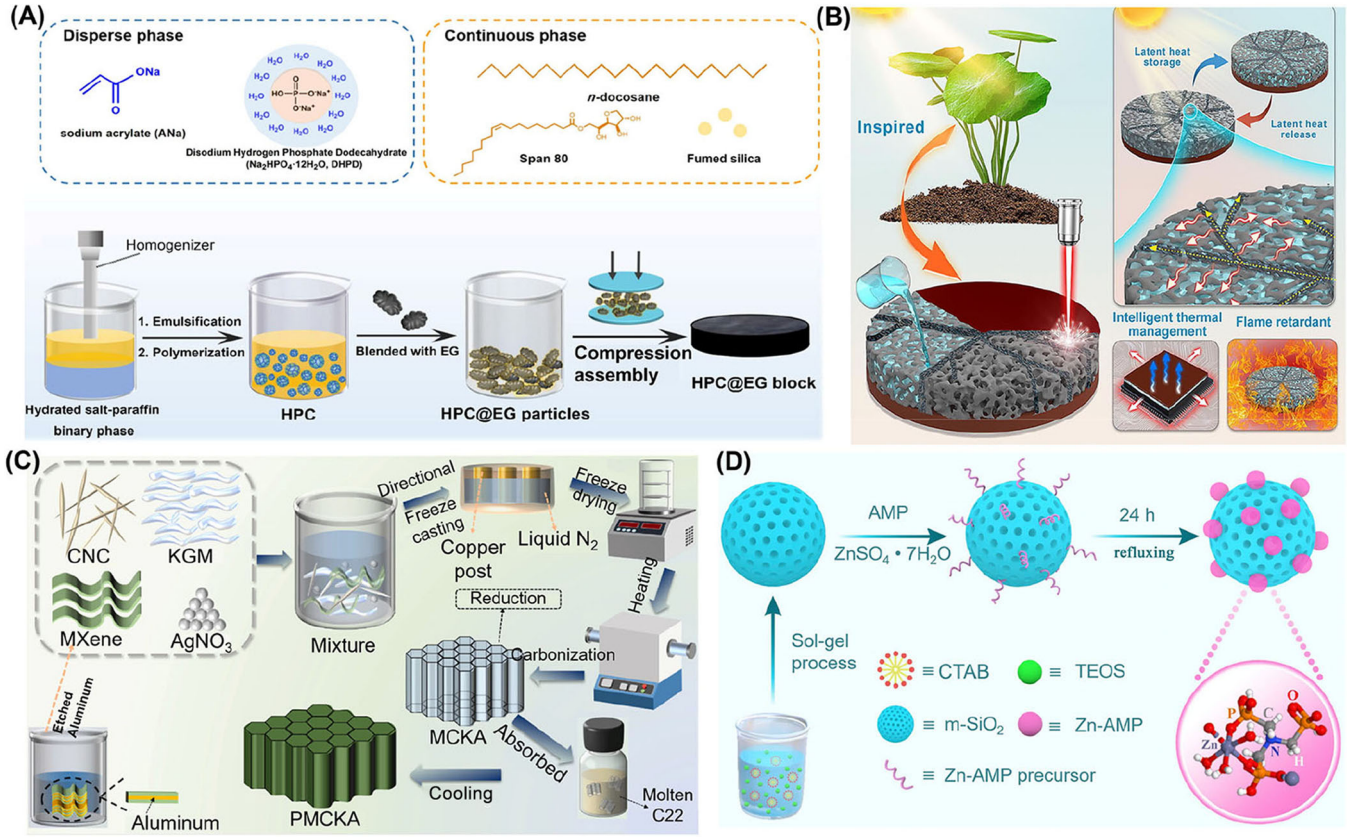

FIGURE 12 | (A) Components of the disperse and continuous phases in a HPC and schematic illustration of the preparation process of HPC@EG. Reproduced with permission: Copyright 2021, Elsevier [173]. (B) Schematic design of a layered energy transfer pathway for PCC of laser-induced graphene. Reproduced with permission: Copyright 2023, Elsevier [174]. (C) Schematic diagram of composite PCM synthesis. Reproduced with permission: Copyright 2022, Elsevier [175]. (D) Synthetic route of mesoporous silica and nano Zn-AMP. Reproduced with permission: Copyright 2020, Elsevier [176]. AMP, amino-tris-(methylenephosphonate); CTAB, cetyltrimethylammonium bromide; KGM, konjac glucomannan; MCKA, MXene/CNC/KGM/Ag; TEOS, cetyltrimethylammonium bromide.

lightweight structure, and enhanced flame retardancy. The MXene aerogel/WPC composites showed superior compressive strength, thermal insulation, and flame-retardant properties, making them effective as PCM substrates.

4.3.1.4 | SiO_2 Aerogels-Based PCMs. Silica is widely used in microencapsulation technology, and the relevant aerogel can also serve extensively as a supporting material for PCM. For example, Fang et al. [181] developed flame-retardant *n*-hexadecane/SiO_2 composites where SiO_2 improved thermal stability and fire resistance (Figure 12D). The addition of EG increased the char residue, improving thermal stability and flammability by forming a continuous, compact residue after combustion. Zhu et al. [176] synthesized mesoporous silica@nano-zinc amino-tris-(methylene phosphonate) spheres, enhancing flame retardancy, smoke suppression, and mechanical properties of ER. The Si, P, N, and Zn components promoted compact char formation and the release of inert substances during combustion.

4.3.1.5 | BN Aerogels-Based PCM. Zhou et al. [182] prepared BN aerogels by self-assembly, lyophilization, and heat treatment. The resulting BN/PEG PCM showed excellent phase-change enthalpy, shape stability, and high thermal conductivity, improving TES and heat dissipation, especially for electronic applications requiring electrical insulation. Pan et al. [183] reported an epoxy-based composite with a 3D carbonized cellulose/boric acid-modified boron nitride aerogel (CCA/m-BN) network, which demonstrated superior flame retardancy by significantly reducing the THR and smoke production. This CCA/m-BN/EP composite, with high thermal conductivity and excellent flame retardancy, shows great potential as a next-generation thermal management material for electronics. We present a summary of the thermal behavioral parameters of inorganic porous support material–based flame-retardant PCMs (Table 5).

4.3.2 | Polymer-Based Support Materials

4.3.2.1 | Polymeric Porous Support Materials. Recently, flame-retardant PI fabrics have been developed through co-polymerization or surface treatment with agents like phosphoric acid [189]. Although PI fabrics offer superior flame resistance compared to most polymers, their fire resistance remains limited. To enhance fire safety, inorganic flame retardants such as graphene oxide [190], CNTs [191], montmorillonite [192], and hydroxyapatite [193] have been incorporated into the polymer matrix.

4.3.2.1.1 | PI aerogel + BN. A form-stable, flame-retardant PCC was developed by Shen et al. [194] using lignin-modified boron nitride (LBN) and PI aerogels with PEG (Figure 13A). The composite showed improved thermal conductivity, enhanced latent heat, and significantly better flame retardancy, with a 23.3% reduction in the pHRR and a 17.3% reduction in the THR compared to pure PEG. In addition, Zhang et al. [195] developed a double-layer smart textile with a flame-retardant outer layer and a phase-changeable inner layer (Figure 13B). This fabric composite extended the pain threshold time to 280.0 s, far outperforming commercial aramid and fiberglass fabrics, thereby demonstrating considerable potential for advanced firefighting protective clothing.

4.3.2.1.2 | PI Aerogel + MXene. MXene/PI@PEG PCCs with high heat storage density, excellent flame retardancy, and good solar thermal conversion were synthesized [184]. The combination of MXene nanosheets and PI reduced the HRR and the THR while increasing the carbon yield, which significantly improved the flame retardancy of the composite.

4.3.2.1.3 | Polyvinyl Alcohol (PVA) Aerogel and MF. Furthermore, Yin et al. [196] designed a coral-like organic–inorganic graphene-modified PVA aerogel (GP) that can host PEG, resulting in PEG-GP with improved flame retardancy and solar-responsive heat storage (Figure 13C). The PEG-GP composite demonstrated a 37.5% reduction in the pHRR and a 25% decrease in the overall heat emission, indicating enhanced fire safety. Hu et al. [200] developed an APP/PEG@PVA-modified melamine foam (PMF) composite by combining IFRs with PMF, yielding a 22.6% oxygen index and increased fire safety. Tian et al. [197] created an ionic liquid crystal (ILC)–armored BNNS/PVA aerogel film with excellent flame retardancy and a maximum HRR of 44.5 kW/m^2 (Figure 13D). The ILC-BNNS enhanced both fire resistance and thermal conductivity, demonstrating the potential for use in thermal interface materials in electronics. Furthermore, Liao et al. [185] used a lightweight, mechanically robust GA within commercial MF (c-GA/MF) to encapsulate PEG (Figure 13E). This c-GA/MF/PEG showed light energy harvesting, TES, and thermal control potential for buildings, as well as improved fire safety.

4.3.2.2 | Polymer Blend–Based PCMs. The flame retardancy of shape-stabilized PCMs based on PW/polymer matrix/organically modified montmorillonite has been improved by using surface coatings, such as acrylic resin/EG, alkyd resin/EG, and ER/EG, as reported by Xu et al. [187]. These coatings dramatically enhanced flame resistance, attaining UL-94 V-0 with reduced smoke output. Huang et al. [198] prepared a flame-resistant, flexible composite PCM for battery heat control. The composite, which contained 15 wt.% flame retardants, performed optimally, with an LOI of 35.9%. This material successfully reduced heat buildup and increased thermal stability during battery operation, as demonstrated by infrared thermal imaging under thermal circumstances (Figure 13F). Ge et al. [199] designed a PW/CNT/BN/silicone gel composite (PCBS4) with superior features such as anti-leakage, mechanical flexibility, re-ignition resistance, and waterproofing (Figure 13G). The combination of PCM with silicone gel improves thermal performance and stability. Similarly, Gao et al. [186] developed a flexible, flame-retardant PCM composite (CPCM) comprising PW, an olefin block copolymer, and MXene that has good thermal stability and flame retardancy. The addition of MXene allows the CPCM to self-extinguish after 12 s. Zheng et al. [201] developed a form-stable PCM (FSPCM) from phosphorus-modified hexadecanol, PEPA, and PER, which has excellent heat storage and flame-retardant properties. FSPCM (P3) with 9% PEPA and 3% PER achieved an LOI of 29.5% and a UL-94 V-0 certification. Liu et al. created a scaffold–PCM crosslinking approach to address

TABLE 5 | Summary of thermal behavioral parameters of inorganic porous support material–based flame-retardant PCMs.

Support materials/ Complex	PCM work substance	PCM fabrication	ΔH_m (J/g)	Thermal conductivity ($W\ m^{-1}\ K^{-1}$)	Self-extinguishing test	LOI (%)/pHRR reduction (%)	UL-94	References
EG	Hydrated salt/PW	Physical blending	177.0	4.35	No open fire	—	—	[173]
GO/polybenzoxazine resin	PEG	Infusion	162.3	1.18	Self-extinguishing	—	—	[174]
CNC/Ag/MXene	PW	Thermal annealing	231.4	0.48	—	—	—	[175]
Silica aerogel	PW	Pressed and molded	79.3	0.23	Self-extinguishing	LOI: 56.31%	V-0	[172]
EG/MXene	PEG	Melt-blended		1.44	Self-extinguishing	—	V-0	[178]
MXene skeleton	Stearyl alcohol	Vacuum impregnation	120.1	0.49	Self-extinguishing	pHRR: 42.8% THR: 32.1%	—	[179]
MXene/polyimide	PEG	Vacuum impregnation	167.9	—	—	pHRR: 26.1% THR: 11.6%	—	[184]
SiO_2/EG	*N*-hexadecane	Sol-gel methods	147.6	—	Self-extinguishing	—	—	[181]
MF/GO	PEG	Immersing	167.6	1.32	—	—	—	[185]
Olefin block copolymer/ MXene	PW	Blended	168.8	0.62	Self-extinguishing			[186]
EG	PW	Melt-blended	—	—	Self-extinguishing	LOI: 30%	V-0	[187]
Polyurethane/EG	PEG	Melt-blended	95.8	1.3	—	pHRR: 29%	—	[188]

inadequate charring in organic PCM, resulting in a composite with high heat storage density, 13.1% char residue, and a low pHRR (231 W/g). Zhang et al. [202] developed flame-retardant PCCs by combining MXene@PTA with phytic acid dicyandiamide in a waterborne polyurethane matrix. This lowered the pHRR and the THR by 6.7%–35.8% and 13.2%–19%, respectively, resulting in a synergistic flame-retardant effect.

We present a summary of the thermal and flame-retardant performance from recent reports on flame-retardant PCM parameters (Table 6). Using aerogels as supporting materials is an effective method for preparing high-enthalpy PCMs, as presented. However, aerogels prepared by freeze-drying are almost entirely open porous, making it challenging to achieve complete leakage-proof performance.

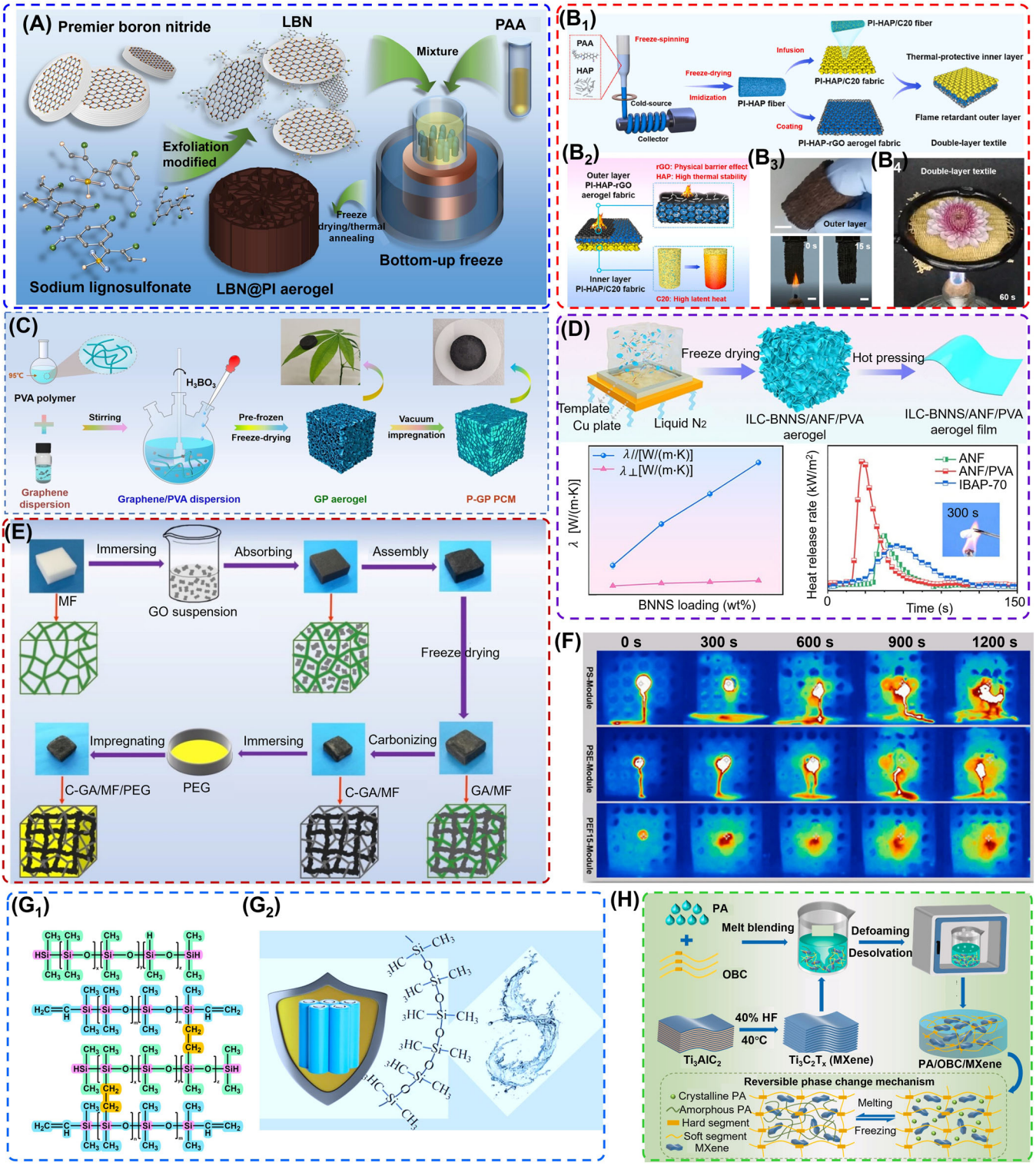

FIGURE 13 | Legend on next page.

4.3.3 | Natural Macromolecule or Wood-Based Porous Materials

4.3.3.1 | SA-Based Aerogel. A double-crosslinked network structure in an SA composite with Al_2O_3 fibers was designed by Xu et al. [203], utilizing Ca^{2+} to induce sol–gel transition and enhance flame retardancy. The Al_2O_3 fiber/SA aerogels showed outstanding flame retardancy, self-extinguishing capabilities, and minimal smoke release (pHRR of 9.7 kW/m^2). Yang et al. [204] developed a bio-based guanosine/boric acid/sodium alginate (GBS) aerogel using guanosine, boric acid, and SA, obtaining exceptional flame retardancy with an oxygen index of 47.0%–51.1% and a V-0 rating while minimizing heat and smoke output.

4.3.3.2 | Wood-Based Support Materials. Wood is a renewable, porous material with a distinct hierarchical structure, excellent mechanical strength, and cheap cost [205]. Delignified wood (DW), following lignin and hemicellulose removal, provides excellent support for *n*-alkane encapsulation. N-alkanes are popular PCMs because of their excellent energy storage, chemical stability, and appropriate working temperature [206]. However, leakage during phase transition limits their ability to store thermal energy efficiently. Recent research has focused on encapsulating *n*-alkanes in wood to overcome this problem.

A shape-stabilized composite PCM was synthesized by Yuan et al. [207] by soaking DW decorated with phytic acid and dopamine in *n*-eicosane. Flame retardancy is enhanced by lowering pHRR from 467.6 to 350.2 W/g and THR from 26.4 to 19.8 kJ/g (Figure 14A). Yue et al. [208] prepared shape-stabilized PCM composites by injecting molten *n*-docosane into phytic acid-modified, zinc oxide-deposited, and surface-carbonized DW. The addition of phytic acid considerably increased flame retardancy, demonstrating their potential for effective thermal storage and fire safety applications (Figure 14B$_1$,B$_2$). Wang et al. [141] synthesized a phosphorus/ammonium-based non-formaldehyde flame retardant (APA) from phytic acid and utilized it to make wood-based form-stable PCM composites. Increasing APA concentration decreased pHRR and THR, improving flame resistance while retaining thermochromic performance following thermal cycling (Figure 14C$_1$,C$_2$).

Finally, we summarize the thermal and flame-retardant properties in the relevant flame-retardant support material or PCM reported in the list in this section (see Table 7). Wood, as a renewable natural material, is rich in cellulose and other polyhydroxy natural macromolecules. Through extensive research, we have observed that phytic acid is widely used for flame-retardant modification of wood-based supporting materials. Depending on the method of treating wood with phytic acid, different phase-change latent heats can be achieved. Typically, for shape-stabilized PCMs supported by materials such as DW, the enthalpy can exceed 160 J/g.

4.3.4 | Advantages and Disadvantages Analysis

The usual flame-retardant strategy is to obtain a multifunctional (such as high thermal conductivity, flame retardancy, and digital shape design) high-performance flame-retardant aerogel by incorporation flame retardants, and then use the flame-retardant porous material as the supporting material of PCM work substances. The aerogel encapsulation pathway has the following typical technical advantages: (1) carried out in separate steps, (2) easy to achieve multifunctions, and (3) high porosity with high PCM loading, thereby ensuring high latent heat. Its typical disadvantage is that many aerogels are expensive, and almost all aerogels are perforated (to ensure convenient adsorption of PCM) and have open pores, so it is difficult to make it completely leakage-free. Moreover, it is challenging to achieve a perfect balance between high PCM loading and high flame retardancy. This is because higher PCM loading often results in a reduced proportion of flame-retardant fillers.

4.4 | Intrinsic Fire-Safety Enhancement

Traditional flame retardancy strategies often rely on physical encapsulation or additive-based approaches, which can result in phase separation and reduced thermal reliability. In contrast, an intrinsically fire-safe design approach, which involves chemically integrating flame-retardant elements or functional groups into the molecular structure of PCM substances, offers a more stable and effective solution by fundamentally altering the material's combustion behavior. This strategy can be implemented in two ways: (1) chemical modification of PCM molecules to introduce flame-retardant functional groups (e.g., phosphorus-, nitrogen-, or silicon-containing moieties) and (2) chain extension or polymerization of typical PCM molecules, such as PEG, to form high-molecular-weight polymers with integrated thermal and flame-retardant properties. These molecular engineering approaches enhance fire resistance by reducing heat release, promoting char formation, and

FIGURE 13 | (A) Preparation of LBN and LBN@PI aerogels. Reproduced with permission: Copyright 2022, Elsevier [194]. (B$_1$) Schematic illustration of fabrication of double-layer textile comprising of PI-hydroxyapatite–reduced graphene oxide (PI-HAP-rGO) aerogel fabric and PI-HAP/eicosane (C20) fabric. (B$_2$) Schematic illustration of the function of double-layer textile. (B$_3$) Photographs of a PI-HAP-rGO aerogel fabric before and after ignition for 15 s. (B$_4$) Photographs of the double-layer textile supporting a flower on an alcohol lamp. Reproduced with permission: Copyright 2022, Elsevier [195]. (C) Schematic diagram for the preparation of PEG-PVA aerogel (P-GP) nanocomposites. Reproduced with permission: Copyright 2023, American Chemical Society [196]. (D) Schematic diagram of the preparation of an ILC-BNNS/aramid nanofiber/PVA aerogel film. Reproduced with permission: Copyright 2023, American Chemical Society [197]. (E) Fabrication process of carbonized–GA/melamine foam (MF)/PEG. Reproduced with permission: Copyright 2020, Elsevier [185]. (F) Infrared thermal imaging cloud images of PS-Module, PSE-Module, and PEF15-Module at the center region. Reproduced with permission: Copyright 2021, Elsevier [198]. (G$_1$) Molecular formula of silica gel and (G$_2$) schematic diagram of waterproof of PCBS4. Reproduced with permission: Copyright 2022, Elsevier [199]. (H) Schematic diagram of the fabrication of a PW/olefin block copolymer (OBC)/MXene composite PCM. Reproduced with permission: Copyright 2023, Elsevier [186].

TABLE 6 | Summary of the thermal and flame-retardant performance of polymeric supporter–encapsulated PCMs.

Support material	PCM work substance	PCM fabrication	ΔH_m (J/g)	Thermal conductivity ($W\,m^{-1}\,K^{-1}$)	UL94	pHRR reduction %	THR reduction %	References
ILC-BNNS	PW	Vacuum impregnation	—	17.7	—	21.0	27.3	[197]
LBN/PI aerogel	PEG	Vacuum impregnation	157.02	0.3286	—	23.3	17.3	[194]
PI-HAP-rGO aerogel fabric	Eicosane	Infusion	193.2	—	V-0	70.0	58.8	[195]
Graphene-modified PVA aerogel	PEG	Vacuum impregnation	164.2	0.7545	—	37.5	25	[196]
Styrene-butadiene-styrene/EG	PW	Vacuum impregnation	120	1.1	V-0	73.1	47.5	[198]
CNT/BN/silicone gel	PW	Vacuum impregnation	55.17	0.72	Self-extinguishing	—	—	[199]
PVA/MF	PEG	Vacuum impregnation	160	0.13	V-0	—	—	[200]
HDPE/SBS	Hexadecanol	Melt blending	122.5	—	V-0	81.0	—	[201]
Waterborne polyurethane	PEG	Vacuum impregnation	121.1	—	—	35.8	19	[202]

Abbreviations: CNT/BN, carbon nanotube/boron nitride; HDPE/SBS, high-density polyethylene/poly (styrene-butadiene-styrene); ILC-BNNS, ionic liquid crystal/boron nitride nanosheets; LBN/PI, lignin-modified boron nitride/polyimide; PI-HAP-rGO, polyimide-hydroxyapatite-reduced graphene oxide; PVA/MF, polyvinyl alcohol/melamine foam.

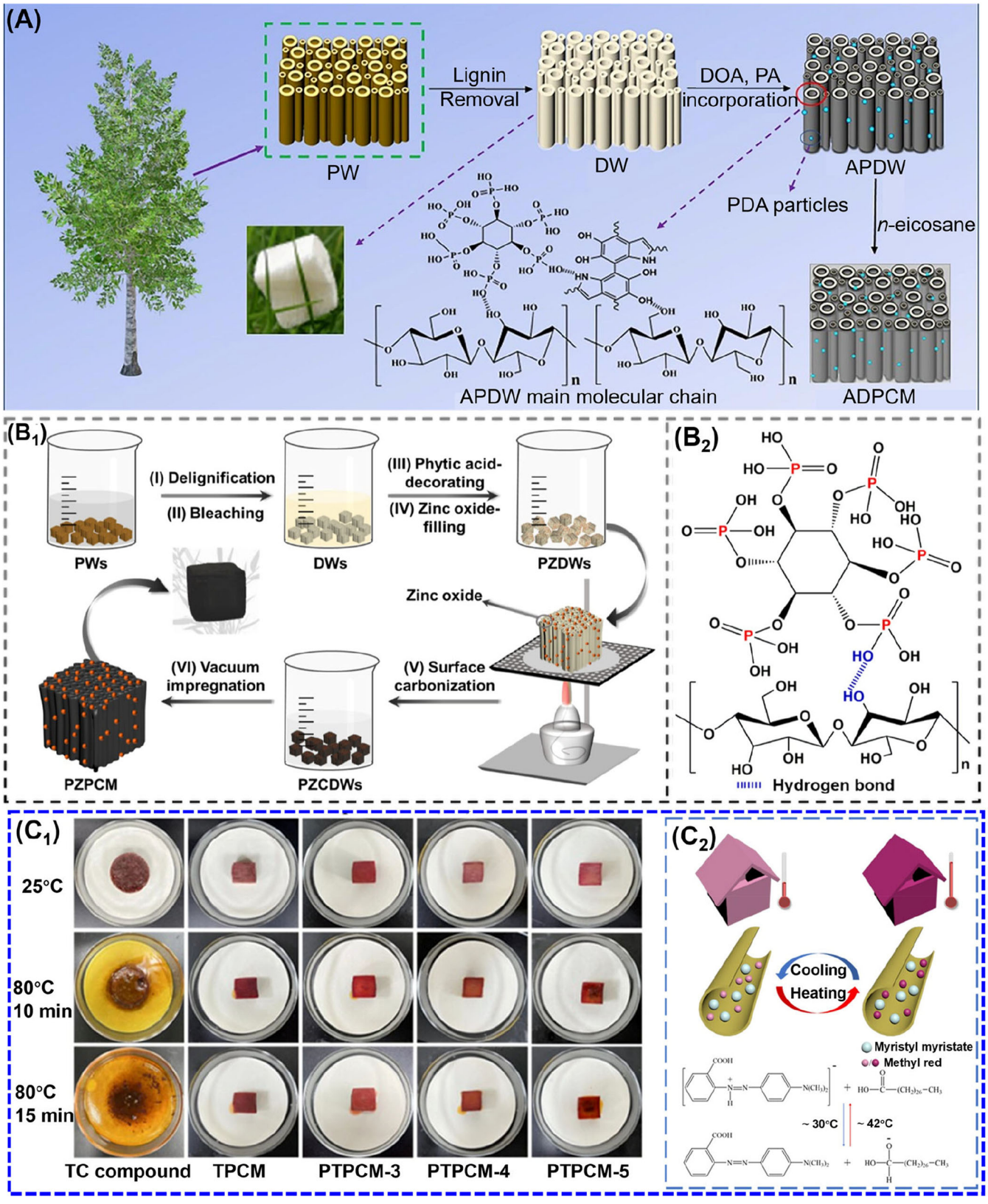

FIGURE 14 | (A) Schematic description of the formation of novel form-stable pristine wood, dopamine-decorated DW, phytic acid/dopamine-decorated DW (APDW), and flame-retardant phase-change composites (ADPCM). Reproduced with permission: Copyright 2022, Elsevier [207]. (B_1) Schematic representation of synthetic phytic acid–modified, zinc oxide–deposited, and surface-carbonized DW PCM composite (PZPCM). (B_2) Main molecular chain of phytic acid-modified DW. Reproduced with permission: Copyright 2023, American Chemical Society [208]. (C_1) Leakage resistance test of the thermochromic compound (TC), TPCM, PTPCM-3, PTPCM-4, and PTPCM-5. (C_2) Thermochromic mechanism of the TC compound. Reproduced with permission: Copyright 2023, American Chemical Society [141].

TABLE 7 | Summary of thermal and flame-retardant performance of wood-based support material fire-safe PCMs.

Support material	PCM type	PCM fabrication	ΔH_m (J/g)	Thermal conductivity (W m^{-1} K^{-1})	pHRR reduction %	THR reduction %	References
APDW	*N*-eicosane	Impregnation	205.2	—	11.6	13.3	[207]
RDP/EP/EG	Lauric acid	Blending	86.02–88.29	0.17	68.6	64.24	[209]
APA-grafted DWs	Myristyl myristate	Vacuum impregnation	165.3	—	6.7	28.5	[141]
PZCDWs	*N*-docosane	Impregnation	185.2	1.200	48.12	15.99	[208]

Abbreviations: APA-grafted DWs, phosphorus–nitrogen–containing intumescent flame retardant–grafted delignified woods; APDW, phytic acid/dopamine-decorated delignified wood; CS/$AlCl_3$/PVA, chitosan/aluminum chloride/polyvinyl alcohol; CS-MA/PA, chitosan-melamine/phytic acid; GBS, guanosine/boric acid/sodium alginate; HANRs/SAB, hydroxyapatite nanorods/sodium alginate/boric acid; PZCDWs, phytic acid–modified, ZnO-deposited, and surface-carbonized delignified woods; RDP/EP/EG, resorcinol bis(diphenyl phosphate)/expanded perlite/EG; SAA, Al_2O_3 fiber/sodium alginate.

suppressing flame propagation without relying solely on external additives.

4.4.1 | Molecular Engineering of PCM Work Substance

In the aforementioned studies, researchers have utilized various techniques to encapsulate materials, including aerogel encapsulation and polymer blending. Fundamentally, these approaches rely on physical methods to support or integrate PCM. Additionally, some studies have reported that chemical methods, such as bonding flame-retardant elements like phosphorus and nitrogen to traditional PCM substances, can effectively enhance the flame-retardant properties of PCM composites [210]. Organic PCMs are flammable, which limits their applications in heat storage and conversion. Chen et al. [140] reported a flame-resistant PCM by combining phosphorus-grafted hexadecanol and PER phosphate. Cone calorimeter data showed a more than 50% reduction in pHRR and THR, and self-extinguishment tests confirmed quicker flame suppression than hexadecanol (Figure 15A). Li et al. [143] created a flame-retardant, form-stable PCM film by chemically attaching stearyl alcohol to phosphorous oxychloride and encapsulating it within a single-wall CNT skeleton. This change greatly increased the heat storage capacity and decreased the pHRR and THR by 24.4% and 24.3%, respectively (Figure 15B).

4.4.2 | PEG Chain Extension

PEG, as a typical PCM work substance, has double-terminal hydroxyl groups and can be used for chain extension to prepare high-molecular-weight polymers. Taking advantage of this principle, researchers often use PEG chain extension to prepare leakage-resistant PEG-based PCMs. Du et al. [211] used nucleophilic substitution to create a trimaleimide end-capped cyclotriphosphazene flame retardant (TMCTP), which they then used to create flame-retardant PCMs with self-healing capabilities and high flame retardancy (Figure 15C). The dynamic covalent binding of TMCTP inside the polymeric network lowered flammability, which improved the material's overall performance. Zhang et al. prepared a form-stable polyether PCM using PEG 10000, toluene-2,4-diisocyanate, and toluene-2,4-diisocyanate as raw materials through two-step polymerization in toluene, with polyurethane acting as the heat storage phase-change segment and the supporting material for the flame retardant (Figure 15D). The composite has a latent heat of 86.69 J/g and an LOI of 21.3, indicating good fire resistance and high TES density. These characteristics provide a new platform for developing form-stable PCMs with good fire resistance, thus opening up a field of energy materials with enhanced fire resistance and energy storage performance. Wang et al. [213] prepared a solid–solid PCM using functionalized graphene oxide and PEG, which reduced the pHRR by 33.4%. Similarly, Luo et al. [188] developed a high flame-retardant, form-stable PEG/EG composite including PEG/EG, diphenylmethane diisocyanate and melamine with DOPO that considerably reduced

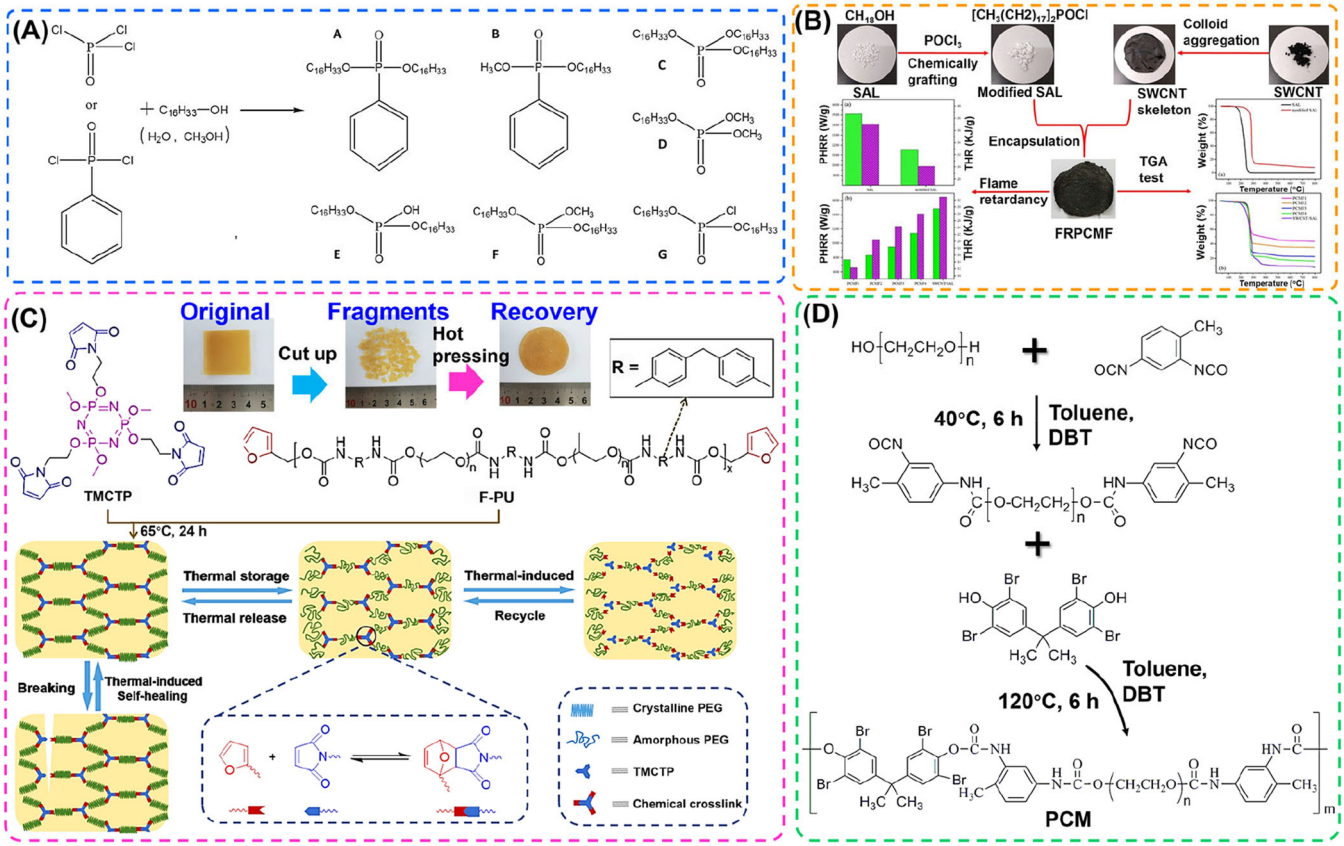

FIGURE 15 | (A) Chemical reaction and formulas of different modified hexadecanol. Reproduced with permission: Copyright 2019, Elsevier [140]. (B) Schematic diagram of the preparation process of the PCMF and comparison of the pHRR and THR of PCMFs and stearyl alcohol (SAL). Reproduced with permission: Copyright 2022, American Chemical Society [143]. (C) Schematic illustration of the synthesis of novel dynamically cross-linked PCM composites (FPCM) and thermally induced recycling of FPCM-3 (Inset). Reproduced with permission: Copyright 2021, American Chemical Society [211]. (D) Schematic of the preparation route for a hybrid form-stable polyether PCM. Reproduced with permission: Copyright 2016, Elsevier [212].

the THR and pHRR, indicating strong fire resistance potential for battery modules.

4.4.3 | Advantages and Disadvantages Analysis

There are usually two general approaches for flame retardancy in this type of PCM. One is to use chemical methods, such as chain extension condensation to obtain high polymers containing flame retardants, while achieving flame retardancy and phase-change effects. After chain expansion, the melting point significantly increases [214], in turn increasing the sensible heat storage capacity. The typical advantage of a PCM obtained using this approach is that it can be flexible and completely leak-free. However, there is also a significant drawback of low latent heat of phase transition. In addition, the selection of PCM functional components is also highly limited, and they must be bifunctional, with PEG diols being a common example. Another approach is to introduce flame-retardant elements into phase-change small molecules. The major change brought about by this is the change in the melting point. The cost often increases because higher purity is required to ensure high crystallinity, which significantly increases the material fabrication cost.

4.5 | A Brief Overview of Flame-Retardant Mechanisms on PCMs

PCMs are typical organic functional materials that generally follow conventional flame-retardant mechanisms. With the rapid development of flame-retardant PCM research, various classical systems have been used to fabricate safe MTPCMs, which predominantly rely on well-established flame-retardant mechanisms. As illustrated in Figure 16, the flame-retardant behavior of these systems aligns with classical mechanistic models. For a comprehensive summary of flame-retardant mechanisms in PCM systems, as well as a discussion of their advantages and limitations, please refer to the review articles [215, 217]. Here, we provide only a brief overview. As shown in Figure 16A, the flame retardants used in flame-retardant PCM systems are similar to those used in traditional flame-retardant materials and primarily include phosphorus-, nitrogen-, silicon-, and nanofiller-based flame retardants and IFRs. These function through various mechanisms such as gas-phase action (dilution effect), condensed-phase char formation, radical trapping, and synergistic effects to achieve effective flame retardancy [218]. In practice, it is often difficult to achieve high-performance flame retardancy using a single mechanism or individual flame retardant. Rather, effective flame-retardant behavior typically results from the synergistic combination of

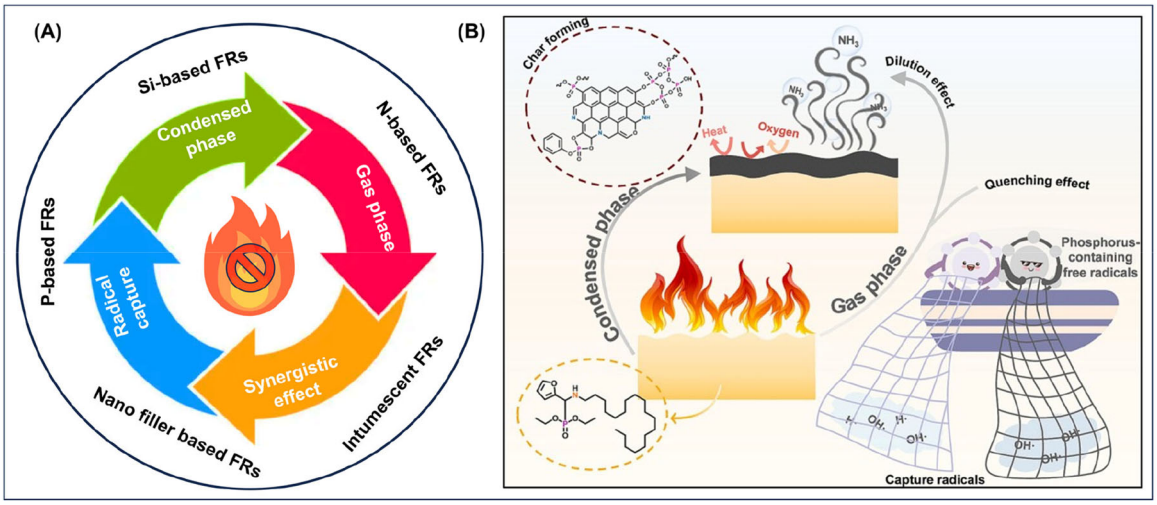

FIGURE 16 | (A) Representative categories of flame retardants and corresponding flame-retardant mechanisms. Reproduced with permission: Copyright 2024, Wiley [215]. (B) Representative examples of synergistic flame-retardant PCM systems. Reproduced with permission: Copyright 2025, Elsevier [216].

multiple flame retardants. For example, the simultaneous incorporation of charring agents along with phosphorus- and nitrogen-based compounds can enable integrated mechanisms, including radical scavenging, flammable gas dilution, and thermal/oxygen barrier formation in the condensed phase—leading to multifunctional and highly efficient flame-retardant effects [216] (Figure 16B).

5 | Remarks and Perspectives

Organic PCMs are classic sustainable energy storage materials and have a long history of research. They have extensive use value and potential applications in traditional building energy conservation, electronic device thermal management, emerging battery thermal management, solar energy capture and storage, and other fields. The related research fits the objectives of the sustainable development goals. Therefore, at present, the research on PCM still attracts a large number of scientific researchers. This review systematically presents the analytical methodologies used in the study of flame-retardant PCMs, including conventional techniques such as the cone calorimeter test, the UL-94 vertical burning test, and the LOI, as well as other methods like direct combustion tests, candle tests, and back-surface temperature monitoring. Furthermore, the recent modification strategies for flame-retardant PCMs are summarized into four main approaches: (1) incorporation of external flame retardants, (2) use of flame-retardant microcapsules, (3) development of flame-retardant support materials, and (4) creation of intrinsic flame-retardant phase-change small molecules. It is worth noting that, for each strategy discussed, we have highlighted both its significant advantages and major limitations, given the broad application prospects of PCMs, the inevitable trend toward the development of environmentally friendly materials, and the various shortcomings and practical challenges associated with current PCM systems. Combining the summary of this review article and the author's research experience, some general insights and prospects will be put forward below for readers to consider and discuss.

5.1 | Sustainable, Fully Bio-Based, and Fire-Safe PCM Development

Sustainable, fully bio-based, and fire-safe PCM development combines the benefits of bio-based materials and fire safety to create innovative solutions for TES and management. The following are some key considerations for sustainable, fully bio-based, and fire-safe PCM development:

(1) Bio-based feedstocks: Sustainable PCMs can be derived from bio-based feedstocks, such as plant oils or agricultural waste, instead of relying on fossil fuel–based sources. Utilizing renewable resources reduces the environmental impact and promotes a circular economy.

(2) Fire safety: Incorporating fire safety considerations into PCM development is crucial to ensuring the materials' safe use. Bio-based PCMs should have inherent fire-resistant properties or be treated with bio-based fire-retardant additives to meet relevant safety standards and sustainable regulations.

(3) Environmental impact: Sustainable PCM development considers the entire life cycle, including the environmental impact of raw material extraction, production processes, use phase, and end-of-life disposal, minimizing energy consumption and emissions during manufacturing, ensuring safe and responsible disposal methods, and promoting recycling and reuse contribute to the sustainability of these materials.

(4) Application-specific requirements: Fully bio-based and fire-safe PCM can find applications in various sectors, including buildings, textiles, electronics, and transportation. Each application may have specific requirements regarding thermal properties, fire safety standards, durability, and compatibility with other materials. Customization of PCM formulations and their integration into different

products and systems require close collaboration between researchers, material manufacturers, and end-users.

5.2 | Multifunctional PCM With Low Cost, High Performance, and Practical Applications

The pursuit of a single performance improvement is difficult to meeting the needs of practical applications, such as weight gain, which is an obvious drawback for the thermal management of sporty devices. Multifunctional PCMs are materials that not only have the ability to store and release thermal energy during phase transitions but also show additional functionalities that enhance their overall performance in specific applications. Some promising examples of multifunctional PCM and their applications are as follows:

(1) Solar-driven interfacial desalination: Given the challenges of freshwater shortage and fossil energy storage, solar-powered interfacial evaporation has been identified as a potential and sustainable saltwater desalination solution. Solar-driven desalination based on PCMs with latent heat storage capability is the key to solving the problem of intermittent solar radiation and is more capable of realizing efficient hydropower cogeneration outside of daylight hours. Several researchers have introduced PCMs in the field of solar-powered desalination, developing high-performance interfacial evaporators with antimicrobial and salt-resistant properties for sustainable desalination production of pure water and efficient dual-hydro cogeneration performance [219–222].

(2) Thermoregulating and moisture management textiles: PCM-enhanced textiles can help regulate body temperature by absorbing excess heat during warm conditions and releasing it when the temperature drops. Additionally, some multifunctional PCMs integrated into textiles can also manage moisture by wicking away perspiration, promoting evaporation, and enhancing overall comfort.

(3) Energy storage and conversion: PCMs can serve as effective TES mediums for various applications, including solar energy systems, batteries, and thermal management in electronics. Multifunctional PCMs with additional properties like high thermal conductivity or electrical conductivity can enhance energy storage and conversion efficiency.

The development of multifunctional PCM requires a combination of materials science, engineering, and application-specific knowledge. Researchers and industry stakeholders collaborate to optimize the properties of PCM and tailor them to meet specific requirements in various sectors. This kind of interdisciplinary approach enables the design and implementation of innovative solutions that offer enhanced performance and multiple functionalities for a wide range of applications.

5.3 | Integrated Structural Materials or Devices

(1) PCMs are integrated with other functional components: For example, for thermal management of chips, thermoelectric converters, sensors, and so forth, Xiaodong Wang's team developed a series of novel phase-change microcapsules, utilizing microcapsule-modified working electrodes to integrate highly electroactive layers with covalently bonded bioenzymes (catalase, penicillinase, horseradish peroxidase, tyrosinase, diamine oxidase, and so on), and designed a thermo-self-regulating smart biosensor, which realizes microenvironmental temperature regulation of biosensors through reversible phase change to prevent enzyme deactivation at high temperatures, thus enhancing the biosensor response to electrochemical biosensing [222–227]. The biosensor developed by the team is expected to be sensitively regulated over a wide temperature range in practical applications.

(2) New topology design: The advanced applications of PCM continue to expand as researchers and engineers explore new possibilities and optimize their performance for specific industries and requirements. These applications offer energy efficiency, thermal comfort, improved system performance, and reduced environmental impact in various sectors, contributing to a more sustainable and efficient future. Jing et al. [228] designed a sandwich-like PCC from crosslinked PI aerogel and medium-erythritol, which provides good long-term high-temperature infrared stealth and thermal camouflage. The composite has potential for use in security and counter-surveillance applications.

Acknowledgments

This study was supported by NEWSAFE (No.: PID2022-143324NA-I00) Projects funded by MICIU (Ministerio de Ciencia, Innovación y Universidades)/AEI (Agencia Estatal de Investigación)/10.13039/501100011033 and, as appropriate, by "ERDF/EU"; and Ramón y Cajal Fellowship (No.: RYC2023-045023-I) funded by MICIU, and, as appropriate, "ESF Investing in your future." This study was also partially supported by INC-UDIT-2025-PRO21 and INC-UDIT-2025-JCR24.

Conflicts of Interest

The authors declare no conflicts of interest.

References

1. J. Liu, X. Zhu, J. Dai, K. Yang, S. Wang, and X. Liu, "Integration of Sustainable Polymers With Phase Change Materials," *Progress in Materials Science* 151 (2025): 101447.

2. F. Zhao, W. Yuan, H. Chen, et al., "Advances in Organic Porous Polymeric-Supported Photothermal Phase Change Materials," *Carbon Energy* 7 (2025): e719.

3. V. J. Reddy, M. F. Ghazali, and S. Kumarasamy, "Advancements in Phase Change Materials for Energy-Efficient Building Construction: A Comprehensive Review," *Journal of Energy Storage* 81 (2024): 110494.

4. M. Chen, H. Liu, H. Zhang, and X. Wang, "Development of $BaSO_4$@*N*-Eicosane Phase-Change Microcapsules With High Corrosion Resistance for Thermal Regulation Application in Architectural Coatings," *Journal of Energy Storage* 57 (2023): 106232.

5. Y. Jung, M. Kim, T. Kim, J. Ahn, J. Lee, and S. H. Ko, "Functional Materials and Innovative Strategies for Wearable Thermal Management Applications," *Nano-Micro Letters* 15, no. 2024 (2023): 160–201.

6. Y. Li, X. Zhao, Y. Tang, X. Zuo, and H. Yang, "Mineral-Based Composite Phase Change Materials Assembled Into 3D Ordered Aerogels for Efficient Wearable Filtration and Thermal Management," *Advanced Functional Materials* 34, no. 39 (2024): 2403059.

7. Z. Zhu, A. Bashir, X. Wu, et al., "Highly Integrated Phase Change and Radiative Cooling Fiber Membrane for Adaptive Personal Thermal Regulation," *Advanced Functional Materials* 35, no. 9 (2024): 2416111.

8. T. Shi, H. Liu, and X. Wang, "Multi-Stimuli-Responsive Shape Memory Flexible Composites Based on Magnetic Melamine/Polydopamine/Phosphorene Complex Foams and Polyethylene Glycol," *Composites, Part A: Applied Science and Manufacturing* 181 (2024): 108117.

9. Z. Huang, R. Wang, W. Jiang, et al., "Nacre-Inspired Flexible and Thermally Conductive Phase Change Composites With Parallelly Aligned Boron Nitride Nanosheets for Advanced Electronics Thermal Management," *Composites Science and Technology* 255 (2024): 110736.

10. E. Alehosseini and S. M. Jafari, "Micro/Nano-Encapsulated Phase Change Materials (PCMs) as Emerging Materials for the Food Industry," *Trends in Food Science & Technology* 91 (2019): 116–128.

11. K. Yuan, Q. Chen, M. Qin, et al., "Micro/Nano Encapsulated Phase Change Materials: Preparation, Principle, and Emerging Advances in Medical Field," *Advanced Functional Materials* 34, no. 23 (2024): 2314487.

12. M. Zare and K. S. Mikkonen, "Phase Change Materials for Life Science Applications," *Advanced Functional Materials* 33, no. 12 (2023): 2213455.

13. K. Matuszek, M. Kar, J. M. Pringle, and D. R. MacFarlane, "Phase Change Materials for Renewable Energy Storage at Intermediate Temperatures," *Chemical Reviews* 123, no. 1 (2022): 491–514.

14. M. Wu, Y. Xuan, X. Liu, Y. Jing, and T. Li, "Flexible, Recyclable, and Highly Conductive Self-Healing Polymer-Based Phase Change Films for Thermal Management," *Advanced Functional Materials* (2025): 2506229.

15. M. Liu, R. Qian, Y. Yang, X. Lu, L. Huang, and D. Zou, "Modification of Phase Change Materials for Electric-Thermal, Photo-Thermal, and Magnetic-Thermal Conversions: A Comprehensive Review," *Advanced Functional Materials* 34, no. 33 (2024): 2400038.

16. S. Yang, Y. Yang, X. Xia, B. Zou, B. Wang, and Y. Zhang, "Biomimetic Stimulus Responsiveness: From Materials Design to Device Integration," *Advanced Functional Materials* 34, no. 33 (2024): 2400500.

17. S. Kahwaji, M. B. Johnson, A. C. Kheirabadi, D. Groulx, and M. A. White, "A Comprehensive Study of Properties of Paraffin Phase Change Materials for Solar Thermal Energy Storage and Thermal Management Applications," *Energy* 162 (2018): 1169–1182.

18. S. Mondal, "Thermo-Regulating Textiles With Phase-Change Materials," in *Functional Textiles for Improved Performance, Protection and Health* (2011), 163–183.

19. L. Liu, Y. Zhang, S. Zhang, and B. Tang, "Advanced Phase Change Materials From Natural Perspectives: Structural Design and Functional Applications," *Advanced Science* 10, no. 22 (2023): 2207652.

20. L. Lu, H. Guo, I. Martin-Fabiani, et al., "Recent Advances and Applications of Flexible Phase Change Composites," *EcoMat* 7, no. 4 (2025): e70004.

21. L. Yu, Y. Jiang, B. Yang, et al., "Reverse Emulsion-Templated Nanoencapsulation of $NaNO_3$ With Crystalline TiO_2 Shell for High-Temperature Heat Energy Storage and Thermal Corrosion Resistance," *Journal of Energy Storage* 128 (2025): 117277.

22. X. Zhang, L. Geng, G. Liang, et al., "Experimental Study on Solid-Solid Phase Change Energy Storage Materials by a Facile Inorganic-Organic Integration Strategy," *Journal of Energy Storage* 113 (2025): 115617.

23. S. Saher, S. Johnston, R. Esther-Kelvin, J. M. Pringle, D. R. MacFarlane, and K. Matuszek, "Trimodal Thermal Energy Storage Material for Renewable Energy Applications," *Nature* 636, no. 8043 (2024): 622–626.

24. Y. Li, T. Wang, J. Zhang, J. Cheng, and Q. Lian, "Multi-Mode Triggered Bio-Based Epoxy Resin/Lauric Acid/Graphene Paper Flexible Phase Change Materials With High Enthalpy Value, Multi-Functionality, and Personal Thermal Management Ability," *Composites, Part A: Applied Science and Manufacturing* 193 (2025): 108849.

25. S. Yang, H. Y. Shi, J. Liu, Y. Y. Lai, Ö. Bayer, and L. W. Fan, "Supercooled Erythritol for High-Performance Seasonal Thermal Energy Storage," *Nature Communications* 15, no. 1 (2024): 4948.

26. T. Shi, X. Gao, H. Liu, and X. Wang, "Multi-Energy Conversion and Electromagnetic Shielding Enabled by Carbonized Polyimide/Kevlar/Graphene Oxide@ZIF-67 Bidirectional Complex Aerogel-Encapsulated Phase-Change Materials," *Nano-Micro Letters* 17, no. 1 (2025): 236–263.

27. Z. M. Png, X. Y. D. Soo, M. H. Chua, et al., "Strategies to Reduce the Flammability of Organic Phase Change Materials: A Review," *Solar Energy* 231 (2022): 115–128.

28. T. B. Freeman, K. E. O. Foster, C. J. Troxler, et al., "Advanced Materials and Additive Manufacturing for Phase Change Thermal Energy Storage and Management: A Review," *Advanced Energy Materials* 13, no. 24 (2023): 2204208.

29. Q. Zhang, Y. Li, C. Liu, et al., "Micro/Nano Encapsulated Phase Change Material: Materials, Preparation, and Emerging Advances in the Solar Energy Field," *Journal of Materials Chemistry A* 12, no. 47 (2024): 32526–32547.

30. X. Deng, C. Li, X. Sun, et al., "Flame-Retardant Wood-Based Composite Phase Change Materials Based on PDMS/Expanded Graphite Coating for Efficient Solar-to-Thermal Energy Storage," *Applied Energy* 368 (2024): 123454.

31. D. Jiao, H. Zhao, H. Sima, C. Cheng, B. Liu, and C. Zhang, "Engineering Flame Retardant Epoxy Resins With Strengthened Mechanical Property by Using Reactive Catechol Functionalized Dopo Compounds," *Chemical Engineering Journal* 485 (2024): 149910.

32. S. Lou, S. Wang, L. Zhang, J. Liu, and T. Tang, "Intrinsic Flame-Retardant Epoxy Resin Based on Phosphorus-Containing Liquid Imidazole Compound: Simultaneously Improving Fire Safety, Mechanical Property and Heat Resistance," *Chemical Engineering Journal* 493 (2024): 152816.

33. S. Araby, B. Philips, Q. Meng, J. Ma, T. Laoui, and C. H. Wang, "Recent Advances in Carbon-Based Nanomaterials for Flame Retardant Polymers and Composites," *Composites, Part B: Engineering* 212 (2021): 108675.

34. L. Ma, J. Gao, Y. Wang, H. Ge, X. Lin, and Z. Zhu, "Preparation of Phosphorus/Nitrogen-Containing MXene Nanohybrids via In Situ Polymerization and Their Application in Epoxy Resins," *Progress in Organic Coatings* 203 (2025): 109163.

35. M. Liu, J. Qiao, X. Zhang, et al., "Flame Retardant Strategies and Applications of Organic Phase Change Materials: A Review," *Advanced Functional Materials* 35, no. 2 (2024): 2412492.

36. G. Z. Yin, J. Hobson, Y. Duan, and D. Y. Wang, "Polyrotaxane: New Generation of Sustainable, Ultra-Flexible, Form-Stable and Smart Phase Change Materials," *Energy Storage Materials* 40 (2021): 347–357.

37. T. Yang, W. P. King, and N. Miljkovic, "Phase Change Material-Based Thermal Energy Storage," *Cell Reports Physical Science* 2, no. 8 (2021): 100540.

38. W. Li, Z. Zheng, Z. Qian, H. Liu, and X. Wang, "Phase Change Material Boosting Electricity Output and Freshwater Production Through Hierarchical-Structured 3D Solar Evaporator," *Advanced Functional Materials* 34, no. 26 (2024): 2316504.

39. H. Zhang, S. Zhou, H. Liu, Z. Qian, and X. Wang, "All-Weather Solar-Powered Desalination and Synchronous Cs^+ Extraction for Salt-Lake Water Enabled by Crown-Ether-Decorated Phase-Change Microcapsules," *Advanced Functional Materials* 34, no. 48 (2024): 2408269.

40. Y. Jin, W. Aftab, X. Geng, et al., "High-Efficiency Thermal-Shock Resistance Enabled by Radiative Cooling and Latent Heat Storage," *Advanced Materials* 36, no. 25 (2024): 2314130.

41. Y. Chen, Y. Meng, J. Zhang, et al., "Leakage Proof, Flame-Retardant, and Electromagnetic Shield Wood Morphology Genetic Composite Phase Change Materials for Solar Thermal Energy Harvesting," *Nano-Micro Letters* 16 (2024): 196.

42. F. Cao, Z. Li, Y. Zhang, et al., "Silica-Based Aerogels Encapsulate Organic/Inorganic Composite Phase Change Materials for Building Thermal Management," *Journal of Energy Storage* 97 (2024): 112858–112867.

43. Y. Lin, Q. Kang, Y. Liu, et al., "Flexible, Highly Thermally Conductive and Electrically Insulating Phase Change Materials for Advanced Thermal Management of 5G Base Stations and Thermoelectric Generators," *Nano-Micro Letters* 15 (2023): 31.

44. Yi-C. Zhou, Y. Jie, B. Lu, B. Rui-Ying, Y. Ming-Bo, and Y. Wei, "Super-Flexible Phase Change Materials With a Dual-Supporting Effect for Solar Thermoelectric Conversion in the Ocean Environment," *Journal of Materials Chemistry A* 11 (2023): 341–351.

45. X. Hu, B. Quan, C. Zhu, et al., "Upgrading Electricity Generation and Electromagnetic Interference Shielding Efficiency via Phase-Change Feedback and Simple Origami Strategy," *Advanced Science* 10, no. 14 (2023): 2206835.

46. T. Shi, H. Liu, and X. Wang, "Unidirectionally Structured Magnetic Phase-Change Composite Based on Carbonized Polyimide/Kevlar Nanofiber Complex Aerogel for Boosting Solar-Thermo-Electric Energy Conversion," *ACS Applied Materials & Interfaces* 16, no. 8 (2024): 10180–10195.

47. Y. Zhang, K. Wu, and Q. Fu, "A Structured Phase Change Material With Controllable Thermoconductive Highways Enables Unparalleled Electricity via Solar-Thermal-Electric Conversion," *Advanced Functional Materials* 32, no. 6 (2022): 2109255–2109262.

48. S. Olson, M. F. Jansen, D. S. Abbot, I. Halevy, and C. Goldblatt, "The Effect of Ocean Salinity on Climate and Its Implications for Earth's Habitability," *Geophysical Research Letters* 49, no. 10 (2022): e2021GL095748.

49. A. K. S. Al-Sayyab, A. Mota-Babiloni, and J. Navarro-Esbrí, "Renewable and Waste Heat Applications for Heating, Cooling, and Power Generation Based on Advanced Configurations," *Energy Conversion and Management* 291 (2023): 117253.

50. R. J. Leamon, S. W. McIntosh, and D. R. Marsh, "Termination of Solar Cycles and Correlated Tropospheric Variability," *Earth and Space Science* 8, no. 4 (2021): e2020EA001223.

51. A. R. Muchtar, B. Srinivasan, S. L. Tonquesse, et al., "Physical Insights on the Lattice Softening Driven Mid-Temperature Range Thermoelectrics of Ti/Zr-Inserted SnTe–An Outlook Beyond the Horizons of Conventional Phonon Scattering and Excavation of Heikes' Equation for Estimating Carrier Properties," *Advanced Energy Materials* 11, no. 28 (2021): 2101122.

52. Z. Tang, P. Cheng, P. Liu, Y. Gao, X. Chen, and G. Wang, "Tightened 1D/3D Carbon Heterostructure Infiltrating Phase Change Materials for Solar–Thermoelectric Energy Harvesting: Faster and Better," *Carbon Energy* 5, no. 6 (2023): e281.

53. L. L. Baranowski, G. J. Snyder, and E. S. Toberer, "Concentrated Solar Thermoelectric Generators," *Energy & Environmental Science* 5, no. 10 (2012): 9055.

54. D. Kraemer, B. Poudel, H. P. Feng, et al., "High-Performance Flat-Panel Solar Thermoelectric Generators With High Thermal Concentration," *Nature Materials* 10 (2011): 532–538.

55. M. H. Jeong, E. J. Bae, B. Park, J. Ha, M. Han, and Y. H. Kang, "High-Performance and Flexible Thermoelectric Generator Based on a Robust Carbon Nanotube/BiSbTe Foam," *Carbon Energy* 7, no. 1 (2024): e650.

56. H. Wang, Y. Peng, H. Peng, and J. Zhang, "Fluidic Phase–Change Materials With Continuous Latent Heat From Theoretically Tunable Ternary Metals for Efficient Thermal Management," *Proceedings of the National Academy of Sciences of United States of America* 119, no. 31 (2022): e2200223119.

57. F. Xue, X. Qi, T. Huang, Cy Tang, N. Zhang, and Y. Wang, "Preparation and Application of Three-Dimensional Filler Network Towards Organic Phase Change Materials With High Performance and Multi-Functions," *Chemical Engineering Journal* 419 (2021): 129620.

58. R. Cao, D. Sun, L. Wang, et al., "Enhancing Solar–Thermal–Electric Energy Conversion Based on m-PEGMA/GO Synergistic Phase Change Aerogels," *Journal of Materials Chemistry A* 8, no. 26 (2020): 13207–13217.

59. H. Y. Zhao, X. Wang, J. Wu, et al., "An Intelligent, Solar-Responsive, and Thermally Conductive Phase-Change System Toward Solar-Thermal-Electrical Conversion Featuring Daytime Blooming for Solar Energy Harvesting and Nighttime Closing for Thermal Preservation," *Advanced Functional Materials* 34, no. 45 (2024): 2406236.

60. L. Li, L. Kong, T. Luo, et al., "Flexible Photothermal Phase Change Material With High Photothermal Properties Achieved by Promoted Dispersion of Hydrophobically Modified Eumelanin and Its Photovoltaic Applications," *Small* 21, no. 22 (2025): 2500951.

61. X. Zeng, S. Chen, Y. Liao, et al., "High Latent Heat and Recyclable Phase-Change Materials for Photothermoelectric Conversion," *ACS Applied Materials & Interfaces* 17, no. 18 (2025): 27155–27166.

62. Y. Tang, X. Zhao, Y. Li, et al., "Nanoclay Hybridized Graphene Aerogels Encapsulating Phase Change Material for Efficient Solar-Driven Desalination and Electricity Generation," *Advanced Functional Materials* 34, no. 48 (2024): 2408693.

63. B. Ai, Z. Liu, X. Hu, et al., "Sandwich-Structured HDPE-Based Medium-Temperature Phase Change Composites With MXene Interlayers for Photo-Thermal-Electrical Applications," *Chemical Engineering Journal* 512 (2025): 162367.

64. Z. Huang, Y. Liu, J. Yang, Dx Sun, Xd Qi, and Y. Wang, "Pine Needle-Like Hierarchical Copper Foam-Based High-Performance Phase Change Composites for All-Weather Solar-Thermal-Electric Conversion," *Chemical Engineering Journal* 514 (2025): 163268.

65. X. L. Shi, J. Zou, and Z. G. Chen, "Advanced Thermoelectric Design: From Materials and Structures to Devices," *Chemical Reviews* 120, no. 15 (2020): 7399–7515.

66. D. Kraemer, J. Sui, K. McEnaney, et al., "High Thermoelectric Conversion Efficiency of MgAgSb-Based Material With Hot-Pressed Contacts," *Energy & Environmental Science* 8, no. 4 (2015): 1299–1308.

67. D. Liu, C. Lei, K. Wu, and Q. Fu, "A Multidirectionally Thermoconductive Phase Change Material Enables High and Durable Electricity via Real-Environment Solar-Thermal-Electric Conversion," *ACS Nano* 14, no. 11 (2020): 15738–15747.

68. J. Yang, L. S. Tang, R. Y. Bao, et al., "An Ice-Templated Assembly Strategy to Construct Graphene Oxide/Boron Nitride Hybrid Porous Scaffolds in Phase Change Materials With Enhanced Thermal Conductivity and Shape Stability for Light–Thermal–Electric Energy Conversion," *Journal of Materials Chemistry A* 4 (2016): 18841–18851.

69. J. Yang, L. S. Tang, R. Y. Bao, et al., "Largely Enhanced Thermal Conductivity of Poly (Ethylene Glycol)/Boron Nitride Composite Phase Change Materials for Solar-Thermal-Electric Energy Conversion and Storage With Very Low Content of Graphene Nanoplatelets," *Chemical Engineering Journal* 315 (2017): 481–490.

70. X. Chen, J. Lin, Y. Feng, et al., "Carbon-Metal Network Boosting Photon/Phonon Transport in Photothermal Phase Change Materials," *Carbon* 238 (2025): 120192.

71. K. Chen, Y. Li, Y. Feng, et al., "In Situ Vertical Alignment of MoS_2 on Co/C Dodecahedron Boosting Phase Change Materials for Solar-Thermoelectric Generation," *Journal of Energy Chemistry* 107 (2025): 548–557.

72. Y. Li, Y. Feng, M. Qin, et al., "Co-Anchored Hollow Carbonized Kapok Fiber Encapsulated Phase Change Materials for Upgrading Photothermal Utilization," *Small* 21, no. 21 (2025): 2500479.

73. J. Weng, X. Yang, D. Ouyang, M. Chen, G. Zhang, and J. Wang, "Comparative Study on the Transversal/Lengthwise Thermal Failure Propagation and Heating Position Effect of Lithium-Ion Batteries," *Applied Energy* 255 (2019): 113761.

74. X. Feng, M. Ouyang, X. Liu, L. Lu, Y. Xia, and X. He, "Thermal Runaway Mechanism of Lithium Ion Battery for Electric Vehicles: A Review," *Energy Storage Materials* 10 (2018): 246–267.

75. R. Kizilel, R. Sabbah, J. R. Selman, and S. Al-Hallaj, "An Alternative Cooling System to Enhance the Safety of Li-Ion Battery Packs," *Journal of Power Sources* 194, no. 2 (2009): 1105–1112.

76. S. Wilke, B. Schweitzer, S. Khateeb, and S. Al-Hallaj, "Preventing Thermal Runaway Propagation in Lithium Ion Battery Packs Using a Phase Change Composite Material: An Experimental Study," *Journal of Power Sources* 340 (2017): 51–59.

77. B. Coleman, J. Ostanek, and J. Heinzel, "Reducing Cell-to-Cell Spacing for Large-Format Lithium Ion Battery Modules With Aluminum or PCM Heat Sinks Under Failure Conditions," *Applied Energy* 180 (2016): 14–26.

78. N. Joshy, M. Hajiyan, A. R. M. Siddique, S. Tasnim, H. Simha, and S. Mahmud, "Experimental Investigation of the Effect of Vibration on Phase Change Material (PCM) Based Battery Thermal Management System," *Journal of Power Sources* 450 (2020): 227717.

79. D. Hu, L. Han, W. Zhou, et al., "Flexible Phase Change Composite Based on Loading Paraffin Into Cross-Linked CNT/SBS Network for Thermal Management and Thermal Storage," *Chemical Engineering Journal* 437 (2022): 135056.

80. J. Weng, Y. He, D. Ouyang, et al., "Honeycomb-Inspired Design of a Thermal Management Module and Its Mitigation Effect on Thermal Runaway Propagation," *Applied Thermal Engineering* 195 (2021): 117147.

81. F. Zhang, A. Lin, P. Wang, and P. Liu, "Optimization Design of a Parallel Air-Cooled Battery Thermal Management System With Spoilers," *Applied Thermal Engineering* 182 (2021): 116062.

82. J. Weng, C. Xiao, D. Ouyang, et al., "Mitigation Effects on Thermal Runaway Propagation of Structure-Enhanced Phase Change Material Modules With Flame Retardant Additives," *Energy* 239 (2022): 122087.

83. S. Wu, T. Li, Z. Tong, et al., "High-Performance Thermally Conductive Phase Change Composites by Large-Size Oriented Graphite Sheets for Scalable Thermal Energy Harvesting," *Advanced Materials* 31, no. 49 (2019): 1905099.

84. P. Jaumaux, J. Wu, D. Shanmukaraj, et al., "Non-Flammable Liquid and Quasi-Solid Electrolytes Toward Highly-Safe Alkali Metal-Based Batteries," *Advanced Functional Materials* 31, no. 10 (2020): 2008644.

85. L. Li, C. Xu, R. Chang, et al., "Thermal-Responsive, Super-Strong, Ultrathin Firewalls for Quenching Thermal Runaway in High-Energy Battery Modules," *Energy Storage Materials* 40 (2021): 329–336.

86. Y. Li, T. Wang, X. Li, G. Zhang, K. Chen, and W. Yang, "Experimental Investigation on Thermal Management System With Flame Retardant Flexible Phase Change Material for Retired Battery Module," *Applied Energy* 327 (2022): 120109.

87. M. Wu, T. Li, P. Wang, S. Wu, R. Wang, and J. Lin, "Dual-Encapsulated Highly Conductive and Liquid-Free Phase Change Composites Enabled by Polyurethane/Graphite Nanoplatelets Hybrid Networks for Efficient Energy Storage and Thermal Management," *Small* 18, no. 9 (2022): 2105647.

88. G. Cheng, Z. Wang, X. Wang, and Y. He, "All-Climate Thermal Management Structure for Batteries Based on Expanded Graphite/Polymer Composite Phase Change Material With a High Thermal and Electrical Conductivity," *Applied Energy* 322 (2022): 119509.

89. J. Zhang, X. Li, G. Zhang, et al., "Experimental Investigation of the Flame Retardant and Form-Stable Composite Phase Change Materials for a Power Battery Thermal Management System," *Journal of Power Sources* 480 (2020): 229116.

90. H. Han, F. Xiong, M. Qin, et al., "Intrinsic Flame-Retardant Phase Change Materials for Battery Thermal Management During Rapid Cycling and Thermal Runaway," *Energy Storage Materials* 77 (2025): 104175.

91. J. Yang, L. Chen, J. Ou, W. Li, and W. Wu, "Room-Temperature Flexible Composite Phase Change Materials for Enhanced Battery Thermal Management," *Applied Thermal Engineering* 265 (2025): 125667.

92. J. Guo, H. Ding, J. Xie, et al., "Bio-Based, Flexible, and Electrically Insulating Phase Change Materials for Advanced Battery Thermal Management," *Journal of Energy Storage* 111 (2025): 115405.

93. C. Zhang, Y. Mao, K. Li, et al., "High Power and Energy Density Graphene Phase Change Composite Materials for Efficient Thermal Management of Li-Ion Batteries," *Energy Storage Materials* 75 (2025): 104003.

94. J. Zhao, Y. Chen, and M. Chen, "Battery Thermal Management With a Modified Metal Alloy/Expanded Graphite/Paraffin Composite Phase Change Material," *Journal of Energy Storage* 113 (2025): 115652.

95. M. Kaempgen, C. K. Chan, J. Ma, Y. Cui, and G. Gruner, "Printable Thin Film Supercapacitors Using Single-Walled Carbon Nanotubes," *Nano Letters* 9, no. 5 (2009): 1872–1876.

96. S. Pan, J. Ren, X. Fang, and H. Peng, "Integration: An Effective Strategy to Develop Multifunctional Energy Storage Devices," *Advanced Energy Materials* 6, no. 4 (2016): 1501867.

97. X. Zhang, Y. Guo, Y. Liu, et al., "Ultrathick and Highly Thermally Conductive Graphene Films by Self-Fusion," *Carbon* 167 (2020): 249–255.

98. Y. Li, J. Chen, Y. Xing, and J. Song, "Thermal Management of Micro-Scale Inorganic Light-Emitting Diodes on an Orthotropic Substrate for Biointegrated Applications," *Scientific Reports* 7, no. 1 (2017): 6638.

99. Y. Shi, C. Wang, Y. Yin, Y. Li, Y. Xing, and J. Song, "Functional Soft Composites as Thermal Protecting Substrates for Wearable Electronics," *Advanced Functional Materials* 29, no. 45 (2019): 1905470.

100. B. Wang, G. Li, L. Xu, J. Liao, and X. Zhang, "Nanoporous Boron Nitride Aerogel Film and Its Smart Composite With Phase Change Materials," *ACS Nano* 14, no. 12 (2020): 16590–16599.

101. X. Li, M. Sheng, S. Gong, et al., "Flexible and Multifunctional Phase Change Composites Featuring High-Efficiency Electromagnetic Interference Shielding and Thermal Management for Use in Electronic Devices," *Chemical Engineering Journal* 430 (2022): 132928.

102. X. Hu, X. Huang, B. Quan, et al., "Tree-Inspired and Scalable High Thermal Conductivity Ethylene–Vinyl Acetate Copolymer/Expanded Graphite/Paraffin Wax Phase Change Composites for Efficient Thermal Management," *Chemical Engineering Journal* 471 (2023): 144720.

103. H. Li, C. Hu, Y. Jiang, et al., "Flexible and Leakage-Proof Sodium Alginate-Based Phase Change Composite Film for Thermal-Comfortable Application of Electronic Devices," *ACS Sustainable Chemistry & Engineering* 11, no. 29 (2023): 10620–10630.

104. X. Zhu, X. Li, J. Shen, et al., "Stable Microencapsulated Phase Change Materials With Ultrahigh Payload for Efficient Cooling of Mobile Electronic Devices," *Energy Conversion and Management* 223 (2020): 113478.

105. W. Lee and J. Kim, "Cellulose Nanofiber Grafting and Aluminum Nitride Deposition on the Surface of Expanded Graphite to Improve the Thermal Conductivity and Mechanical Properties of Phase Change Material Composites," *Composites, Part B: Engineering* 230 (2022): 109526.

106. A. G. Anter, A. A. Sultan, A. A. Hegazi, and M. A. El Bouz, "Thermal Performance and Energy Saving Using Phase Change Materials (PCM) Integrated in Building Walls," *Journal of Energy Storage* 67 (2023): 107568.

107. M. Mahdaoui, S. Hamdaoui, A. Ait Msaad, et al., "Building Bricks With Phase Change Material (PCM): Thermal Performances," *Construction and Building Materials* 269 (2021): 121315.

108. R. Kalbasi, B. Samali, and M. Afrand, "Taking Benefits of Using PCMs in Buildings to Meet Energy Efficiency Criteria in Net Zero by 2050," *Chemosphere* 311, no. 2 (2023): 137100.

109. Z. X. Li, A. A. A. A. Al-Rashed, M. Rostamzadeh, R. Kalbasi, A. Shahsavar, and M. Afrand, "Heat Transfer Reduction in Buildings by Embedding Phase Change Material in Multi-Layer Walls: Effects of Repositioning, Thermophysical Properties and Thickness of PCM," *Energy Conversion and Management* 195 (2019): 43–56.

110. J. Lei, J. Yang, and E. H. Yang, "Energy Performance of Building Envelopes Integrated With Phase Change Materials for Cooling Load Reduction in Tropical Singapore," *Applied Energy* 162 (2016): 207–217.

111. Z. Zhang, N. Zhang, Y. Yuan, P. E. Phelan, and S. Attia, "Thermal Performance Analysis of an Existing Building Heating Based on a Novel Active Phase Change Heater," *Energy and Buildings* 278 (2023): 112646.

112. K. Faraj, M. Khaled, J. Faraj, F. Hachem, and C. Castelain, "Phase Change Material Thermal Energy Storage Systems for Cooling Applications in Buildings: A Review," *Renewable and Sustainable Energy Reviews* 119 (2020): 109579.

113. G. Zhang, N. Xiao, B. Wang, and A. G. Razaqpur, "Thermal Performance of a Novel Building Wall Incorporating a Dynamic Phase Change Material Layer for Efficient Utilization of Passive Solar Energy," *Construction and Building Materials* 317 (2022): 126017.

114. E. Rodriguez-Ubinas, L. Ruiz-Valero, S. Vega, and J. Neila, "Applications of Phase Change Material in Highly Energy-Efficient Houses," *Energy and Buildings* 50 (2012): 49–62.

115. P. Schossig, H. Henning, S. Gschwander, and T. Haussmann, "Micro-Encapsulated Phase-Change Materials Integrated Into Construction Materials," *Solar Energy Materials and Solar Cells* 89 (2005): 297–306.

116. D. Li, Y. Zheng, C. Liu, and G. Wu, "Numerical Analysis on Thermal Performance of Roof Contained PCM of a Single Residential Building," *Energy Conversion and Management* 100 (2015): 147–156.

117. J. Yu, Q. Yang, H. Ye, et al., "Thermal Performance Evaluation and Optimal Design of Building Roof With Outer-Layer Shape-Stabilized PCM," *Renewable Energy* 145 (2020): 2538–2549.

118. S. S. Chandel and T. Agarwal, "Review of Current State of Research on Energy Storage, Toxicity, Health Hazards and Commercialization of Phase Changing Materials," *Renewable and Sustainable Energy Reviews* 67 (2017): 581–596.

119. J. Giro-Paloma, M. Martínez, L. F. Cabeza, and A. I. Fernández, "Types, Methods, Techniques, and Applications for Microencapsulated Phase Change Materials (MPCM): A Review," *Renewable and Sustainable Energy Reviews* 53 (2016): 1059–1075.

120. H. Zhang, F. Xing, H. Z. Cui, et al., "A Novel Phase-Change Cement Composite for Thermal Energy Storage: Fabrication, Thermal and Mechanical Properties," *Applied Energy* 170 (2016): 130–139.

121. L. Pan, Q. Tao, S. Zhang, et al., "Preparation, Characterization and Thermal Properties of Micro-Encapsulated Phase Change Materials," *Solar Energy Materials and Solar Cells* 98 (2012): 66–70.

122. Z. Sun, T. Shi, Y. Wang, J. Li, H. Liu, and X. Wang, "Hierarchical Microencapsulation of Phase Change Material With Carbon-Nanotubes/Polydopamine/Silica Shell for Synergistic Enhancement of Solar Photothermal Conversion and Storage," *Solar Energy Materials and Solar Cells* 236 (2022): 111539.

123. T. Makuta, K. Kadoya, H. Izumi, and M. Miyatake, "Synthesis of Cyanoacrylate-Covered Xylitol Microcapsules for Thermal Storage," *Chemical Engineering Journal* 273 (2015): 192–196.

124. C. Y. Zhao and G. H. Zhang, "Review on Microencapsulated Phase Change Materials (MEPCMs): Fabrication, Characterization and Applications," *Renewable and Sustainable Energy Reviews* 15, no. 8 (2011): 3813–3832.

125. X. Yu, Y. Li, X. Yin, et al., "Corncoblike, Superhydrophobic, and Phase-Changeable Nanofibers for Intelligent Thermoregulating and Water-Repellent Fabrics," *ACS Applied Materials & Interfaces* 11, no. 42 (2019): 39324–39333.

126. C. Wang, J. Wang, L. Zhang, and S. Fu, "Thermoregulatory Elasticity Braided Fibers Designed With Core–Sheath Structure for Wearable Personal Thermal Management," *Journal of Materials Chemistry C* 12, no. 7398 (2024): 7398–7406.

127. Y. He, Q. Liu, M. Tian, et al., "Highly Conductive and Elastic Multi-Responsive Phase Change Smart Fiber and Textile," *Composites Communications* 44 (2023): 101772.

128. Z. Niu, S. Qi, S. S. A. Shuaib, and W. Yuan, "Flexible, Stimuli-Responsive and Self-Cleaning Phase Change Fiber for Thermal Energy Storage and Smart Textiles," *Composites, Part B: Engineering* 228 (2022): 109431.

129. J. Wu, M. Wang, L. Dong, et al., "A Trimode Thermoregulatory Flexible Fibrous Membrane Designed With Hierarchical Core-Sheath Fiber Structure for Wearable Personal Thermal Management," *ACS Nano* 16, no. 8 (2022): 12801–12812.

130. Q. Zhang, T. Xue, J. Tian, Y. Yang, W. Fan, and T. Liu, "Polyimide/Boron Nitride Composite Aerogel Fiber-Based Phase-Changeable Textile for Intelligent Personal Thermoregulation," *Composites Science and Technology* 226 (2022): 109541.

131. Z. Guo, F. Lin, J. Qiao, et al., "A Modified Kapok Fiber Based Phase Change Composite for Highly-Efficient Solar-Thermal Conversion," *Nano Energy* 108 (2023): 108205.

132. G. Li, G. Hong, D. Dong, W. Song, and X. Zhang, "Multiresponsive Graphene-Aerogel-Directed Phase-Change Smart Fibers," *Advanced Materials* 30, no. 30 (2018): 1801754.

133. M. Kong, X. Guo, S. Zhang, Y. Zhang, and B. Tang, "Structural Colored Textiles With High Color Visibility and Stability for Intelligent Thermoregulating Performance," *Chemical Engineering Journal* 473 (2023): 145332.

134. C. Liang, W. Zhang, C. Liu, et al., "Multifunctional Phase Change Textiles With Electromagnetic Interference Shielding and Multiple Thermal Response Characteristics," *Chemical Engineering Journal* 471 (2023): 144500.

135. Y. Su, W. Zhu, M. Tian, Y. Wang, X. Zhang, and J. Li, "Intelligent Bidirectional Thermal Regulation of Phase Change Material Incorporated in Thermal Protective Clothing," *Applied Thermal Engineering* 174 (2020): 115340.

136. T. Ma, L. Li, Q. Wang, and C. Guo, "High-Performance Flame Retarded Paraffin/Epoxy Resin Form-Stable Phase Change Material," *Journal of Materials Science* 54, no. 1 (2018): 875–885.

137. R. N. Walters, N. Safronava, and R. E. Lyon, "A Microscale Combustion Calorimeter Study of Gas Phase Combustion of Polymers," *Combustion and Flame* 162, no. 3 (2015): 855–863.

138. Y. H. Huang, Y. X. Cheng, R. Zhao, and W. L. Cheng, "A High Heat Storage Capacity Form-Stable Composite Phase Change Material With Enhanced Flame Retardancy," *Applied Energy* 262 (2020): 114536.

139. Y. Zhao, Q. Zeng, X. Lai, et al., "Multifunctional Cellulose-Based Aerogel for Intelligent Fire Fighting," *Carbohydrate Polymers* 316 (2023): 121060.

140. R. Chen, X. Huang, R. Zheng, D. Xie, Y. Mei, and R. Zou, "Flame-Retardancy and Thermal Properties of a Novel Phosphorus-Modified PCM for Thermal Energy Storage," *Chemical Engineering Journal* 380 (2020): 122500.

141. J. Wang, H. Yue, Z. Du, X. Cheng, H. Wang, and X. Du, "Flame-Retardant and Form-Stable Delignified Wood-Based Phase Change Composites With Superior Energy Storage Density and Reversible Thermochromic Properties for Visual Thermoregulation," *ACS Sustainable Chemistry & Engineering* 11, no. 9 (2023): 3932–3943.

142. D. Li, Y. Tang, X. Zuo, X. Zhao, X. Zhang, and H. Yang, "Preparation of Hierarchical Porous Microspheres Composite Phase Change Material for Thermal Energy Storage Concrete in Buildings," *Applied Clay Science* 232 (2023): 106771.

143. J. Li, R. Chen, Y. Luo, et al., "SWCNT-Encapsulated Phosphorus-Grafted Stearyl Alcohol as a Flame-Retardant Phase-Change Material With Superior Thermal Properties," *ACS Applied Energy Materials* 5, no. 2 (2022): 1869–1882.

144. Z. Zhang, Z. Zhang, T. Chang, J. Wang, X. Wang, and G. Zhou, "Phase Change Material Microcapsules With Melamine Resin Shell via Cellulose Nanocrystal Stabilized Pickering Emulsion In-Situ Polymerization," *Chemical Engineering Journal* 428 (2022): 131164.

145. D. Xu, Q. Huang, L. Yang, et al., "Experimental Design of Composite Films With Thermal Management and Electromagnetic Shielding Properties Based on Polyethylene Glycol and MXene," *Carbon* 202 (2023): 1–12.

146. G. Z. Yin, X. M. Yang, J. Hobson, A. M. López, and D. Y. Wang, "Bio-Based Poly (Glycerol-Itaconic Acid)/PEG/APP as Form Stable and Flame-Retardant Phase Change Materials," *Composites Communications* 30 (2022): 101057.

147. Z. Xu, W. Chen, T. Wu, C. Wang, and Z. Liang, "Thermal Management System Study of Flame Retardant Solid–Solid Phase Change Material Battery," *Surfaces and Interfaces* 36 (2023): 102558.

148. Y. Cai, Y. Hu, L. Song, H. Lu, Z. Chen, and W. Fan, "Preparation and Characterizations of HDPE–EVA Alloy/OMT Nanocomposites/Paraffin Compounds as a Shape Stabilized Phase Change Thermal Energy Storage Material," *Thermochimica Acta* 451 (2006): 44–51.

149. P. Zhang, Y. Hu, L. Song, H. Lu, J. Wang, and Q. Liu, "Synergistic Effect of Iron and Intumescent Flame Retardant on Shape-Stabilized Phase Change Material," *Thermochimica Acta* 487 (2009): 74–79.

150. Y. Jiang, P. Yan, Y. Wang, C. Zhou, and J. Lei, "Form-Stable Phase Change Materials With Enhanced Thermal Stability and Fire Resistance via the Incorporation of Phosphorus and Silicon," *Materials & Design* 160 (2018): 763–771.

151. L. Li, G. Wang, and C. Guo, "Influence of Intumescent Flame Retardant on Thermal and Flame Retardancy of Eutectic Mixed Paraffin/Polypropylene Form-Stable Phase Change Materials," *Applied Energy* 162 (2016): 428–434.

152. M. Kang, Y. Liu, W. Lin, C. Liang, and J. Cheng, "The Thermal Behavior and Flame Retardant Performance of Phase Change Material Microcapsules With Halloysite Nanotube," *Journal of Energy Storage* 60 (2023): 106632.

153. P. S. Jijoe, S. R. Yashas, and H. P. Shivaraju, "Fundamentals, Synthesis, Characterization and Environmental Applications of Layered Double Hydroxides: A Review," *Environmental Chemistry Letters* 19, no. 3 (2021): 2643–2661.

154. Z. Zhang, W. Du, Y. Liu, et al., "Thermal Management Ability and Flame Retardancy of Silicone Rubber Foam Filled With Flame Retardant Phase Change Capsules," *Applied Clay Science* 240 (2023): 106977.

155. Z. Zhang, Y. Liu, W. Du, et al., "Construction of Layered Double Hydroxide-Modified Silica Integrated Multilayer Shell Phase Change Capsule With Flame Retardancy and Highly Efficient Thermoregulation Performance," *Journal of Colloid and Interface Science* 632 (2023): 311–325.

156. S. D. Jiang, G. Tang, J. Chen, Z. Q. Huang, and Y. Hu, "Biobased Polyelectrolyte Multilayer-Coated Hollow Mesoporous Silica as a Green Flame Retardant for Epoxy Resin," *Journal of Hazardous Materials* 342 (2018): 689–697.

157. Z. T. Hu, V. H. Reinack, J. An, et al., "Ecofriendly Microencapsulated Phase-Change Materials With Hybrid Core Materials for Thermal Energy Storage and Flame Retardancy," *Langmuir* 37, no. 21 (2021): 6380–6387.

158. X. Du, Y. Fang, X. Cheng, Z. Du, M. Zhou, and H. Wang, "Fabrication and Characterization of Flame-Retardant Nanoencapsulated *n*-Octadecane With Melamine−Formaldehyde Shell for Thermal Energy Storage," *ACS Sustainable Chemistry & Engineering* 6, no. 11 (2018): 15541–15549.

159. H. Liao, W. Duan, Y. Liu, Q. Wang, and H. Wen, "Flame Retardant and Leaking Preventable Phase Change Materials for Thermal Energy Storage and Thermal Regulation," *Journal of Energy Storage* 35 (2021): 102248.

160. P. A. Advincula, A. C. de Leon, B. J. Rodier, J. Kwon, R. C. Advincula, and E. B. Pentzer, "Accommodating Volume Change and Imparting Thermal Conductivity by Encapsulation of Phase Change Materials in Carbon Nanoparticles," *Journal of Materials Chemistry A* 6, no. 6 (2018): 2461–2467.

161. M. Kang, Y. Liu, C. Liang, et al., "Phase Change Material Microcapsules With DOPO/Cu Modified Halloysite Nanotubes for Thermal Controlling of Buildings: Thermophysical Properties, Flame Retardant Performance and Thermal Comfort Levels," *International Journal of Heat and Mass Transfer* 207 (2023): 124045.

162. X. Du, S. Wang, Z. Du, X. Cheng, and H. Wang, "Preparation and Characterization of Flame-Retardant Nanoencapsulated Phase Change Materials With Poly(Methylmethacrylate) Shells for Thermal Energy Storage," *Journal of Materials Chemistry A* 6, no. 36 (2018): 17519–17529.

163. X. Zhao, Y. Tang, W. Xie, D. Li, X. Zuo, and H. Yang, "3D Hierarchical Porous Expanded Perlite-Based Composite Phase-Change Material With Superior Latent Heat Storage Capability for Thermal Management," *Construction and Building Materials* 362 (2023): 129768.

164. S. Niu, M. Kang, Y. Liu, et al., "The Preparation and Characterization of Phase Change Material Microcapsules With Multifunctional Carbon Nanotubes for Controlling Temperature," *Energy* 268 (2023): 126652.

165. Q. Xu, X. Liu, Q. Luo, et al., "Bioinspired Spectrally Selective Phase-Change Composites for Enhanced Solar Thermal Energy Storage," *Advanced Functional Materials* 35, no. 1 (2024): 2412066.

166. T. Luo, L. Kong, J. Lu, et al., "Neuron-Inspired Flexible Phase Change Materials for Ambient Energy Harvesting and Respiration Monitoring," *Advanced Materials* 36, no. 50 (2024): 2411820.

167. J. X. Wang, Y. Mao, and N. Miljkovic, "Nano-Enhanced Graphite/Phase Change Material/Graphene Composite for Sustainable and Efficient Passive Thermal Management," *Advanced Science* 11, no. 38 (2024): 2402190.

168. X. Hao, D. Li, X. Peng, W. Lan, and C. Liu, "In Situ Construction of Biomass Derived 3D Carbon Framework for Efficient Electromagnetic Interference Shielding and Joule Heating Performance," *Chemical Engineering Journal* 479 (2024): 147681.

169. C. Qiu, H. Jiang, P. Liu, et al., "An Ultrastrong Wood-Based Phase Change Material for Efficient Photothermal Conversion and Thermal Energy Conservation," *Composites, Part B: Engineering* 279 (2024): 111460.

170. W. Fan, X. Zhang, Y. Zhang, Y. Zhang, and T. Liu, "Lightweight, Strong, and Super-Thermal Insulating Polyimide Composite Aerogels Under High Temperature," *Composites Science and Technology* 173 (2019): 47–52.

171. L. Dou, X. Zhang, X. Cheng, et al., "Hierarchical Cellular Structured Ceramic Nanofibrous Aerogels With Temperature-Invariant Superelasticity for Thermal Insulation," *ACS Applied Materials & Interfaces* 11, no. 32 (2019): 29056–29064.

172. J. Niu, S. Deng, X. Gao, H. Niu, Y. Fang, and Z. Zhang, "Experimental Study on Low Thermal Conductive and Flame Retardant Phase Change Composite Material for Mitigating Battery Thermal Runaway Propagation," *Journal of Energy Storage* 47 (2022): 103557.

173. Y. Wang, F. Wang, L. Zhao, et al., "Shape-Stable and Fire-Resistant Hybrid Phase Change Materials With Enhanced Thermoconductivity for Battery Cooling," *Chemical Engineering Journal* 431 (2022): 133983.

174. X. Zhu, J. Liu, W. Zhao, W. Yu, and X. Liu, "Design of Phase Change Composite With Hierarchical Energy-Transfer Pathway via Laser-Induced Graphene for Efficient Energy Storage, Conversion, and Utilization," *Chemical Engineering Journal* 460 (2023): 141882.

175. D. Huang, Z. Wang, X. Sheng, and Y. Chen, "Bio-Based MXene Hybrid Aerogel/Paraffin Composite Phase Change Materials With Superior Photo and Electrical Responses Toward Solar Thermal Energy Storage," *Solar Energy Materials and Solar Cells* 251 (2023): 112124.

176. M. Zhu, L. Liu, and Z. Wang, "Mesoporous Silica via Self-Assembly of Nano Zinc Amino-Tris-(Methylenephosphonate) Exhibiting Reduced Fire Hazards and Improved Impact Toughness in Epoxy Resin," *Journal of Hazardous Materials* 392 (2020): 122343.

177. A. H. Alkhazaleh, W. Almanaseer, M. Ismail, S. Almashaqbeh, and M. M. Farid, "Thermal and Mechanical Properties of Cement Based-Composite Phase Change Material of Butyl Stearate/Isopropyl Palmitate/Expanded Graphite for Low Temperature Solar Thermal Applications," *Journal of Energy Storage* 50 (2022): 104547.

178. Y. Wang, L. Zhao, W. Zhan, Y. Chen, and M. Chen, "Flame Retardant Composite Phase Change Materials With MXene for Lithium-Ion Battery Thermal Management Systems," *Journal of Energy Storage* 86 (2024): 111293.

179. Y. Luo, Y. Xie, H. Jiang, et al., "Flame-Retardant and Form-Stable Phase Change Composites Based on MXene With High Thermostability and Thermal Conductivity for Thermal Energy Storage," *Chemical Engineering Journal* 420 (2021): 130466.

180. C. Liang, H. Qiu, P. Song, X. Shi, J. Kong, and J. Gu, "Ultra-Light MXene Aerogel/Wood-Derived Porous Carbon Composites With Wall-Like "Mortar/Brick" Structures for Electromagnetic Interference Shielding," *Science Bulletin* 65, no. 8 (2020): 616–622.

181. G. Fang, H. Li, Z. Chen, and X. Liu, "Preparation and Characterization of Flame Retardant N-Hexadecane/Silicon Dioxide Composites as Thermal Energy Storage Materials," *Journal of Hazardous Materials* 181, no. 1 (2010): 1004–1009.

182. Z. Zhou, H. Xia, J. Hu, and L. Wang, "Enhanced Thermal Energy Storage of Polyethylene Glycol Composite With High Thermal Conductive Reaction-Bonded BN Aerogel," *Composites Communications* 49 (2024): 101965.

183. D. Pan, J. Dong, G. Yang, et al., "Ice Template Method Assists in Obtaining Carbonized Cellulose/Boron Nitride Aerogel With 3D Spatial Network Structure to Enhance the Thermal Conductivity and Flame Retardancy of Epoxy-Based Composites," *Advanced Composites and Hybrid Materials* 5 (2022): 58–70.

184. Y. Cao, M. Weng, M. H. H. Mahmoud, et al., "Flame-Retardant and Leakage-Proof Phase Change Composites Based on MXene/Polyimide Aerogels Toward Solar Thermal Energy Harvesting," *Advanced Composites and Hybrid Materials* 5 (2022): 1253–1267.

185. H. Liao, W. Chen, Y. Liu, and Q. Wang, "A Phase Change Material Encapsulated in a Mechanically Strong Graphene Aerogel With High Thermal Conductivity and Excellent Shape Stability," *Composites Science and Technology* 189 (2020): 108010.

186. S. Gao, J. Ding, W. Wang, and J. Lu, "MXene Based Flexible Composite Phase Change Material With Shape Memory, Self-Healing and Flame Retardant for Thermal Management," *Composites Science and Technology* 234 (2023): 109945.

187. L. Xu, X. Liu, Z. An, and R. Yang, "EG-Based Coatings for Flame Retardance of Shape Stabilized Phase Change Materials," *Polymer Degradation and Stability* 161 (2019): 114–120.

188. Y. Luo, D. Zhou, W. Yang, et al., "Phosphorus-Nitrogen Based Flame Retardant Polyurethane Composite Phase Change Materials for Battery Thermal Safety System," *Applied Thermal Engineering* 258 (2025): 124763.

189. P. Qi, F. Chen, Y. Li, et al., "A Review of Durable Flame-Retardant Fabrics by Finishing: Fabrication Strategies and Challenges," *Advanced Fiber Materials* 5, no. 3 (2023): 731–763.

190. B. Sang, Z. Li, X. Li, L. Yu, and Z. Zhang, "Graphene-Based Flame Retardants: A Review," *Journal of Materials Science* 51, no. 18 (2016): 8271–8295.

191. W. Chai, X. Su, Y. Xia, et al., "Construction of a Novel Halogen-Free and Phosphorus-Free and Synergistic Flame Retardant System With Low Addition in Simultaneously Improving the Flame Retardancy, Water Resistance and Mechanical Properties for Silicone Rubber," *Applied Clay Science* 238 (2023): 106926.

192. Q. X. Yu, R. X. Bei, J. H. Liu, et al., "Bioinspired Polyimide Film With Fire Retardant and Gas Barrier Properties by Gravity-Induced Deposition of Montmorillonite," *Aggregate* 4, no. 6 (2023): e392.

193. J. Zhu, R. Xiong, F. Zhao, et al., "Lightweight, High-Strength, and Anisotropic Structure Composite Aerogel Based on Hydroxyapatite Nanocrystal and Chitosan With Thermal Insulation and Flame Retardant Properties," *ACS Sustainable Chemistry & Engineering* 8, no. 1 (2019): 71–83.

194. R. Shen, L. Liu, Y. Cao, L. Zhang, X. Sheng, and Y. Chen, "Biomass Modified Boron Nitride/Polyimide Hybrid Aerogel Supported Phase Change Composites With Superior Energy Storage Capacity and Improved Flame Retardancy for Solar-Thermal Energy Storage," *Solar Energy* 242 (2022): 287–297.

195. Q. Zhang, L. Ma, T. Xue, J. Tian, W. Fan, and T. Liu, "Flame-Retardant and Thermal-Protective Polyimide-Hydroxyapatite Aerogel Fiber-Based Composite Textile for Firefighting Clothing," *Composites, Part B: Engineering* 248 (2023): 110377.

196. L. Yin, D. Xie, K. Gong, C. Shi, X. Qian, and K. Zhou, "Phase Change Materials Encapsulated in Coral-Inspired Organic–Inorganic Aerogels for Flame-Retardant and Thermal Energy Storage," *ACS Applied Nano Materials* 6, no. 10 (2023): 8752–8762.

197. R. Tian, X. Jia, C. Huang, et al., "Flexible, Flame-Resistant, and Anisotropic Thermally Conductive Aerogel Films With Ionic Liquid Crystal-Armored Boron Nitride," *ACS Applied Materials & Interfaces* 15, no. 22 (2023): 27223–27233.

198. Q. Huang, X. Li, G. Zhang, J. Weng, Y. Wang, and J. Deng, "Innovative Thermal Management and Thermal Runaway Suppression for Battery Module With Flame Retardant Flexible Composite Phase Change Material," *Journal of Cleaner Production* 330 (2022): 129718.

199. X. Ge, X. Li, Y. Jin, G. Zhang, J. Deng, and J. Ge, "Experimental Investigation on Thermal Management System of Composite Phase Change Material Coupled With Serpentine Tubes for Battery Module," *Applied Thermal Engineering* 219 (2023): 119501.

200. J. Hu, S. Xu, Y. Wang, et al., "Integration of Safety and Energy Storage: Experimental Study on Thermal and Flame-Retardant Properties of Ammonium Polyphosphate/Polyvinyl Alcohol/Modified Melamine Foam as a Composite Phase Change Material," *Journal of Energy Storage* 84 (2024): 110852.

201. R. Zheng, R. Chen, D. Xie, et al., "Fabrication of Flame-Retardant Phase-Change Materials for Photo-to-Heat Conversion and Flame-Retardant Mechanism," *Journal of Energy Storage* 84 (2024): 110724.

202. X. Zhang, F. Wang, and L. He, "Flame-Retardant Shape-Stabilized Phase Change Composites With Superior Solar-to-Thermal Conversion," *Solar Energy Materials and Solar Cells* 274 (2024): 112996.

203. H. Xu, C. Liu, W. Guo, et al., "Sodium Alginate/Al_2O_3 Fiber Nanocomposite Aerogel With Thermal Insulation and Flame Retardancy Properties," *Chemical Engineering Journal* 489 (2024): 151223.

204. L. Yang, H. Zhang, C. Wang, et al., "Novel Aerogels Based on Supramolecular G-Quadruplex Assembly With Intrinsic Flame Retardancy and Thermal Insulation," *Journal of Colloid and Interface Science* 672 (2024): 618–630.

205. C. Montanari, Y. Li, H. Chen, M. Yan, and L. A. Berglund, "Transparent Wood for Thermal Energy Storage and Reversible Optical Transmittance," *ACS Applied Materials & Interfaces* 11, no. 22 (2019): 20465–20472.

206. H. Yang, Y. Liu, J. Li, C. Wang, and Y. Li, "Full-Wood Photoluminescent and Photothermic Materials for Thermal Energy Storage," *Chemical Engineering Journal* 403 (2021): 126406.

207. S. Yuan, H. Wang, X. Li, Z. Du, X. Cheng, and X. Du, "Flame Retardant and Form-Stable Phase Change Composites Based on Phytic Acid/Dopamine-Decorated Delignified Wood for Efficient Solar-Thermal Energy Conversion and Storage," *Composites, Part A: Applied Science and Manufacturing* 160 (2022): 107048.

208. H. Yue, J. Wang, H. Wang, Z. Du, X. Cheng, and X. Du, "Flame-Retardant and Form-Stable Phase-Change Composites Based on Phytic Acid/ZnO-Decorated Surface-Carbonized Delignified Wood With Superior Solar-Thermal Conversion Efficiency and Improved Thermal Conductivity," *ACS Applied Materials & Interfaces* 15, no. 6 (2023): 8093–8104.

209. A. H. Alkhazaleh, W. Almanaseer, and A. Alkhazali, "Experimental Investigation on Thermal Properties and Fire Performance of Lauric Acid/Diphenyl Phosphate/Expanded Perlite as a Flame Retardant Phase Change Material for Latent Heat Storage Applications," *Sustainable Energy Technologies and Assessments* 56 (2023): 103059.

210. G. Liang, X. Zhang, J. Zhao, et al., "Intrinsic Flame-Retardant Solid–Solid Organic Phase Change Materials for High-Security Thermal Management," *Small* (2025): 2503431.

211. X. Du, L. Jin, S. Deng, et al., "Recyclable, Self-Healing, and Flame-Retardant Solid-Solid Phase Change Materials Based on Thermally Reversible Cross-Links for Sustainable Thermal Energy Storage," *ACS Applied Materials & Interfaces* 13, no. 36 (2021): 42991–43001.

212. Y. Zhang, B. Tang, L. Wang, R. Lu, D. Zhao, and S. Zhang, "Novel Hybrid Form-Stable Polyether Phase Change Materials With Good Fire Resistance," *Energy Storage Materials* 6 (2017): 46–52.

213. F. Wang, P. Zhang, Y. Mou, et al., "Synthesis of the Polyethylene Glycol Solid-Solid Phase Change Materials With a Functionalized Graphene Oxide for Thermal Energy Storage," *Polymer Testing* 63 (2017): 494–504.

214. W. Aftab, J. Shi, M. Qin, et al., "Molecularly Elongated Phase Change Materials for Mid-Temperature Solar-Thermal Energy Storage and Electric Conversion," *Energy Storage Materials* 52 (2022): 284–290.

215. M. Liu, J. Qiao, X. Zhang, et al., "Flame Retardant Strategies and Applications of Organic Phase Change Materials: A Review," *Advanced Functional Materials* 35, no. 2 (2024): 202412492.

216. K. Li and B. Yuan, "Developing Flame-Retardant Properties Into Intrinsic Phase Change Materials: A Molecular Design Study Inspired by Phosphorus-Nitrogen Synergy," *Chemical Engineering Journal* 509 (2025): 161287.

217. Y. Xiao, T. Li, Y. Yang, et al., "Exploring Flame-Retardant, Shape-Stabilized Multi-Functional Composite Phase Change Materials," *Solar Energy Materials and Solar Cells* 282 (2025): 113369.

218. X. Wang, T. Wang, R. Wei, et al., "Preparation and Performance Study of an Innovative Wood-Based Phase Change Material With High Thermal Conductivity and Fire Retardancy," *Journal of Energy Storage* 121 (2025): 116589.

219. W. Li, Z. Zheng, H. Liu, and X. Wang, "A Solar-Driven Seawater Desalination and Electricity Generation Integrating System Based on Carbon Black-Decorated Magnetic Phase-Change Composites," *Desalination* 562 (2023): 116713.

220. H. Yang, Z. Hu, S. Wu, et al., "Directional-Thermal-Conductive Phase Change Composites Enabling Efficient and Durable Water-Electricity Co-Generation Beyond Daytime," *Advanced Energy Materials* 14, no. 43 (2024): 2402926.

221. Y. Li, Y. Shi, H. Wang, et al., "Recent Advances in Carbon-Based Materials for Solar-Driven Interfacial Photothermal Conversion Water Evaporation: Assemblies, Structures, Applications, and Prospective," *Carbon Energy* 5, no. 11 (2023): e331.

222. S. Chen, Z. Zheng, H. Liu, and X. Wang, "Highly Efficient, Antibacterial, and Salt-Resistant Strategy Based on Carbon Black/Chitosan-Decorated Phase-Change Microcapsules for Solar-Powered Seawater Desalination," *ACS Applied Materials & Interfaces* 15, no. 13 (2023): 16640–16653.

223. H. Liu, X. Tian, H. Liu, and X. Wang, "Electrochemical Biosensor Based on Tyrosinase-Immobilized Phase-Change Microcapsules for Ultrasensitive Detection of Phenolic Contaminants Under In Situ Thermal Management," *Journal of Industrial and Engineering Chemistry* 120 (2023): 349–360.

224. X. Tian, H. Liu, H. Liu, and X. Wang, "Immobilizing Diamine Oxidase on Electroactive Phase-Change Microcapsules to Construct Thermoregulatory Smart Biosensor for Enhancing Detection of Histamine in Foods," *Food Chemistry* 397 (2022): 133759.

225. J. Xiong, Z. Sun, J. Yu, H. Liu, and X. Wang, "Thermal Self-Regulatory Smart Biosensor Based on Horseradish Peroxidase-Immobilized Phase-Change Microcapsules for Enhancing Detection of Hazardous Substances," *Chemical Engineering Journal* 430 (2022): 132982.

226. G. Liao, H. Liu, and X. Wang, "More Accurate and More Efficient: Penicillinase-Immobilized Phase-Change Microcapsules for Detection and Removal of Penicillins Under Microenvironmental Thermal Management," *Journal of Environmental Chemical Engineering* 11, no. 1 (2023): 109148.

227. H. A. M. Saeed, W. Xu, and H. Yang, "The Application of Cellulosic-Based Materials on Interfacial Solar Steam Generation for Highly Efficient Wastewater Purification: A Review," *Carbon Energy* 6, no. 9 (2024): e540.

228. J. Jing, H. Liu, and X. Wang, "Long-Term Infrared Stealth by Sandwich-Like Phase-Change Composites at Elevated Temperatures via Synergistic Emissivity and Thermal Regulation," *Advanced Functional Materials* 34, no. 2 (2023): 2309269.